Membrane Technology For Phosphorus Recovery from Wastewater

Kedwell, Katie Charlotte

Publication date:
2019

Document Version
Publisher's PDF, also known as Version of record

MEMBRANE TECHNOLOGY FOR PHOSPHORUS RECOVERY FROM WASTEWATER

BY
KATIE CHARLOTTE KEDWELL

DISSERTATION SUBMITTED 2019

AALBORG UNIVERSITY
DENMARK

MEMBRANE TECHNOLOGY FOR PHOSPHORUS RECOVERY FROM WASTEWATER

by

Katie Charlotte Kedwell

AALBORG UNIVERSITY
DENMARK

PhD Dissertation

March 2019

Department of Chemistry and Bioscience

.

Dissertation submitted: 25th March 2019

PhD supervisor: Associate Prof. Morten L. Christensen,
Aalborg University

Co-supervisors: Assistant Prof. Cejna A. Quist-Jensen,
Aalborg University

Assistant Prof. Mads K. Jørgensen,
Aalborg University

PhD committee: Associate Professor Rudi P. Nielsen (chairman)
Aalborg University

Associate Professor Anders Bentien
Aarhus Universitet

Assistant Professor Irena Petrinic
University of Maribor

PhD Series: Faculty of Engineering and Science, Aalborg University

Department: Department of Chemistry and Bioscience

ISSN (online): 2446-1636
ISBN (online): 978-87-7210-412-6

Published by:
Aalborg University Press
Langagervej 2
DK – 9220 Aalborg Ø
Phone: +45 99407140
aauf@forlag.aau.dk
forlag.aau.dk

Printed in Denmark by Rosendahls, 2019

PREFACE

This dissertation is submitted in partial fulfilment of the requirements for obtaining the degree of doctor of philosophy (Ph.D.). The dissertation consists of abstracts in English and Danish, a short thesis and four supporting papers.

The study was carried out at the Section of Chemistry, Department of Chemistry and Bioscience at Aalborg University in the period from October 2015 to February 2019. The study was financed by Innovation Fund Denmark, under the RecoverP project (Grant number: 4106-00014B). Part of the work was carried out at Katholieke Universiteit Leuven, Department of Chemical Engineering (Leuven, Belgium).

ENGLISH SUMMARY

Phosphorus is essential in many industries, particularly agriculture. However, phosphorus is a finite resource, and reserves are limited. Northern Europe has no phosphorus reserves, while Morocco has the World's largest reserves of phosphate rock. Phosphorus has been used at an increasing rate, consequently, it is estimated that phosphorus reserves will be depleted within the next 200 years.

Phosphorus can be recovered from waste streams. The most promising of which is wastewater. During wastewater treatment phosphorus is removed by biological or chemical means. This means sewage sludge contains a high concentration of phosphorus. In some places sludge is spread on fields as a fertilizer. However, this raises issues surrounding odour, heavy metal contamination, and poor public opinion. Sludge can be incinerated and phosphorus recovered from the ashes, but the incineration process is energy intensive, and heavy metal contamination is sometimes still an issue.

Biologically bound phosphorus is released during digestion; therefore digested sludge liquors contain a high concentration of phosphorus, but much less solids than sludge itself. Phosphorus products can then be precipitate from digested sludge liquors. Struvite is an extremely effective fertilizer, since it contains nitrogen, phosphorus, and magnesium. Addition of magnesium is needed in order to precipitate struvite, often in the form magnesium chloride.

The objective of this study is to increase the efficiency of struvite precipitation through concentrating digested sludge liquors (thus reducing the amount of magnesium additive) or through removal of phosphorus to a 'clean' stream, free of heavy metals or biological contamination. This can be achieved by using forward osmosis and selectrodialysis, respectively.

TFC forward osmosis membrane was tested, using a seawater draw solution. Water permeability of 0.29 LMH bar^{-1} was achieved when concentrating digester centate, and a VCR of 7 was achieved using seawater draw. Membrane fouling was not found to be a problem during 68 hour operation. Biomimetic membrane achieved a water flux of 0.092 LMH bar^{-1}. Using biomimetic membrane phosphorus permeability was found to decrease with increasing pH, while ammonium permeability increased with increasing pH. This shows increasing rejection with increasing charge on the ion. However, it was also found that sodium ions from the draw acted as co-ions for ammonium flux across the membrane. Consequently, pH adjustment could not prevent draw solution contamination.

Selectrodialysis was investigated for recovery of ammonium and phosphate in separate streams simultaneously. Initial recovery rates of 0.072 and 1.31 mmol m^{-2} s^{-}

[1] were found for phosphate and ammonium respectively. After 3 hours of operation 90% phosphate and 72% ammonium was recovered into the concentrate streams. Simulations of membrane area and power usage were carried out for increasing recovery.

Finally, an economic analysis of implementing both technologies at Aaby wastewater treatment plant (Aarhus, Denmark) is carried out. It was found that the cost of treatment (including construction, plant etc.) must be below €6.75 per cubic meter of digester centrate treated. Any cost incurred below this value would allow a profit to be made. Only forward osmosis was below this threshold. The membrane area required for selectrodialysis was large, incurring high costs.

.

DANSK RESUME

Fosfor er vigtig i mange brancher, især i landbruget. Imidlertid er fosfor en begrænset ressource, hvor Nordeuropa ingen fosforreserver har, mens Marokko har verdens største reserver af fosfatsten. Fosfor bliver brugt i stigende grad, og det vurderes derfor, at fosforreserverne vil blive udtømt inden for de næste 200 år.

Derfor kunne en løsning på dette problem være at genindvinde fosfor fra spildstrømme, hvor den mest lovende er spildevand. Under spildevandsrensning fjernes fosfor enten biologiske og/eller kemisk. Det betyder, at spildevandsslam indeholder en høj koncentration af fosfor. Nogle steder spredes slammet på marker som gødning. Dette medfører imidlertid nogle udfordringer såsom lugt, tungmetalforurening og general dårligt omdømme i befolkningen. Derimod kan slammet forbrændes, hvorved fosfor kan udvides fra asken, men forbrændingsprocessen er energiintensiv, og forurening af tungmetaller er stadigt et problem.

En anden metode, er at fjerne fosfor fra udrådnet slam. Biologisk bundet fosfor frigives under udrådning og derfor indeholder væskefasen fra dette slam (rejektvand) en høj koncentration af fosfor, men med et lavere tørstofindhold. Fra denne væskefase kan forskellige fosforprodukter udfældes såsom Struvit. Dette produkt kan bruges til gødning, da det indeholder både nitrogen, fosfor og magnesium. Tilsætning af magnesium er nødvendig for at udfælde struvit, ofte i form af magnesiumklorid.

Formålet med dette PhD projekt er at øge effektiviteten af struvitudfældningen ved at opkoncentrere rejektvandet fra det udrådnede slam, således at tilsætning af magnesium kan reduceres, eller ved at fjerne fosfor til en "ren" strøm, fri for tungmetaller og biologisk kontaminering. Dette kan opnås ved at benytte forskellige membranprocesser - henholdsvis direkte osmose og selektiv elektrodialyse.

En TFC osmosemembran blev testet ved at anvende havvand fra Limfjorden , som trækopløsning. En vandpermeabilitet på 0,29 LMH bar-1 blev opnået ved opkoncentrering af rejektvand, og en opkoncentreringsfaktor på 7 blev opnået under anvendelse af havvand fra Limfjorden. Fouling af membranen er ikke et problem i løbet af 68 timers drift. En anden membran, som efterligner naturen, en såkaldt ”biomimetic” membran opnåede en vandflux på 0,092 LMH bar-1. Ved brug af denne membran faldt fosforpermeabiliteten med stigende pH, mens ammoniak/ammoniumpermeabiliteten steg med stigende pH. Dette viser en stigende tilbageholdelse af ioner ved højere ladning. Det blev imidlertid også fundet, at natriumioner fra trækopløsningen fungerede som med-ioner for ammoniumtransporten over membranen, hvorved ammonium blev transporteret over

i trækopløsningen, mens natrium blev transporteret til rejektvandet. Derfor kunne pH-justering ikke forhindre forurening af trækopløsningen.

Selektiv elektrodialyse blev undersøgt for at genvinde ammonium og fosfat i separate strømme samtidigt. Genindvindingen til start blev fundet til 0,072 og 1,31 mmol m-2 s-1 for henholdsvis fosfat og ammonium. Efter 3 timers drift blev 90% fosfat og 72% ammonium genindvundet i koncentratstrømmene. Simuleringer af det nødvendige membranareal og strømforbrug blev udført for at undersøge muligheden for at genindvinde disse næringsstoffer.

Endelig blev der gennemført en økonomisk analyse af implementeringen af begge teknologier på Aaby rensningsanlæg (Aarhus, Danmark). Det blev konstateret, at omkostningerne (herunder konstruktion, anlæg mv.) skal være under 6,75 € pr. m^3 af behandlet rejektvand for at opnå en fortjeneste. Kun direkte osmose lå under denne værdi. Det membranareal, der kræves til selektiv elektrodialyse, var for stort og medførte for høje omkostninger på nuværende tidspunkt.

LIST OF SUPPORTING PAPERS

Paper I

K.C. Kedwell, C.A. Quist-Jensen, G. Giannakakis, M.L. Christensen, Forward osmosis with high-performing TFC membranes for concentration of digester centrate prior to phosphorus recovery, Sep. Purif. Technol. 197 (2018) 449–456. doi:10.1016/j.seppur.2018.01.034.

Paper II

K.C. Kedwell, M.L. Christensen, C.A. Quist-Jensen, M.K. Jørgensen, Effect of reverse sodium flux and pH on ammoniacal nitrogen transport through biomimetic membranes, Sep. Purif. Technol. 217 (2019) 40–47. doi:10.1016/j.seppur.2019.02.001.

Paper III

K.C. Kedwell, M.K. Jørgensen, C.A. Quist-Jensen, T.D. Pham, B Van der Bruggen, M.L. Christensen, Selective electrodialysis for simultaneous but separate phosphate and ammonia recovery, *Submitted to Environmental Technology*

OTHER PUBLICATIONS

Separate but simultaneous recovery of phosphate and ammonium using selective electrodialysis. / Kedwell, Katie Charlotte; Pham, Tien Duc; Jensen-Quist, Cejna Anne; Jørgensen, Mads Koustrup; Van der Bruggen, Bart; Christensen, Morten Lykkegaard.. 2018. Poster session presented at 17th Nordic Filtration Symposium, Aalborg, Denmark

Ammonia transfer in forward osmosis during operation to concentrate digester centrate. / Kedwell, Katie Charlotte; Quist-Jensen, Cejna Anna; Jørgensen, Mads Koustrup; Christensen, Morten Lykkegaard. 2018. Poster session presented at Euromembrane 2018, Valencia, Spain.

Forward osmosis for phosphorus recovery from wastewater. / Kedwell, Katie Charlotte; Giannakakis, Georgios; Quist-Jensen, Cejna Anna; Jørgensen, Mads Koustrup; Christensen, Morten Lykkegaard. Conference Handbook - 9th International Membrane Science & Technology Conference. 2016. p. 163-165 T4.3.

Fouling of forward osmosis membranes during phosphorus recovery from wastewater. / Kedwell, Katie Charlotte; Giannakakis, Georgios; Jørgensen, Mads Koustrup; Quist-Jensen, Cejna Anna; Christensen, Morten Lykkegaard. IFOS 2016 Abstract Book. UTS ePRESS, 2016. p. 18.

ACKNOWLEDGEMENTS

Firstly, I would like to thank my supervisor, Associate Professor Morten L. Christensen, for his guidance over the past three years. Likewise, my thanks also go to Assistant Professors Cejna A. Quist-Jensen and Mads K. Jørgensen for their help and interesting discussions. I owe a huge thank you to Lisbeth Wybrandt, Henriette Casper Jensen, and Kamilla Smith Hansen for all their help in the lab and translations of procedures. Also, thank you to Professor Bart van der Bruggen for having me at his lab in Belgium, and a special thanks to Duc and Kenneth for their help during my time there.

Thank you to my fellow PhD students; Malwina, Nadieh, Laura, Kamilla, Chao, Martin, Yang, and Kate, who were always there for a chat or cup of coffee. Special thanks to Trine, who helped me settle into the lab and life in Belgium (especially as it was on one leg).

Lastly, I'd like to thank my parents, Derek and Jeanette, for their ongoing support, and Paul for his encouragement and patience, especially while we were living in different countries.

TABLE OF CONTENTS

TABLE OF FIGURES/TABLES

CHAPTER 1. INTRODUCTION

Since the industrial revolution, humanity has been using finite resources at an ever increasing rate. As such it is necessary to find ways of reducing their use, or find alternative renewable resources which can be used in their place. The most notable example of this in recent years is oil. In order to reduce its use, alternative automotive fuels have been studied, such as the use of electric vehicles. However, some finite resources have no alternative, such as phosphorus which is contained in every living cell. Consequently, it is necessary to identify opportunities to reuse or recycle phosphorus from waste streams.

1.1. PHOSPHORUS CYCLE AND SOURCES OF RECOVERY

Phosphorus is essential to everyday life. It is mined as rock, with the largest reserves (over half of the world's phosphate reserves) found in Morocco [1]. Through the use of intensive farming methods phosphorus use in fertilizers has significantly increased. 'Peak phosphorus', is the term used to describe the time when the global phosphorus production rate is at its maximum. A number of estimates have been made as to when peak phosphorus will occur, with many studies citing that it will be reached by 2035 [2]. However, another study calculated that it was reached in 1989 [3]. Similarly, the estimated lifetime of phosphorus reserves has been calculated to be anywhere between 50 and 400 years [3–5]. Therefore, it is essential to develop new and cost effective method to recover phosphorus before reserves are depleted.

1.1.1. PHOSPHORUS CYCLE

Prior to industrialization the phosphorus cycle was closed (Figure 1a). However, modern human activity has caused the cycle to be broken (Figure 1b). In industrialized countries faecal matter (containing phosphorus) goes to wastewater treatment plants (WWTPs). This prevents faeces decomposing and in many countries the phosphorus is not returned back into the soil. As such, farmers add fertilizer to the soil to ensure an appropriate phosphorus concentration. This may causes problems with a high run-off of phosphorus, if the phosphorus is not bound in the soil, resulting in higher phosphorus concentrations in water bodies.

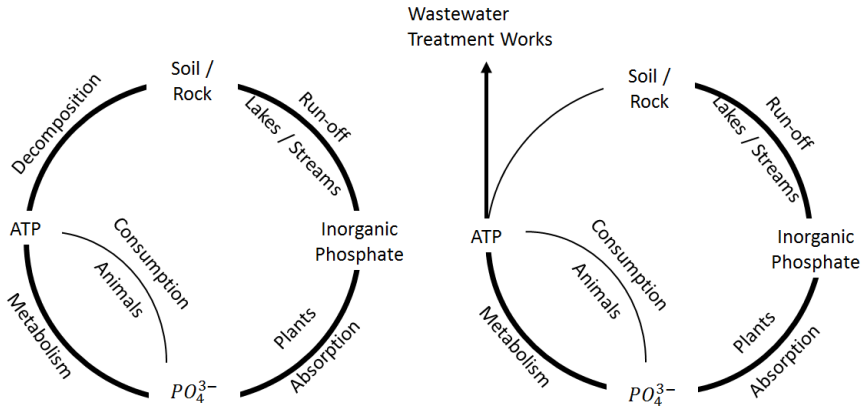

Figure 1(a) Phosphorus cycle (b) phosphorus cycle broken by human activity

Recovery of phosphorus from WWTPs or other phosphorus-rich waste streams is a good opportunity to reduce a country's dependence on imported phosphorus, and create a more sustainable reliance on the declining mass of minable phosphate rock.

1.1.2. USES OF PHOSPHORUS

Phosphorus has many uses; the following section highlights some, but not all, industrial uses of phosphorus. Phosphoric acid is the most common starting point for other uses of phosphorus [6].

Around 90% of phosphorus is used in food production. With the most common use being fertilizers (80%). The application of phosphorus fertilizers has played a key role in agricultural prosperity and reducing global hunger [7]. Phosphorus is vital for the survival of crops as it plays a role in photosynthesis, and many other biochemical processes, such as root development, uniform crop maturity and disease resistance [8]. In the last 40 years fertilizer use has increased 700% [9], with China, India and the US accounting for 50% of its use [7]. Not only plants require phosphorus for growth, animals and people also require it. Phosphorus is a key component of DNA, and is vital in cellular energy production. It is therefore added to animal food stuffs (7%) to promote healthy bone growth/density [10] and skeletal tissue. A further 1-2% is used in food additives. [11,12]

Table 1 shows some of the uses of phosphorus, and in which form it is used. It is important to understand which form of phosphorus is required for certain applications to ensure correct recovery, identify potential customers/ users, and ensure it is adequately pure for proper use.

Phosphorus is also used in the following industries/products;

- Pigments and dyes (phosphinines [13]);
- Glasses (phosphorus oxynitride [14]);
- Phospho-ceramic construction materials (phospho-silicate [15]);
- Industrial phosphate esters (triaryl/alkyl phosphates for use in fire retardants [16]);
- Pesticides (dialkyl phosphates [17]);
- Medicinal compounds;
- Pyrotechnics (white, yellow or red phosphorus [18]);
- Catalysts and synthetic reagents (i.e. surface-phosphated NiO catalysts [19]);
- Electronic/electrical materials (black phosphorus [20]).[6]

Table 1 Phosphorus uses and the type of phosphorus product used [21,22]

Phosphorus Use	**Phosphorus form**
Fertilizer	Superphosphate [$Ca(H_2PO_4)_2•H_2O+CaSO_4•2H_2O$] Concentrated superphosphate [$Ca(H_2PO_4)2•H_2O$] Ammonium phosphate ($NH_4H_2PO_4$) Diammonium phosphate [$(NH_4)_2HPO_4$] Nitric phosphates Calcium phosphate Magnesium ammonium phosphate (struvite) [$NH_4MgPO_4·6H_2O$]
Food industry	Polyphosphates Disodium phosphate Phosphoric acid Mono –calcium phosphate Sodium acid pyrophosphate

	Tetra-sodium pyrophosphate
Detergents	Sodium tripolyphosphate Tetrapotassium pyrophosphate
Metal surface treatments	Phosphoric acid
Toothpaste	Sodium hexametaphosphate Sodium monofluorophosphate
Fire retardants	Ammonium phosphate
Refractory industries	Aluminium phosphate

Since heavy metal contamination is often an issue when recovering phosphorus, the use of recovered products in direct human consumption is not legal, i.e in toothpaste, detergents, or food additives. Furthermore, there would be poor public opinion of using consumables containing phosphorus recovered from certain waste streams, such as wastewater. In order to ensure safe processes/use, many industries require a phosphorus compound with high purity. For example, the fire retardant industry requires a pure product in order to produce high-quality, potentially life-saving products. On the other hand, use of recovered phosphorus as a fertilizer has high potential. Phosphorus from waste streams is already used on agricultural land, but has poor public opinion due to odour and the potential for heavy metal contamination. As such, a market already exists for recovered phosphorus. Struvite is a widely studied phosphorus recovery product, and has a sale value of €225 per ton [23]. Struvite is of particular interest if it can be used in organic farming.

Recovered phosphorus products show poor or no water solubility compared to commercially available fertilizer. Consequently, it may not be suitable for application requiring a liquid product. However, application in field trials shows improved agricultural output even though recovered fertilizers showed no water solubility. [24] Consequently, recovered phosphorus is best suited to fertilizer application.

1.2. WASTE STREAMS WITH HIGH PHOSPHORUS CONTENT

Different waste streams exist with high phosphorus content that could be recovered. Thus, once a suitable application has been selected, it is necessary to identify a waste stream suitable for recovery/reuse. When looking for waste streams with high phosphorus content, one may look no further than phosphorus mines themselves.

Thirty to 40% of mined phosphorus is lost during mining and processing [25]. While this may appear to be the perfect place to recover phosphorus, phosphorus mining wastes also contain considerable quantities of heavy metals and radioactive material. These pose a threat to human health, and complicate the recovery of phosphorus. Furthermore, this would only be suitable in the few regions where phosphate mines exist. [25,26]

Surface run-off contains phosphorus [27]. White et al. (1977) measured the phosphorus content of surface run-off from catchments of the Taita experimental basin in New Zealand. Catchments included a hill pasture, fertilized with lime and super phosphate, and forested land, both native and exotic. It was reported that the hill pasture lost 3 times as much reactive phosphate, and up to 5 times as much total phosphate as forested land [28]. This is further supported by research in the United Kingdom which shows up to 2 kg P ha^{-1} y^{-1} being lost from land treated with slurry [29].

Animal manure contains phosphorus, cattle and swine faeces have been found to contain 6.7 and 29.1 g kg^{-1} total-P respectively [30]. In 1997, livestock farms in the US produced 0.7 million tons of recoverable phosphorus [31]. Livestock manure is often spread on fields; however, it suffers from poor public opinion due to odour and health concerns. Furthermore, livestock is often concentrated on large farms, as such; phosphorus from manure is not evenly distributed across a country or continent, and can only be transported short distances. While the spreading of manure has been found to be effecting in increasing the phosphorus content of soil, some (depending on animal feed etc.) of the phosphorus is inorganic and not soluble in water, and as such cannot be used by plants. One method to overcome this is by treating the manure with hydrothermal carbonization, then acid treating the product. Though this method 80-90% of phosphorus can be recovered [32].

Municipal wastewater not only covers human excreta, but also some surface run-off, and phosphorus from household items (i.e detergents and toothpaste). Consequently wastewater contains 75-300 mg P L^{-1} [33]. Treatment of wastewater involves phosphorus removal by biological or chemical means. This results in a sludge which has high phosphorus concentration. Biologically bound phosphorus is released during sludge digestion, with digester liqours (high phosphorus content) being returned to the head of the WWTP. This continuous cycle means that wastewater treatment is more costly, due to the costs of chemical dosing to remove the phosphorus and due to struvite build up in pipes and digesters.

Since WWTPs already require phosphorus removal, it may be cost effective to introduce phosphorus recovery to this waste stream. As such, the remainder of this dissertation will focus on recovery from wastewater. In Denmark, phosphorus in wastewater amounts to 20-25% of the 11,000 tonnes of phosphorus imported each year.

1.3. WHERE ON THE WASTEWATER TREATMENT PLANT SHOULD RECOVERY OCCUR?

There are a number of places in a WWTP from which phosphorus can be recovered. **Error! Reference source not found.** shows a typical bio-P WWTP. As seen in the figure there are a number of treatment steps by which phosphorus can be removed/recovered. Firstly, wastewater itself can be used. Raw municipal wastewater contains 5-20 mg L^{-1} total phosphorus, some of which is chemically or biologically bound [34]. Raw wastewater also contains a relatively high suspended solids concentration, and contains other objects such as toilet paper, wet wipes, and other waste. Even after screening, which removes larger objects and solids, the phosphorus concentration is relatively low, so extensive treatment would need to occur in order to achieve a desirable phosphorus concentration, or recovery would be inefficient.

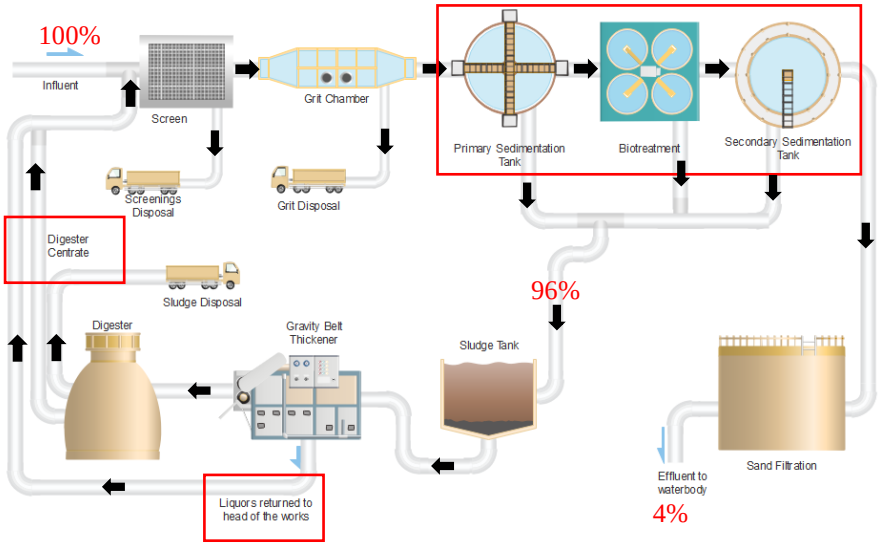

Figure 2 Process flow diagram of a typical bio-P WWTP red boxes highlight area where phosphorus is removed, percentages show the percent of phosphorus present in influent sludge and effluent at Aaby WWTP..

Phosphorus is partly recovered during primary sedimentation; but the phosphorus is biologically or chemically bound. Thus, this fraction of phosphorus cannot be recovered easily, and the concentration is relatively low.

During bio-treatment wastewater is pumped through an aerated tank in which bacteria, which may include phosphate accumulating organisms, treat the raw wastewater, achieving several results:

- Phosphate removal;
- Driving off gases;
- Coagulation of suspended solids;
- Generating a biological floc
- Oxidation of nitrogenous and carbonaceous matter.

Phosphorus is removed by phosphate accumulating organisms and chemical precipitation. Chemical precipitation involves the dosing of a coagulant and mixing. Commonly used coagulants are salts of iron, aluminium, or calcium. Ferric ions and phosphate react slowly, as such lime can be added in order to raise pH, and hasten coagulation. Solids are removed in the secondary sedimentation tank. Consequently, it is not possible to recover phosphate from the liquors as the majority of incoming phosphorus is contained in sludge.

A large fraction of phosphorus in EBPR plants is biologically bound (up to 10-15% [34]) , but the phosphorus is released during aerobic digestion. The amount of phosphorus released can be increased by lowering pH in the digester to between 4 and 6 [35]. Digested sludge is dewatered and the liquors sent to the head of the WWTP for further treatment, the dry solids are often disposed of or burnt to ash and used as fertilizer. Phosphorus can then be recovered from the sludge ash, separating phosphorus from heavy metals in the sludge ash. Digested sludge liquors contain a high concentration of phosphate, usually 75-300 mg L^{-1}, compared to 4-12 mg L^{-1} for influent [36]. Not only does digester centrate contain phosphorus, but it also contains other resources, such as ammonia. Consequently, digester centrate (the liquors from centrifuging digested sludge) may be used as a source of phosphorus.

1.4. METHODS OF PHOSPHORUS RECOVERY CURRENTLY AVAILABLE

There are several phosphorus recovery methods available on the market. Table 2 shows a number of commercially available phosphorus recovery technologies. Some methods have been developed to extract phosphorus from sludge ash. However heavy metal contamination is a commonly mentioned issue when using sludge ashes. Sulzle Kopf reports nickel contamination of 129 mg kg^{-1} ashes, but German consent is only 80 mg L^{-1}. Ravita has solved this issue, and heavy metal concentrations were found to be low, but phosphorus recovery was also lower than that of Sulzle Kopf – 55-63% for Ravita compared to 80% for Sulzle Kopf. Suez Phosphogreen reported low heavy metal contamination, but also has a P recovery of ~50%. As seen in the table, most technologies do not achieve phosphorus recovery higher than 90%. Furthermore, the use of technologies requiring heat, such as incineration of sludge to create sludge ash, has high operational cost. As such, it is necessary to look into developing new recovery methods or making existing processes more efficient.

Figure 3 shows a typical bio-P WWTP, red boxes indicate streams often used for phosphorus recovery. These include sludge (extraction e.g. by acidification), digester centrate or filtrate (precipitation/crystallization), sludge ash (shown as sludge disposal), or digested sludge liquors (digester centrate) (precipitation/crystallization).

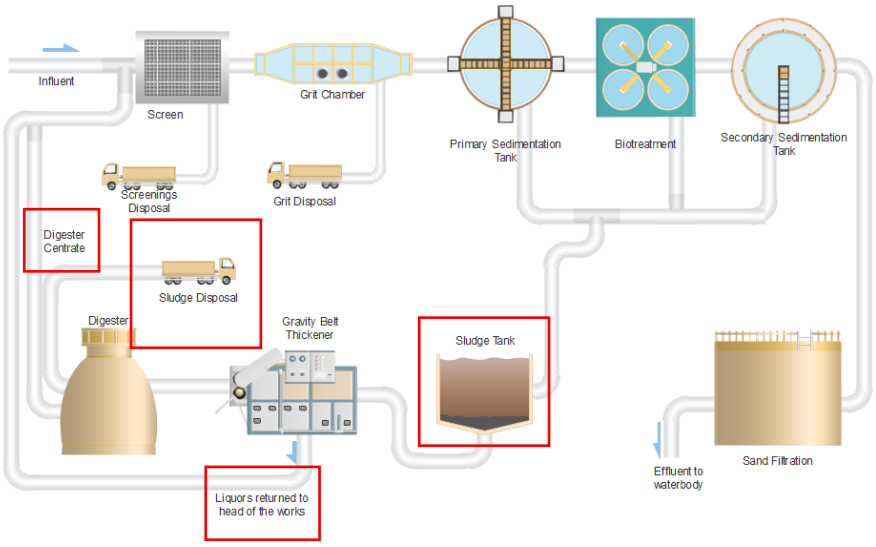

Figure 3 Typical places phosphorus is recovered from wastewater

Table 2 Commercially available P recovery technologies

	Process	Country	Phosphorus Recovery (%)	Method	Ref
Aqueous Phase	EkoBalans	Sweden	>75	Struvite precipitation	[37]
	Suez Phosphogreen	France	~50	Struvite precipitation	[38]
	DHV Crystalactor	Netherlands	85-95	Struvite crystallization	[24]

	Ostara Pearl	Canada	85-95	Struvite crystallization	[24]
	P-RoC	Austria	85-95	Struvite crystallization	[24]
	PRISA	-	85-95	Struvite precipitation/crystallization	[24]
Sewage sludge	Stuttgart process	Germany	>65	Wet chemical leaching	[39]
	Gifhorn process	Not specified	~80	Wet chemical leaching	[40]
	Aqua Reci	Sweden	Not reported	Super critical water oxidation	[41]
	MEPHREC	Germany	~70	Metallurgic melt-gassing	[40]
Sludge ashes	LEACHPHOS	Switzerland	~60-70	Acidic wet-chemical, leaching	[40]
	PASCH	Germany	~60-70	Acidic wet-chemical, leaching	[40]
	RecoPhos	Austria	~85	Acidic wet-chemical, extraction	[40]
	Thermphos	China	~85	Thermo-electrical (produces P_4)	[40]
	Sulzle Kopf	Germany	80	Gasification ashes as P-fertilizer	[42]
	Eliquo Stulz	Germany	80	Sludge ashes	[43]
	Ravita	Finland	55-63	Recovery as phosphoric acid	[44]

	Outotec AshDec	Germany	Not reported	Sludge ashes	[45]
	Ash2Phos	Sweden	90-95	Sludge ashes	[46]

Worldwide, 1.7 million tonnes of incinerated sewage sludge ash (ISSA) is produced annually. The majority of this is produced in North America, Europe, and Japan. While the phosphorus content of ISSA is similar to that of low-grade phosphate ore, most ISSA is sent to landfill. This is partially due to public concerns over pathogen transfer to crops, and accumulation of heavy metals in agricultural soils. Most countries in Europe have regulations to prevent heavy metal contamination of soil. While some concentrate on limiting sludge exposure on certain soils, such as the Safe Sludge Matrix in the UK, others concentrate on creating 'high quality' sludge, i.e. one with low heavy metals content. This is achieved by limiting the concentration of heavy metals in wastewater, by restricting the substances disposed of in sinks etc. both in the home and workplace (i.e labs etc.). [47]

In order to produce ISSA, sludge goes through a number of processes. Firstly, it is thickened to give solids content of 3-8 wt%, and is then dewatered to a solids content of 18-35 wt%. Sewage sludge needs to have a solids content of 28-33 wt% in order to burn auto-thermally. Sludge is incinerated in a fluidized bed incinerator. A sand bed near the bottom of the incinerator helps to avoid temperature spikes in the incinerator. The sand bed tends to have a temperature of 750^{o}C, and the overhead freeboard zone has a temperature of 800-900^{o}C. The incinerator has a residence time of only 1-2 seconds [48], and in this time organic matter is combusted to CO_2 and other trace gases with water removed as vapour. Major components of ISSA are Si, Al, Ca, Fe and P [49]. The concentration of Fe and Al depends greatly on the method of phosphorus removal used, due to Al and Fe use in chemical dosing. [47]

ISSA often has low bioavailability of phosphorus, and contains heavy metals [50–52]. Bioavailability is characterized by a Na/P ratio >1.75 in the starting materials [52], or by a pot experiment, which involves growing plants in soil with known nutrient value, then testing the soil composition and plant growth after a set period of time [53]. Pot experiments are not as accurate as field trials, which can last multiple years [54]. In Germany it was estimated that half of the 19,000 ton year^{-1} ISSA only half is suitable for use [52]. Consequently it requires treatment before use. Two methods of treatment have been widely investigated; these are an electrodialytic process or acid leaching.

Using the electrodialytic process phosphate is concentrated at the anode, and heavy metals at the cathode [55]. The anolyte was found to be 98% phosphorus, and 2% heavy metals. Copper was found to have an 80% removal, but lead and iron

removals were found to be as low as 4 and 6% respectively [55]. Electrodialytic process can take place with or without ion exchange membranes. Using ion exchange membranes has been found to give better separation from heavy metals and 96% phosphorus recovery [56].

Acid leaching involves dissolving ISSA in acid. Takahashi et al. (2001) investigated the use of dissolving ISSA in H_2SO_4 (pH 2). Lead is insoluble in H_2SO_4, and is therefore removed from the product. Phosphorus was then recovered by filtration, and precipitated at pH 10. While the remaining solution was easily disposed of, due to its low salts concentrations, the phosphate product was found to contain heavy metals. [57]

Another study used 0.5 M HCl, and produced 97% struvite purity with low heavy metals concentration. Furthermore, the struvite product was found to have 94% bioavailability. However, in order to achieve this a molar ratio of 1.6:1.6:1 Mg:N:P was required. [58]

Consequently, treatment using this method would either be costly, or risk heavy metal contamination. Furthermore, this method of recovery is only possible if incineration is the usual method of sludge disposal [59].

Extraction via wet chemical leaching takes place by dissolving phosphorus in an acidic (pH < 2) or basic solution. Using acidic wet chemical leaching will give aluminium, calcium, or iron phosphates. It has been found that a ratio of 2.7 to 14.1 mol H^+/mol P is required for phosphorus recovery >66.5% when using ISSA and HCl or H_2SO_4. pH is raised slightly in order to avoid heavy metal removal alongside phosphorus recovery. Heavy metal contamination can be reduced further by precipitating heavy metals with sulphide. This results in the precipitation of Al-P (Ca is precipitated as $CaSO_4$), while heavy metals remain in solution [57]. Since Al-P cannot be used as a fertilizer, further treatment is necessary to create a usable product. This can be achieved by dissolving Al-P in alkaline solution, which causes the precipitation of Ca-P. A minimum of 4 mol OH^-/mol P is required. Ions can then be recovered using an ionic exchanger [60] or filtration [61]. [62]

Alternatively, alkaline wet chemical leaching can be used to produce Ca-P. In this process amphoteric Al-P compounds dissolve, while heavy metals remain in ISSA. pH > 13 can then be used to precipitate a very low impurity Ca-P product using the addition of $CaCl_2$. Waste with low Ca concentration is able to achieve up to 75% phosphorus recovery, however this is dependent on both the Al and Ca concentration. However, if Ca concentration is high, for example due to hard drinking water, only 0-35% phosphorus can be recovered [62].

In Northern Europe water tends to be hard, as such this method of recovery would not be appropriate. Furthermore, the process is energy intensive when producing

ISSA, and requires a large volume of acid/base. This will incur a high cost, and the use of concentrated acids will be considered a health and safety risk/ require special equipment and/ training. As such it may be necessary to use an alternative recovery method, such as struvite crystallization.

The presence of struvite ($MgNH_4PO_4 \cdot 6H_2O$) at WWTPs was first noted in the 1930s, when a crystalline substance was found in sludge supernatant lines [63]. Struvite often forms in pipework and digesters at WWTPs, causing process inefficiency and disruption. However, controlling the precipitation process can produce a fertilizer and reduce struvite blockages in the rest of the WWTP.

Below is the general reaction by which struvite forms [64].

$$Mg^{2+} + NH_4^+ + PO_4^{3-} + 6H_2O \rightleftharpoons MgNH_4PO_4 \cdot 6H_2O \quad pK = 13.26$$

Solubility product

$$K_{str} = [Mg^{2+}][NH_4^+][PO_4^{3-}] = 2.51\ 10^{-13}\ M^3 \text{ [65]}$$

Doyle and Parsons (2002) compared the solubility product of struvite from a number of papers, and found that precipitation occurs above pH = 8 [66–70], and calcium phosphate apatite occurs at pH>9.5 [64]. Above pH = 9.5 ammonium removal decreases, due to the change in ammonium to ammonia with increasing pH [67].

The conditional solubility product for struvite can be calculated from Equation 1 or Equation 2

Equation 1

$$K'_{str} = \alpha_{Mg2+} C_{Mg} \alpha_{NH4+} C_N \alpha_{PO43-} C_P$$

Equation 2

$$K'_{str} = K_{str} \cdot (\alpha_{PO_4^{3-}} \cdot \alpha_{NH_4^+} \cdot \alpha_{Mg^{2+}})^{-1}$$

Where C_{Mg}, C_N, and C_P are the dissolved concentration of magnesium, ammonium and phosphate respectively, and α_{Mg2+}, α_{NH4+}, and α_{PO43-} are the fraction of magnesium as Mg^{2+}, ammonium as NH_4^+ and phosphate as PO_4^{3-}.

A number of reactions take place for struvite to form, these are shown below.

Magnesium forms metal hydroxides

$MgOH^+$ (aq) $Mg^{2+}(aq) + H_2O(l) \rightleftharpoons MgOH(aq) + H^+(aq)$, $\log K_{Mg1} = -11.4$

$Mg(OH)_2$ (aq) $MgOH(aq) + H_2O(l) \rightleftharpoons Mg(OH)_2(aq) + H^+(aq)$, $\log K_{Mg2} = -4.4$

Thus,

$$\alpha_{Mg^{2+}} = \frac{[Mg^{2+}]}{[Mg^{2+}] + [MgOH^+] + [Mg(OH)_2]}$$

$$\alpha_{Mg^{2+}} = \frac{[Mg^{2+}]}{[Mg^{2+}] + [Mg^{2+}] \cdot \frac{K_{Mg1}}{[H^+]} + [Mg^{2+}] \cdot K_{Mg1} \cdot \frac{K_{Mg2}}{[H^+]^2}}$$

$$\boldsymbol{\alpha_{Mg^{2+}}} = \frac{1}{1 + \frac{K_{Mg1}}{[H^+]} + K_{Mg1} \cdot \frac{K_{Mg2}}{[H^+]^2}}$$

Ammonium forms ammonia at high pH;

$NH_4^+(aq) + H_2O(l) \rightleftharpoons NH_3(aq) + H_3O^+(aq)$, $\log K_{N1} = -9.3$

$$\alpha_{NH_4^+} = \frac{[NH_4^+]}{[NH_4^+] + [NH_3]}$$

$$\alpha_{NH_4^+} = \frac{1}{1 + \frac{K_{N1}}{[H^+]}}$$

Finally the phosphate reaction;

H_3PO_4 (aq) $H_3PO_4(aq) + H_2O(l) \rightleftharpoons H_2PO_4^-(aq) + H_3O^+(aq)$, $\log K_{P1} = -2.1$

$H_2PO_4^-$ (aq) $H_2PO_4^-(aq) + H_2O(l) \rightleftharpoons HPO_4^{2-}(aq) + H_3O^+(aq)$, $\log K_{P2} = -7.2$

HPO_4^{2-} (aq) $HPO_4^{2-}(aq) + H_2O(l) \rightleftharpoons PO_4^{3-}(aq) + H_3O^+(aq)$, $\log K_{P3} = -12.3$

$$\alpha_{PO_4^{3-}} = \frac{[Mg^{2+}]}{[H_3PO_4] + [H_2PO_4^-] + [HPO_3^{2-}] + [PO_4^{3-}]}$$

$$\alpha_{PO_4^{3-}} = \frac{1}{[H^+]^3 \cdot \frac{1}{K_{P3}} \cdot \frac{1}{K_{P2}} \cdot \frac{1}{K_{P1}} + [H^+]^2 \cdot \frac{1}{K_{P3}} \cdot \frac{1}{K_{P2}} + [H^+] \cdot \frac{1}{K_{P3}} + 1}$$

The solubility constant describes the dissociation of molecules in aqueous solutions, as with the struvite equilibrium shown previously. Figure 4 shows the log of the solubility product for struvite, as seen in the figure, the solubility is lowest around pH 10, which as previously discussed, is in the optimal range for struvite recovery.

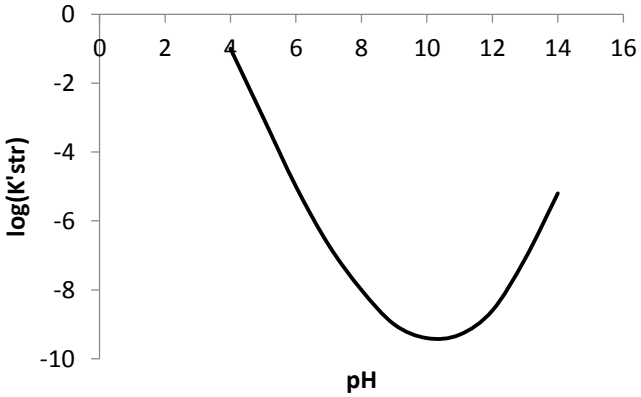

Figure 4 Log of the struvite solubility product as a function of pH

While struvite precipitates most efficiently between pH 9 and 11, it is often precipitated between pH 7 and 8 in order to avoid the co-precipitation of other salts and heavy metals alongside struvite. As such, at pH 7-8:

$$Mg^{2+} + NH_4^+ + HPO_4^{2-} + 6H_2O \rightarrow MgNH_4PO_4 \cdot 6H_2O + H^+$$

Sodium hydroxide (NaOH) is usually dosed into the rector in order to control the pH, and prevent acidification. However, aeration can be used to strip carbon dioxide, which also increases pH. [64]

A fluidised bed reactor is commonly used for struvite recovery. In this, a column reactor is used, with the addition of a seed material, upon which struvite precipitates (commonly used seed materials can be seen in Table 3). The feed solution is pumped into the base of the reactor, along with NaOH and a source of magnesium.

Large particles form in the bottom of the reactor, where saturation is highest, while smaller particles form higher in the column. As these increase in size they fall to lower levels in the reactor, aiding the formation of larger particles. Effluent is taken out of the top of the reactor and returned to the head of the WWTP, while a recycle loop takes P-rich waste from high in the reactor column back to the base of the reactor. A simple schematic of this can be seen in Figure 5.

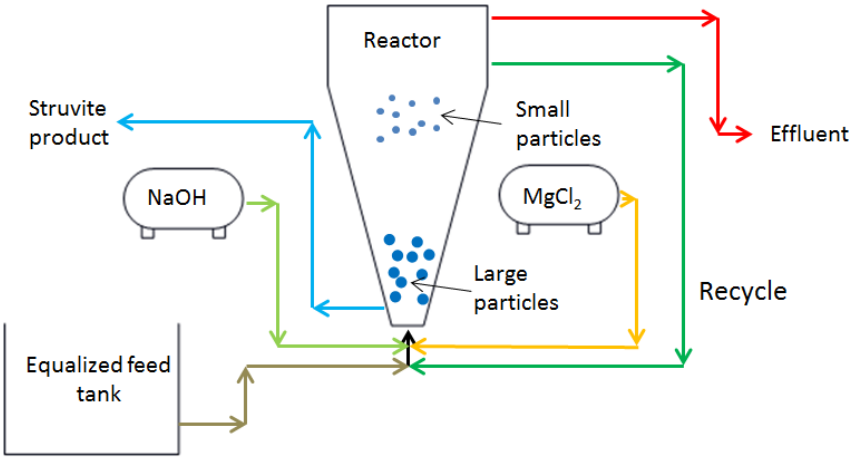

Figure 5 Fluidised struvite reactor

There are three stages to precipitation:

- Saturation; this occurs with the addition of Mg^{+}, and pH adjustment using NaOH or aeration. Under saturated conditions struvite will spontaneously precipitate.
- Nucleation; is the initial stage in crystal growth, it involves the coming together of particles in a particular pattern, typical of a crystalline solid, this forms the basis on which other particles deposit, leading to crystal growth. I.e. small particles in a reactor.
- Crystal growth; occurs when a crystal becomes larger by addition of ions in the crystal lattice, as with the growth of larger particles at the base of the reactor.

Since magnesium concentration tends to be low in wastewater, it is often dosed to the reactor in order to ensure maximum phosphate recovery, usually in the form $MgCl_2$ or $Mg(OH)_2$. In order to achieve a phosphate recovery of ~85% a P:Mg ratio of 1:1.3 is required, as shown in Figure 6. Magnesium chloride is one of the most costly parts of the process. Seawater contains Mg and can be used as Mg source but

also contains high concentration of chloride, which have to be reduced prior to use [71].

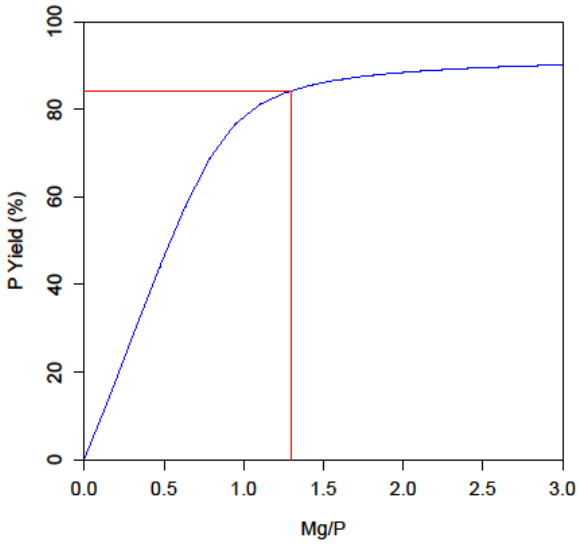

Figure 6 P yield as a function of Mg/P ratio, calculated using MINTEQ (Ammonium = 50 mgL^{-1}, phosphate = 3.16 mgL^{-1}, Magnesium =4.108 mgL^{-1}, pH=7.5)

Table 3 shows results from some studies into struvite precipitation. As seen in the table, most studies utilize aeration for pH adjustment. Aeration provides a more effective phosphate recovery (>80%), than using NaOH (62-97%). This is due to the removal of carbonate during aeration. A seed material is sometimes used to aid struvite precipitation. Seed materials are often used when using a fluidized bed reactor. This is a material on which struvite can precipitate. Seed materials can be a number of substances, including; quartz [72], silica sand [72], pumice [73], clay [74], and metals [75].

Table 3 Struvite precipitation in literature

Method	**Phosphate Recovery (%)**	**Seed Material**	**Influent**	**Ref**
Aeration	>80	Struvite crystals	Digester liquors	[76]

Aeration	84.1-90.5	-	Swine wastewater	[77]
Aeration	80	-	Belt press liquors	[78]
Aeration	-	Wire mesh	Swine wastewater	[75]
Aeration	80	-	Digested sludge	[79]
Aeration	62-81	Quartz	Digester supernatant	[72]
Aeration and 60% magnesium hydroxide slurry	94	500g crushed and sieved (1mm) struvite	Digester centrate	[80]
Aeration and seawater and bittern as Mg^+ source	97.1-99.5	-	Urine	[81]
Mg^+ from seawater	>70	-	Belt press liquors	[82]
$MgCl_2$ and pH adjustment using NaOH	97	-	Digester centrate	[83]
pH adjustment using NaOH	75-92	-	Synthetic wastewater	[84]
pH adjustment using NaOH	62	-	Synthetic wastewater	[85]
pH adjustment with NaOH	>91.8	-	Sludge	[86]

Going forward phosphorus recovery for struvite crystallization will be investigated. This is due to the lower cost of struvite recovery compared to that of, for example, sludge ashes, which require high energy input. Furthermore, struvite is a suitable fertilizer which does not require additional processing, and the combination of nitrogen phosphorus and magnesium is highly desirable in agriculture. Furthermore, struvite is already found in wastewater treatment plants, and is therefore relatively simple to recover from wastewater compared to other recoverable compounds.

CHAPTER 2. MEMBRANE TECHNOLOGY FOR PHOSPHORUS RECOVERY AS STRUVITE

Membrane technology uses a selective barrier (membrane) to separate one or more components of a stream by sieving, sorption or diffusion. Membranes are usually selective to particle size, molecular weight, or charge. Membrane performance is determined by:

- Flux (movement of permeate through the membrane)
- Selectivity
- Stability (mechanical, chemical, or thermal)
- Fouling
- Cost.

There are two types of membrane filtration; dead-end and cross-flow. During dead-end filtration the feed flows perpendicular to the membrane and all water introduced to the system passes through the membrane. This causes a thick build-up of particles on the membrane surface, which can become dense when applying hydraulic pressure, known as a cake layer. This can hinder permeate flux, resulting in flux decline over time. Consequently dead-end filtration requires regular membrane cleaning, or replacement, as such it is also known as batch filtration. A simple schematic of dead-end filtration can be seen in Figure 7.[87]

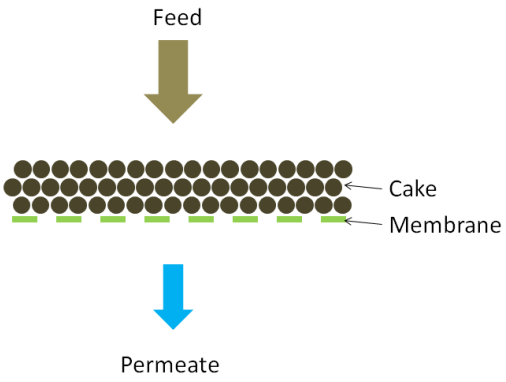

Figure 7 Dead-end filtration

Cross-flow filtration uses a flow tangential to the membrane. As the feed flows across the membrane surface the pressure difference causes components smaller than the membrane pore size to pass the membrane (permeate), the remaining feed then flows back to the feed reservoir, or to another location, this is known as the retentate. This setup can be seen in Figure 8. Cross-flow filtration is useful for applications where the feed requires concentration, rather than gaining a clean permeate. The addition of the retentate stream encourages a lesser degree of fouling (smaller cake formation) as the solids are taken with the flow back to the feed reservoir. Unlike dead-end filtration, cross-flow filtration allows for continuous use, as cake can be removed by increasing the flow rate of the feed.[88]

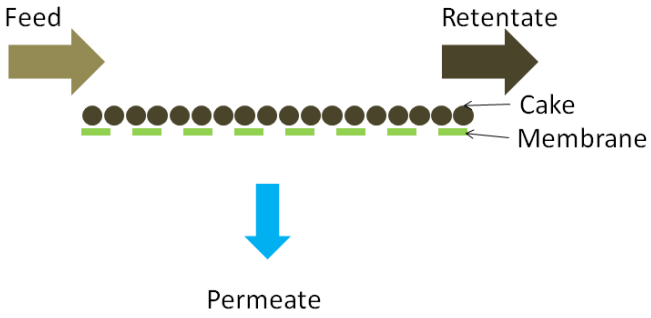

Figure 8 Cross-flow filtration

Membrane pore size varies depending on which type of membrane is used. This enables the user to determine which membrane is best for their application, i.e, to retain whatever feed component is necessary. Membranes with smaller pore size are more likely to foul as the membrane rejects a greater number of feed components, and a larger pressure is required to force permeate through smaller pores. Figure 9 shows the pore size distribution of various membrane technologies.

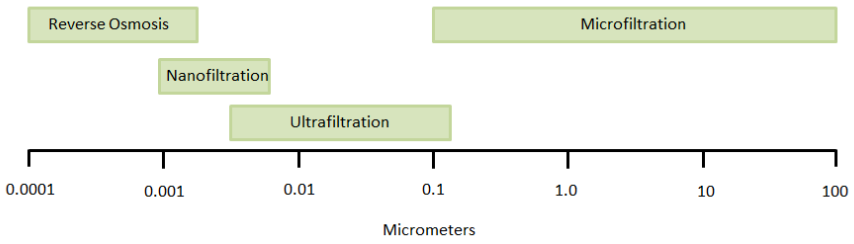

Figure 9 Membrane pore size distribution (pressure driven processes)

While the most common driving force is pressure gradient (as with reverse osmosis, nanofiltration, ultrafiltration, and microfiltration) other driving forces can be used. Forward osmosis utilizes an osmotic pressure difference; this involves the movement of water from a less concentrated solution to a more concentrated solution. Electrodialysis uses an electrical field gradient, which draws ions through ion selective membrane. Lastly, temperature can be used, as in membrane distillation.

The following sections outline the two technologies used for phosphorus recovery in this dissertation.

2.1. FORWARD OSMOSIS

Struvite crystallization can be made more efficient (and cost effective) by concentrating the phosphorus and thereby reducing the quantity of magnesium needed, ie. reducing the P:Mg ratio from 1:1.3 to 1:1. From calculations carried out in MINTEQ, it is possible to achieve this by increasing the phosphorus and magnesium concentration. Figure 10 shows the recovery achievable for digester centrate, and digester centrate concentrated 3-fold. Digester centrate is used as a feed solution due to its high phosphorus concentration relative to other streams on the WWTP. As seen in the figure, once concentrated, a greater phosphorus yield is possible with less added magnesium.

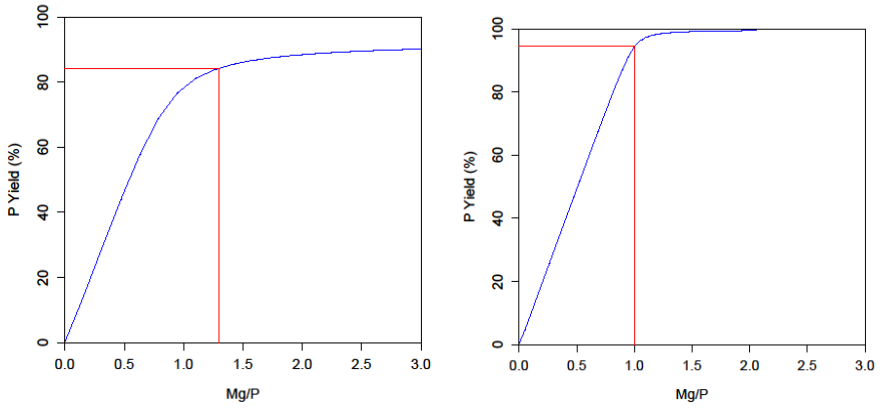

Figure 10 P Yield as struvite for (a) un-concentrated digester centrate (Ammonium = 50 mgL^{-1}, phosphate = 3.16 mgL^{-1}, Magnesium = 4.108 mgL^{-1}, pH=7.5), (b) digester centrate concentrated 3-fold (Ammonium = 150 mgL^{-1}, phosphate = 9.48 mgL^{-1}, Magnesium = 12.324 mgL^{-1}, pH=7.5)

Forward osmosis is a membrane technology by which water is moved from a solution of low osmotic potential to a solution of high osmotic potential through a

water permeable membrane [89], as shown in Figure 11. No hydraulic pressure is required, which reduces fouling and energy costs [90].

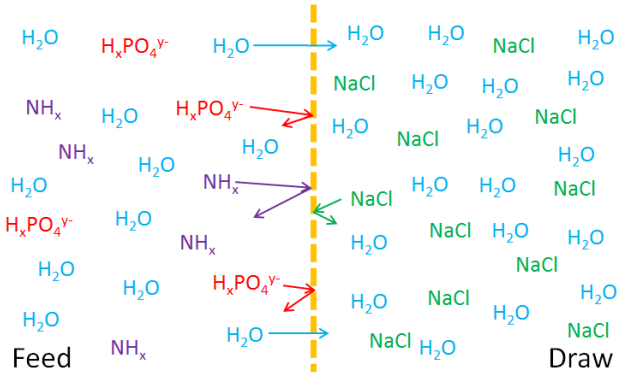

Figure 11 Simplified schematic of forward osmosis process

Figure 11 shows a simplified example of how forward osmosis works. As seen in the figure, draw solution consists of NaCl solution, while the feed (in this case digester centrate) contains water and components such as phosphoric acid ($H_xPO_4^{y-}$) or ammoniacal nitrogen (NH_x) (other components are also rejected by the membrane, but these have been left out of the simplified schematic), which are rejected by the membrane. On the other hand water passes through the membrane, from feed to draw.

Forward osmosis membrane comprise of a porous support layer and thin active layer, which rejects contaminants, such as phosphate or ammonium. Membranes can be orientated with the active layer facing either the draw solution (AL-DS) or feed solution (AL-FS), as shown in Figure 12.

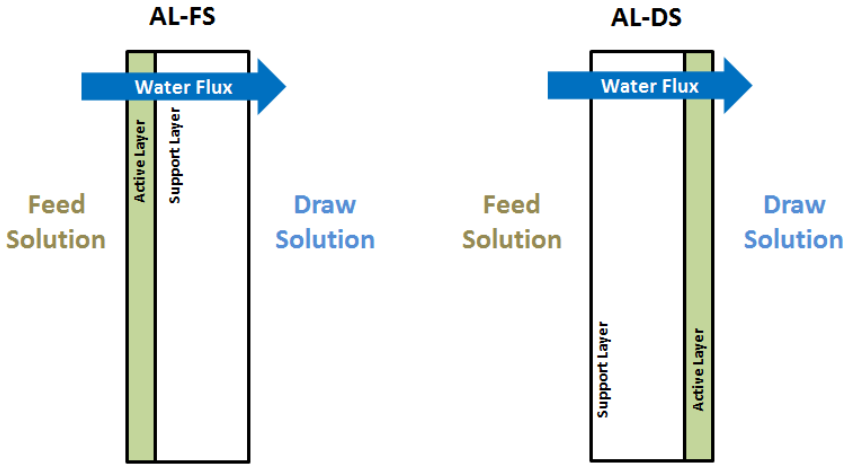

Figure 12 Simple diagram showing membrane orientation.

2.1.1. FOULING, SCALING, AND CONCENTRATION POLARIZATION

There are certain phenomena which inhibit/reduce water flux through the membrane. These are concentration polarisation, reverse salt flux, fouling, and for some processes scaling.

Table 4 Types of concentration polarization

	Dilutive	**Concentrative**
Internal	If AL-FS membrane orientation is used, the draw solution enters the porous support layer. Water then moves through the membrane diluting the draw solution in the support layer. [91]	Occurs when AL-DS membrane orientation is used. The feed solution enters the porous support layer of the membrane and water diffuses across the dense active layer, but salt in the feed is trapped in the support layer leading to an increased concentration on the feed side of the active layer. [92]
External	Occurs when the draw solution concentration is diluted by	Occurs when there is a build-up of solutes on the active layer surface

	permeate water at the membrane surface.	(similar to that in pressure driven membrane processes)

Concentration polarization occurs in two forms; internal and external, with both having dilutive or concentrative forms.

Table 4 describes all four of these forms of concentration polarization. The type of internal concentration polarization depends on membrane orientation, i.e whether the active layer of the membrane is AL-FS or AL-DS [93] and are depicted in Figure 13. Concentration polarization reduces the osmotic pressure difference between the feed and draw solutions, thus reducing the driving force for water flux. Therefore, it has a negative impact on water flux. External concentration polarization can be mitigated by ensuring turbulent flow e.g. via the application of spacers adjacent to the membrane or high cross-flow of water [94]. Internal concentration polarization can only be reduced by decreasing the thickness of the membrane support layer.

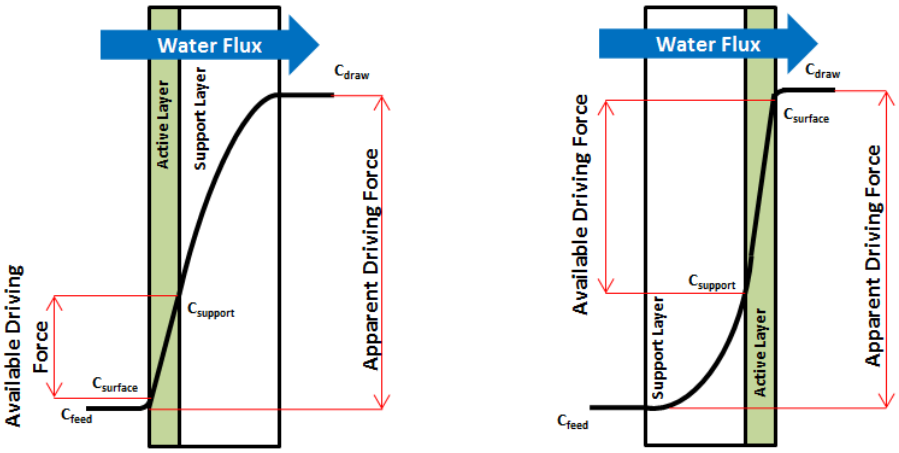

Figure 13 Diagram of dilutive (left) and concentrative (right) internal concentration polarization.

The use of more concentrated draw solutions increases the severity of internal concentration polarization [95], as this encourages a higher water flux. This in turn causes a more concentrated or dilute layer to form within the porous membrane support layer (depending on membrane orientation). Increasing support layer thickness also causes more severe internal concentration polarization [96], as seen when using reverse osmosis membranes in forward osmosis mode [97] (reverse osmosis membranes are thicker than forward osmosis membranes). Other than using

less concentrated draw solutions, increasing feed solution temperature [92], and ultrasound [98] have been found to aid in mitigating internal concentration polarization.

There are a number of equations used to model the effect of concentration polarization on water flux. Water flux (J_w (L m^{-2} h^{-1} (LMH))) can be calculated using Equation 3, where A is the water permeability coefficient (LMH bar^{-1}), $\pi_{D,b}$ is the osmotic pressure of the draw solution (bar) and $\pi_{F,b}$ is the osmotic pressure of the feed solution (bar).

Equation 3

$$J_w = A(\pi_{D,b} - \pi_{F,b})$$

Equation 3 assumes that salt does not cross the membrane, and there is an absence of dilutive or concentrative ECP. This can only be used when permeate flux is very low, for higher flux, the equation is modified to form Equation 4, which includes the effects of concentrative and dilutive ECP. k is the mass transfer coefficient, as per Equation 5.[92]

Equation 4

$$J_w = A\left[\pi_{D,b}\exp\left(-\frac{J_w}{k}\right) - \pi_{F,b}\exp\left(\frac{J_w}{k}\right)\right]$$

Equation 5

$k = \frac{ShD}{d_h}$ where; $Sh = 1.85\left(ReSc\frac{d_h}{L}\right)^{0.33}$ (laminar flow)

$$Sh = 0.04Re^{0.75}Sc^{0.33} \text{ (turbulent flow)}$$

Equation 6 can be used to calculate the effect of concentrative ICP and dilutive ECP on permeate flux when membrane is AL-DS. K, how easily a solute can diffuse in and out of the support layer, is defined by Equation 7. K is a measure of the severity of ICP. B is the salt permeability coefficient; τ is the tortuosity of the support layer, t_m the thickness and ε the membrane porosity. B can be ignored when using a membrane with high salt rejection and high permeate flux.[92]

Equation 6

$$J_w = A\left[\pi_{D,b}\exp\left(-\frac{J_w}{k}\right) - \pi_{F,b}\exp(J_wK)\right]$$

Equation 7

$$K = \left(\frac{1}{J_w}\right) \ln \frac{B + A\pi_{D,m} - J_w}{B + A\pi_{F,b}} = \frac{t_m \tau}{D\varepsilon}$$

For AL-FS configurations, Equation 8 can be used to calculate dilutive ICP and concentrative ECP. For this case, K can be determined using Equation 9.

Equation 8

$$J_w = A\left[\pi_{D,b} \exp(-J_w K) - \pi_{F,b} \exp\left(\frac{J_w}{k}\right)\right]$$

Equation 9

$$K = \left(\frac{1}{J_w}\right) \ln \frac{B + A\pi_{D,b}}{B + J_w + A\pi_{F,m}}$$

Equation 4 is suitable for use when using a symmetric membrane. However, most forward osmosis membranes are asymmetric, as such, only Equation 6 and Equation 8 should be used to calculate the effects of concentration polarization. [92]

When using digester centrate as a feed solution, fouling occurs [99] due to a build-up of bacterial clusters, biopolymers, and inorganic scales [100]. Fouling in forward osmosis tends to be less dense than that of pressure driven membrane processes such as reverse osmosis [101–103]. Reverse salt flux (the flux of salts from the draw solution to feed solution) exacerbates the cake enhanced osmotic pressure in the fouling layer, leading to an elevated osmotic pressure on the feed side. This results in a lower water flux [104] and may potentially also induce fouling. In forward osmosis, fouling has been found to be negligible [89,105], or easily reversed by cleaning [106–109], however limited studies have been carried out on untreated digester centrate. Methods of cleaning include; increasing cross flow velocity (from 8.5 to 25.6 cm s^{-1} [109]), chemical cleaning [108], or osmotic backwash [107]. Chemical and physical cleaning have been found to restore water flux to 96% and 90% of the initial water flux, respectively [108]. Scaling is a form of inorganic fouling and occurs when salt precipitates on the membrane surface [110]. It occurs when the feed solution reaches supersaturation, which triggers precipitation [111]. Scaling can be mitigated by pH adjustment [112].

2.1.2. DRAW SOLUTION SELECTION

Ideal draw solutions have a reasonably higher osmotic pressure than the feed solution [113]; however, finding a suitable draw solution is one of the main challenges in forward osmosis. Too low an osmotic pressure and the flux will be low and the feed solution will not be adequately concentrated (for VCR = 3 osmotic pressure of digester centrate at Aaby WWTP is ~15 bar (Paper 1)) too high, and the process will experience an increase in concentration polarization [96].

Many studies have been carried out to find suitable draw solutions for forward osmosis, the necessary traits of such a solution are; easily recoverable, cost efficient, and have a relatively low molecular weight, which leads to high osmotic pressure [113]. Existing studies have focused on the use of fertilizer [114–116], hydrogels [117–120], $MgCl_2$ [96,121], and NaCl [121–126] as draw solution. NaCl solution is the most widely used draw solution; however, this requires using another membrane process, such as reverse osmosis, to recover initial draw solution concentration.

These draw solutions require treatment post forward osmosis. This incurs a further cost for treatment. However, there are many sources of salt solutions readily available in nature, the most prevalent of which is seawater, and includes salt lakes, such as the Dead Sea. These naturally occurring salt water sources can be used a draw solution, then, providing there is not high contamination from the feed solution, can be discharged without treatment [58]. Furthermore, salt solutions are a common side product of the food production industry, cheese brine being a commonly known example, and are costly to dispose of.

Table 5 shows some of the draw solutions used in recent studies. As seen in the table, osmotic pressures of the tested draw solutions range from 14 bar to over 200 bar. The osmotic pressure of digester centrate is 1.8 bar [124] (approximately, depending on treatment plant, time of year etc.), as such, all draw solutions in Table 5 are capable of treating digester centrate. However, all exhibit a reverse salt flux, which lowers the effectiveness of the draw solution by raising osmotic pressure in the feed, and leads to the potential for ions to diffuse from feed to draw, thus losing resources to be recovered, or contaminating water produced during forward osmosis desalination. Consequently, it is necessary to understand the mechanism by which reverse salt flux occurs for particular membranes, and if it affects the rejection of ions in the feed, such as ammonium, which has been highlighted as an issue for concentration of wastewater [108,127].

Solute flux, J_s (mol m^{-2} h^{-1}), was calculated with the following equation:

Equation 10

$$J_s = \frac{C_{s,F,initial}V_{initial} - C_{s,F,final}V_{final}}{A_m * t}$$

where $C_{s,F,initial}$ and $C_{s,F,final}$ are the initial and final feed solute concentrations (mol), respectively, A_m is the effective membrane area (m^2), and t is the time in hours. J_s can then be used in Equation 11 to calculate solute rejection.

Equation 11

$$R\ (\%) = \left(1 - \frac{J_s}{J_w C_{Feed}}\right) * 100$$

Table 5 Draw solutions used in forward osmosis

Draw Solution	Concentration (M)	Membrane	Osmotic Pressure (bar)	Reverse Salt Flux (gMH)	Salt Rejection (%)	Ref
Magnesium Acetate	0.54-1.85	CTA	14-42	0.63-1.06	-	[128]
Sodium propionate	0.32-1.06	CTA	14-42	0.8-2.29	-	
Sodium acetate	0.52-1.69	CTA	14-42	1.5-3.55	-	
Sodium formate	0.32-1.03	CTA	14-42	3.86-7.63	-	
EDTA sodium salt	0.7	CTA	-	0.17-0.3	-	[129]
Ammonia-carbon dioxide	1.1-6	CTA	48.5-252.8	-	95-99	[113]

NaCl	0.05-1.5	TFC	-	-	<90	[130]
KCl	2	CA	90.5	59.6	-	[114]
$NaNO_3$	2	CA	82.2	84.9	-	
NH_4NO_3	2	CA	65.8	227.9*	-	

*Initial values given in mmol m^{-2} s^{-1}, hence reverse salt flux higher than initial concentration

If the feed solution requires concentrating beyond the capabilities of the draw solution or the flux is too low, pressure assisted osmosis (PAO) can be used. PAO involves the addition of pressure to the feed side of forward osmosis setup, as show in Figure 14. This allows the concentration of the feed solution above that of osmotic equilibrium [131], i.e. the feed will have an osmotic pressure higher than the draw solution after treatment.

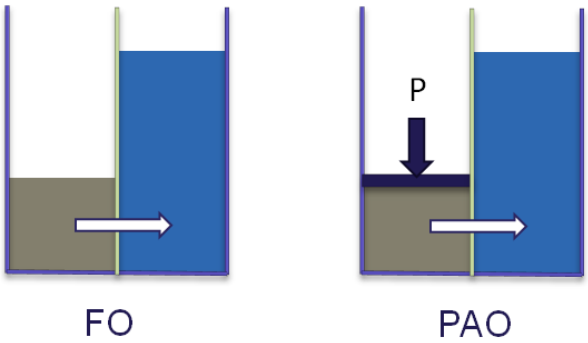

Figure 14 Simplified schematic of FO and PAO

Further dilution of the draw solution has benefits for draw solution disposal or regeneration. When using a fertilizer draw solution it is possible to dilute the draw solution to a suitable concentration for direct fertigation [131], which would need diluting when using traditional forward osmosis. Draw solution regeneration using reverse osmosis is more energy efficient when using PAO, as the draw solution is highly diluted, which reduces the fouling propensity when using reverse osmosis [132]. Water flux increased 9% and 29% for 2 and 4 bar applied pressure respectively [133]. For 10 bar applied pressure water flux increased ~x20 times, whereas an increase in draw solution concentration, from 0.1 M to 3 M $(NH_4)_2SO_4$ corresponded to an water flux increase of 38% [131].

2.1.3. REGENERATION OF DRAW SOLUTION

After the concentration of the feed solution, the draw solution is diluted. In order to reuse draw solution, and recover water, it is necessary to regenerate them by removing water, and increasing the concentration once more. This is usually carried out using reverse osmosis [96,121,134], nanofiltration [135,136], ultrafiltration [137], or membrane distillation [138], depending on the draw solution used. Other thermal processes, such as heating an ammonia-carbon dioxide draw solution to 60°C to recover the ammonia and carbon dioxide [139], have been used, however these have been found to be energy demanding, and costly [140].

As discussed in the previous section, 100% rejection of the draw is rarely, if ever, achieved. Regeneration of the draw solution also offers another opportunity for loss of initial draw solution concentration. Table 6 shows the rejection of the most commonly used draw solution regeneration methods. Membrane distillation has the highest rejection; however, its initial/setup costs were high. Nanofiltration had variations in rejection (99.7% vs 35.5%) for the same membrane; as such it may not be reliable. This can be explained, as nanofiltration is not selective for monovalent salts (i.e. brackish water), and as such can only be used for certain draw solutions. Reverse osmosis has the highest overall rejection, with all draw solutions being rejected >98.7%.

Table 6 Draw solution rejection during regeneration

Regeneration Method	**Draw solution**	**Rejection (%)**	**Ref.**
Reverse Osmosis	Magnesium acetate	>99	[128]
	Magnesium formate	98.7	
	Sodium acetate	>99	
	Sodium propionate	>99	
	Sodium chloride	98.9	
Nanofiltration	Na_2SO_4	97.7	[136]

	Brackish water	35.5	
Ultrafiltration	Super hydrophilic nanoparticles	90.5-92.7	[137]
Membrane distillation	Sodium Chloride	~100	[141]

2.1.4. TYPES OF MEMBRANES

Forward osmosis membrane have three key properties; low structural parameter (maximize water flux, S = thickness × tortuosity / porosity for the support layer [142]), high selectivity, low reverse salt flux [143]. Conventionally, reverse osmosis membranes, with thinner support layers, have been used for forward osmosis application. These membranes have a cellulose triacetate (CTA) or thin film composite (TFC) active layer, and a porous support structure (usually polysulfone or polyethersulfone). The active layer is usually formed by inter-facial polymerization and has a thickness of 100-200 µm.

However, a new generation of membranes are being utilized, with promising results, these membranes make use of biomimetic active layers. These membranes utilize aquaporin proteins, which are highly selective, resulting in high rejection. A comparison of commercially available membranes can be found in Table 7. Further discussion on water flux, ammonia and phosphorus rejection, can be found in section 2.1.5.

Table 7 Comparison of commercially available membranes (from supplier data sheets and press releases)

Supplier	**Membrane Type**	**Pure water flux (LMH) using 1M NaCl draw solution**	**Operation pH range**	**Reverse draw solute Flux (gMH)**
Aquaporin A/S	Biomimetic	7	2-11	<2.5
Porifera	TFC	22-27	2-11	4.4-16.2
HTI	TFC	20	2-12	82

	CTA	9	Not Reported	Not Reported
$FTSH_2O$	CTA	Not Reported	3-7	Not Reported

2.1.5. MEMBRANE PERFORMANCE

Water flux can be affected by a number of parameters other than just the type of membrane used. The draw and feed solution used can greatly affect the water flux due to osmotic pressure difference, fouling, scaling or concentration polarization. Since different studies use different draw solutions it is beneficial to compare water transport across the membrane by comparison of water permeability (LMH bar^{-1}), as per Equation 3. Osmotic pressure of digester centrate is 1.8 bar and water permeability has been found to be 0.28 LMH bar^{-1} when using digester centrate feed solution and TFC forward osmosis membrane [124].

Figure 15 shows reported membrane permeability for TFC, CTA, biomimetic, and nanocomposite membranes. As seen in the figure, most reported water permeability fall between 0.14-0.3 LMH bar^{-1}. This is typically true of traditional membranes (TFC and CTA). However, recently new membranes have been developed, and these membranes have higher water permeability [144,145]. These membranes rely on altering the surface of the membrane with ester substrates or nanocomposite fibres. Goh et al. (2013) fabricated a multi-walled carbon nanotube membrane (CNT) membrane which achieved 4.48 LMH bar^{-1} [146].

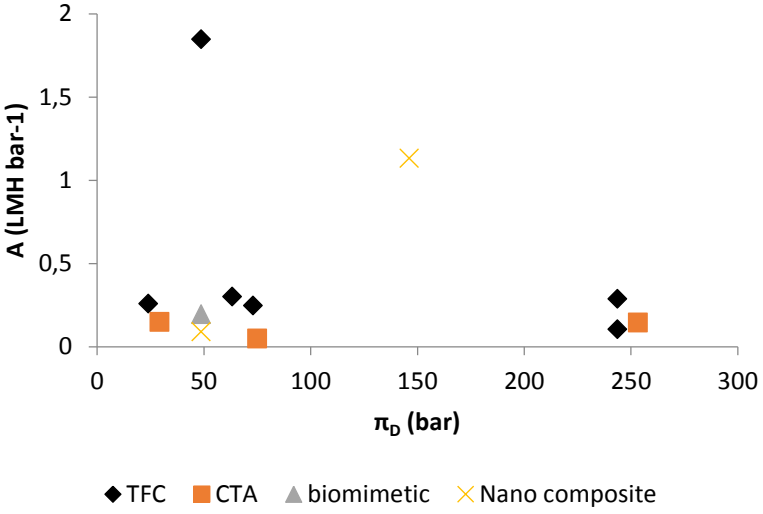

Figure 15 Water Permeability (A) for increasing draw solution osmotic pressure (π_D) for TFC [96,101,144,147,148], CTA [113,149], biomimetic [150], and nanocomposite membranes [145,151].

When recovering resources, it is essential to have a membrane with a low permeability of resources such as ammonia and phosphorus. Membrane permeability has been studied extensively in forward osmosis, with most studies using membranes supplied by HTI [99,123,152,153].

While most studies found a near complete rejection of phosphate [154], >92% [149,152,153], ammonia rejection is still much lower (calculated using Equation 11). Rejection of ammoniacal nitrogen has been measured to be 62-93.3% [108,127] for CTA membranes in forward osmosis treatment of reject water [155]. Ammoniacal nitrogen has potential to cause eutrophication if discharged to watercourses [156], and in drinking water ammoniacal nitrogen in excess of 0.2 mg L^{-1} will cause odour and taste issues [157]. In addition, low rejection of ammoniacal nitrogen results in loss of nutrient to be recovered and contamination of the draw solution [158], which then may have to be treated prior to discharge [159]. Ammoniacal nitrogen has a small hydrated/molecular radius (330 pm for ammonium and 180 pm for ammonia [160]), consequently it can pass the membrane with greater ease than larger ions. Ammonium has been found to aid reverse salt flux by acting as a co-ion for reverse sodium flux [97,161], while ammonia has been seen to diffuse across the membrane, aided by its small size and neutrality [97,162].

2.2. ELECTRODIALYSIS AND SELECTIVE ELECTRODIALYSIS

Since wastewater contains a large quantity of biological contaminants it could be beneficial to create a phosphorus product which does not contain any potential hazards. Electrodialysis/selectrodialysis is an alternative technology to forward osmosis, though which phosphorus is extracted from the feed (diluate), creating a more 'pure' product stream than forward osmosis.

Electrodialysis involves the movement of ions across selectively permeable membranes via the application of potential difference across the membrane stack. A typical stack consists of diluate, concentrate, brine, and electrode rinse, as shown in Figure 16. Membranes are selective towards anions or cations, and are used in an alternating configuration, separating the different solutions. Net spacers separate the membranes, allowing greater turbulence, reducing concentration polarisation. Since the process relies on charge to move ions, uncharged compounds are unaffected.

Diluate is the solution from which ions are to be recovered; the concentrate is the stream in which ions are recovered, and the electrode rinse is usually 20 g L^{-1} Na_2SO_4, which protects the electrodes.

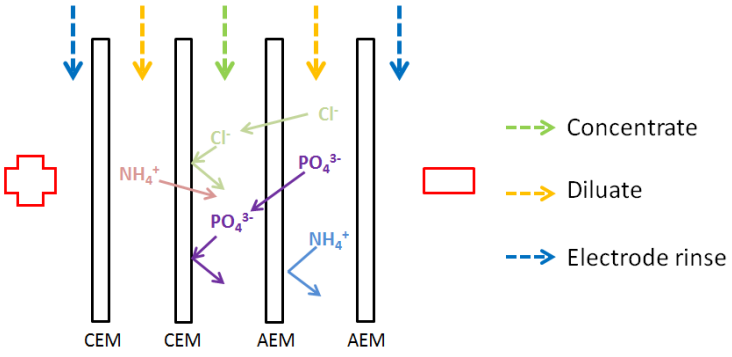

Figure 16 Example electrodialysis set-up using anion exchange membrane (AEM) and cation exchange membrane (CEM)

Selective electrodialysis (selectrodialysis) uses a similar process, but utilizes membranes which are selective to charge (i.e. monovalent or multivalent); an example for phosphorus recovery can be seen in Figure 17. Selectrodialysis also makes use of a brine solution; this enables monovalent ions to pass out of the concentrate if they are not required in the concentrate. Since there can be many different combinations of membranes there are many possibilities to improve the quality of the concentrate product.

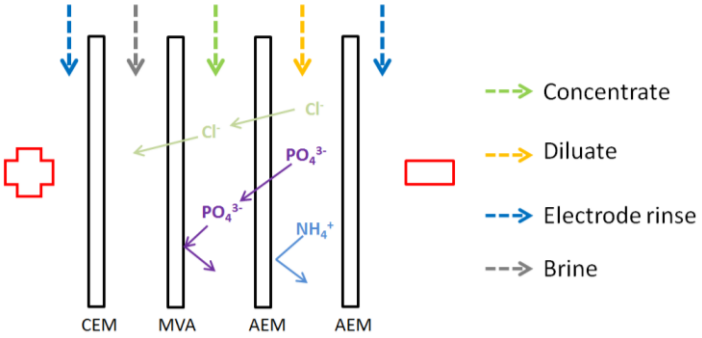

Figure 17 Example selectrodialysis set-up using monovalent anion exchange membrane (MVA)

Electrodialysis/selectrodialysis separates ions by charge, and thereby obtains high concentration phosphorus, and low impurity concentration if the membrane setup is done properly. This is especially useful in cases of recovery from a diluate which contains contaminants, such a biological contamination or heavy metals. Allowing nutrients to be recovered and used without the health and safety risk, such as that presented by spreading sludge on fields, or heavy metal contamination in struvite precipitation or the use of sludge ashes. Below are some of the equations associated with electrodialysis/selectrodialysis.

Equation 12 can be used to calculate the current efficiency of the electrodialysis process:

Equation 12

$$CE = \frac{z_A \left(\frac{m_A(t)}{M_A}\right) F}{nIt}$$

Where z is the charge on the ion, $m_A(t)$ is the total weight of the transferred ions (either phosphate or ammonium), M_A is the molar mass of the ion, F is Faraday's constant (96485 A·s·mol-1), n is the number of cell trios, I is the applied current (A), and t is the time period (s).

The membrane transport number t_i' can be calculated using a modified Nernst equation, as in Equation 13 [163].

Equation 13

$$E_m = \frac{RT}{nF}(2t_i' - 1)\ln\left(\frac{a_1}{a_2}\right)$$

where E_m is the potential difference across the cell, a_1 and a_2 are the mean activities of electrolyte solutions and n is the electrovalence of counter-ion.

The separation efficiency (S_B^A) between components A and B can be calculated using Equation 14. If $0<S_B^A<1$ ion A transported slower than ion B, whereas if $-1<S_B^A<0$ ion A was transported faster than ion B. $c_A(t)$ and $c_B(t)$ are the concentrations of ion A and B in the diluate [164].

Equation 14

$$S_B^A(t) = \frac{\left(\frac{C_A(t)}{C_A(0)}\right) - \left(\frac{C_B(t)}{C_B(0)}\right)}{\left(1 - \left(\frac{C_A(t)}{C_A(0)}\right)\right) + \left(1 - \left(\frac{C_B(t)}{C_B(0)}\right)\right)}$$

Lower current utilization efficiency is seen above the limiting current density (i_{lim}). If electrodialysis is run above the limiting current density the cost per unit of recovered product will be higher than if it is run using a lower current density than the limiting current density. The limiting current density can be calculated using Equation 15.

Equation 15

$$i_{lim} = \frac{CDzF}{\delta(t_m - t_s)}$$

where, C is the diluate concentration, D the diffusion coefficient, δ the boundary layer thickness, t_m and t_s the ion transport numbers in the membrane and the solution respectively. The recovery can be calculated using Equation 16.

Equation 16

$$R = \left(\frac{C_{C,t}V_{C,t} - C_{C,i}V_{C,i}}{C_{D,i}V_{D,i}}\right) \approx \left(\frac{C_{C,t} - C_{C,i}}{C_{D,i}}\right)$$

Where $C_{C,t}$ is the concentration in the concentrate compartment at a given time, and $C_{C,i}$ is the initial concentration in the concentrate compartment. If the volume change in the diluate and concentrate were negligible the shortened expression can be used.

2.2.1. MEMBRANES

Two types of membranes are used in electrodialysis, anion exchange membrane (AEM) and cation exchange membrane (CEM). Electrodialysis membrane is electrically conductive, which allows only ions with positive or negative charge to pass. CEMs only allow the transfer of cations, and usually consist of a polymer with negatively charged groups, such as; $–SO_3^-$, $-COO^-$, $-PO_3^{2-}$, $-PO_3H^-$, or $–C_6H_4O^-$. AEM usually consist of a membrane matrix with a positive charge such as; $–NH_3^+$, $–NRH_2^+$, $–NR_2H^+$, $–NR_3^+$, $–PR_3^+$, $–SR_2^+$. A simplified schematic of the membranes can be seen in Figure 18. [165,166]

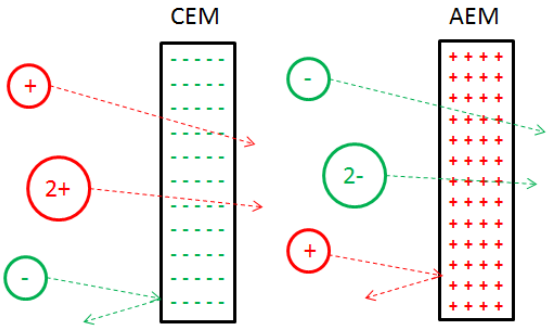

Figure 18 Simplified diagrams of CEM and AEM electrodialysis membranes

Selectrodialysis uses monovalent anion exchange (MVA) and monovalent cation exchange (MVC) membranes (Figure 19) which are selective to monovalent ions, i.e multivalent ions are rejected by the membrane. These membranes have a surface charge, negative for MVA and positive for MVC membranes. Electrostatic repulsion between multivalent ions and the charged membrane surface provides monovalent selectivity. [167]

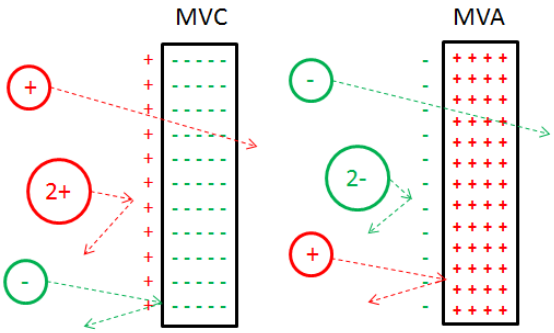

Figure 19 Simplified diagrams of MVC and MVA selectrodialysis membranes

2.2.2. PERFORMANCE

A number of studies have taken place on the use of electrodialysis or selectrodialysis for phosphate removal from wastewater. Using electrodialysis combined with gas stripping, phosphorus and ammonia were removed in the ranges 86-94% and 96-100%, respectively [168]. Another study reported phosphorus removal of 77% (the decrease in the diluate concentration), however, recovery was reported to be 65% (the increase in the concentrate concentration) [169]. These studies used diluate streams of synthetic anaerobic digestion side streams and diluted hydrolysed urine, respectively. Ammonia has been found to achieve an ionic flux of 0.27 mol m^{-2} h^{-1}, with an average total current efficiency of 76%. This leads to a power consumption of 4.9 kWh per kg N. In a separate study phosphate ionic flux was found to be 16 mmol m^{-2} h^{-1}, costing 16.6 kWh per kg phosphate produced [170]. Equation 17 can be used to calculate specific power consumption.

Equation 17

$$Specific\ Power\ Consumption = \frac{E \int_0^t I dt}{V_D}$$

Where I is the current (A), V_D is the diluate volume, and E is the energy supplied (J).

Phosphorus recovery using selectrodialysis often relies on MVA membrane to allow monovalent anions to move out of the concentrate, but retain the multivalent phosphate ions. Zhang et al. (2009) found that MVA membranes were effective in separating mono-and multi-valent ions from one another [171]. A phosphorus efficiency of 26.6% was achieved using MVA membrane and synthetic diluate (KH_2PO_4 and NaCl solution) [172]. The main concern with this method is that wastewater contains a large number of ions, as such there is a competitive influence on phosphorus concentrating efficiency [173].

2.2.3. POTENTIAL CHALLENGES

Key issues in electrodialysis/selectrodialysis are:

- Membrane fouling, particularly of the AEM membrane (due to macromolecules) [174–176].
- Scaling [177,178].
- Product use, i.e to crystallize or use liquid product.
- Energy requirement.
- Concentrate pH (to ensure phosphate has a multi-valent charge and cannot pass MVA membrane).
- Phosphate interactions with cations.

In this dissertation forward osmosis will be used to concentrate real digester centrate and selectrodialysis will be used to create a phosphorus product free of biological contamination and heavy metals.

CHAPTER 3. OBJECTIVES

The objective of this PhD project is to gain knowledge on the subject of membrane technology for phosphorus recovery. The main focus will be on forward osmosis and selective electrodialysis.

While these topics are not novel, most studies use synthetic or filtered digester centrate. This allows for overambitious results, since digester centrate contains a significant quantity of large molecules and solids which could present issues in membrane fouling or clogging. Studies supporting this thesis have used digester centrate collected from Aaby WWTP (Aarhus, Denmark).

This project will concern:

1) Testing of forward osmosis membranes (biomimetic and TFC) for orthophosphate rejection, ammonia rejection, suitability of seawater as a draw solution, and water permeability,

2) Selectrodialysis for simultaneous phosphate and ammonia recovery.

3) Cost analysis for the implementation of forward osmosis or selectrodialysis at Aaby WWTP.

CHAPTER 4. FORWARD OSMOSIS

Forward osmosis was used to concentrate digester centrate from Aaby WWTP (Aarhus, Denmark). The following chapter discusses results obtained using biomimetic and TFC forward osmosis membranes. All experiments were carried out using a lab-scale setup with 140cm^2 effective membrane area. Results in this chapter are published in [124,179].

4.1. FEED SOLUTION OSMOTIC PRESSURE

Digester centrate was collected from Aaby WWTP (Aarhus, Denmark) an 84,000 PE municipal WWTW, using denitrification/nitrification and enhanced biological phosphorus removal (EBPR) treatment. At the plant, ferric chloride was added to control the concentration of total-P, excess EBPR sludge was pre-thickened and added to a mesophilic digester with a residence time of 20-22 days. This sludge was then dewatered in a decanter centrifuge and the digester centrate collected for this study. The composition of digester centrate collected from Aaby WWTP can be found in Table 8.

Table 8 Digester centrate composition

Parameter	**Digester Centrate**
Ortho-P (mM)	1±0.03
Total P (mM)	9.4±0.3
Ammoniacal nitrogen (mM)	122±5
Mg^+ (mM)	0.04±0.0009
Ca^+ (mM)	1±0.05
Na^+ (mM)	3.7±1.0
Cl^- (mM)	209±51
pH	8.0±0.2
Electrical Conductivity (mS cm^{-1})	13.189±0.007
Osmotic Pressure (bar)	1.8±0.3

It is essential to know the osmotic pressure of the feed and draw solutions to ensure an adequate driving force between the two. Using the osmotic pressure difference water permeability can be determined, per Equation 3, which is key in evaluating a membranes performance. Determining feed solution osmotic pressure can be challenging, as digester centrate contains many components. There are three methods which may be suitable for this application. First, there is the determination of osmotic pressure using water activity, a_w, which is the partial vapour pressure of a substance (digester centreate) divided by the standard state partial vapour pressure of pure water (Equation 18).

Equation 18

$$\pi = -\left(\frac{RT}{V_m}\right)\ln(a_w)$$

where; V_m (m^3) is the partial molar volume of water, R is the ideal gas constant (0.0831 L bar mol^{-1} K^{-1}), T is the temperature in Kelvin and a_w is the water activity. It is assumed that all solutes are fully rejected by the membrane and therefore contribute to the osmotic pressure difference across the membrane.

From a number of feed solution samples concentrated to a specific VCR it is possible to plot a graph of feed osmotic pressure by VCR, as seen in Figure 20. From these data a line of best fit can be determined and used to estimate feed solution osmotic pressure. However, this graph can only be used for a short period of time due to seasonal changes in composition, and only for digester centrate collected from Aaby WWTP, since digester centrate composition varies between WWTPs. Nevertheless, producing the data necessary to plot Figure 20 is relatively fast and precise, with ±0.003 a_w error (provided by supplier). Plus, inline osmotic pressure can be determined from the VCR of the feed.

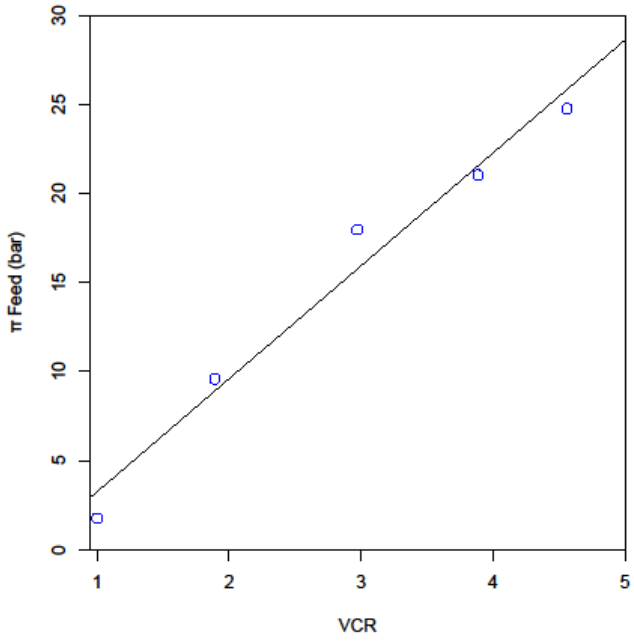

Figure 20 Feed osmotic pressure for various VCR calculated using water activity.

The second method of determining feed solution osmotic pressure is experientially. This is achieved by taking draw solutions of various, and known, osmotic pressure and running forward osmosis for a short period of time. From this mass changes can be plotted against time, as in Figure 21. For draw solutions with a higher osmotic pressure than that of the feed, water will move into the draw solution, i.e positive $\Delta m/\Delta t$. For lower osmotic pressure water will move into the feed solution, i.e negative $\Delta m/\Delta t$. If both feed and draw have the same osmotic pressure, $\Delta m/\Delta t$ will be 0.

This is time consuming, as there is potential for the need to run many experiments in order to find a suitable range of draw solutions. Lastly, as with the method using a_w, it would need to be repeated periodically and for different WWTPs, and an inline determination of osmotic pressure would be impossible.

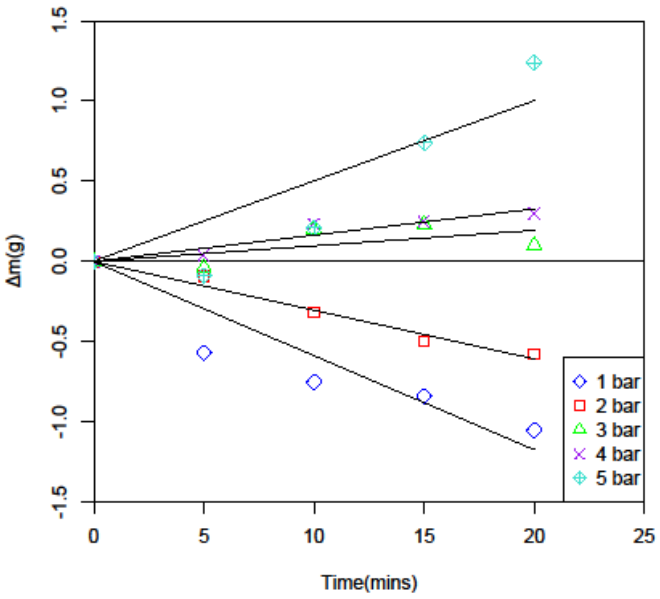

Figure 21 Experimental determination of osmotic pressure.

The final method is to calculate the osmotic pressure using known concentrations of solutes found in digester centrate. However, there are many compounds present in digester centrate, and it would be impossible to find all of them, and give an inaccurate osmotic pressure if any were excluded. Wastewater contains macromolecules which also contribute to osmotic pressure, but the effect of these cannot be calculated. Furthermore, as with the experimental method, this method cannot be used inline. Consequently, feed solution osmotic pressures have been determined using the feed solution a_w, and was found to be 1.8±0.3 bar.

4.2. NATURALLY OCCURRING SALT WATER AS A DRAW SOLUTION

Many counties have access to seawater; however, the salinity in natural water sources varies around the world. This can cause issues when looking to utilize these saline waters as draw solution for forward osmosis since not all saline waters are of an adequate salinity to facilitate efficient flux, and consequently VCR. As such it is necessary to ascertain whether using seawater is commercially viable, firstly in the region in which you intend to apply forward osmosis, and secondly, for the depth below sea level from which seawater will be taken.

Table 9 Salinity of naturally occurring salt waters, and this flux and VCR these are capable of achieving when concentrating digester centrate

Ref.	Location	Salinity (PSU)	Min Temp (°C)	Max Temp (°C)	Min Temperature			Max Temperature		
					Osmotic Pressure (bar)	Max Flux (LMH)	VCR	Osmotic Pressure (bar)	Max Flux (LMH)	VCR
[180]	Baltic Sea	10	1	16	6.9	6.3	1.7	7.3	6.6	1.7
[181]	Caspian Sea	12.5	0	28	8.6	7.8	1.9	9.5	8.6	2.0
[182]	Atlantic / Pacific Ocean	35	0	30	24.2	21.8	4.1	26.8	24.2	4.4
[183]	North Sea	34-35	6	17	24.7	22.3	4.1	25.7	23.2	4.3
[184]	Red Sea	36-41	21	31	30.5	27.5	4.9	31.5	28.5	5.1
[185]	Hypersaline Lake (i.e Dead Sea)	>300	20	39	222.3	200.9	31.5	236.7	213.9	33.5

Table 9 shows some examples of salinities around the world. Salinity as low as 10 PSU can be seen, such as in the Baltic Sea, a relatively low salinity, which can be attributed to dilution by a vast number of estuaries. Waters with salinity this low are not suitable for use in forward osmosis for phosphorus recovery from wastewater, as a minimum VCR of 3 is required to reduce the magnesium demand from 1.3:1 to 1:1 Mg:P. These osmotic pressures can only achieve a VCR of 1.7 for digester centrate collected from Aaby WWTP. Similar can be said of the Caspian Sea, as such, all saline waters with salinity under 14.87 PSU (relating to a VCR of 3) should be disregarded for this purpose. The average salinity of seawater globally is 35 PSU, as seen for the Atlantic/Pacific Ocean and North Sea. This corresponds to a theoretical VCR between 4.1 and 4.4, thus reducing the magnesium demand to 1:1 Mg:P. The Dead Sea, one of many hypersaline lakes located worldwide, has an extremely high salinity. While this may appear desirable, using such a high osmotic pressure will give rise to an extremely high flux, forcing the foulants in the wastewater into the membrane with a greater force, consequently forming a much thicker and less readily-removed fouling layer than solutions with lower salinity. Additionally, concentration polarization will have a far greater effect for osmotic pressures as high as this. The combination of increased fouling and concentration polarization would therefore, lead to a decrease in average flux, a need for a greater number of cleaning cycles, and an increase in pumping costs due to increased viscosity. As such, it would not be cost-efficient to use hypersaline lakes without first diluting them, however, the effects of using a high salinity draw solution can be reduced by using a counter current flow configuration, as this makes the osmotic pressure difference more uniform over the length of the membrane.

Table 10 Effect of seawater salinity with increasing depth below sea level [186]

Depth (m)	Salinity (PSU)	Temperature (°C)	Osmotic Pressure (bar)	Max Flux (LMH)	VCR
0	35,84	23,3	26,9	24,3	4,4
200	35,91	16,3	26,3	23,7	4,4
400	35,48	11,72	25,5	23,1	4,3
600	35,19	9,31	25,1	22,7	4,2
1000	35	5,99	24,7	22,3	4,1

Location is not the only parameter to affect the osmotic pressure of seawater, temperature and salinity change with depth below seawater surface. Table 10 shows

salinity for the first 1000m below surface level for the North Atlantic Ocean. The osmotic pressure falls by 2.2 bar, resulting in a 6.8% decrease in potential VCR. For varying depths salinity does not significantly change, however temperature does, this, along with

Figure 22, shows that temperature does not play a key role in the osmotic pressure of seawater, as such; seasonal changes in temperature should not affect the forward osmosis process.

One problem with using seawater as draw solution and discharging it back into the sea without treatment is the risk of contamination, which has potential to cause eutrophication [58], amongst other problems i.e. micro-pollutants/heavy metal contamination. This has been investigated later in the chapter.

Seawater has varying salinity and temperature in different parts of the world, and in different seasons. As such, it is necessary to calculate the osmotic pressure, flux, and VCR seawater is capable of achieving. Too low a salinity and it will not be able to concentrate digester centrate to an adequate VCR, too high and the user risks the adverse effects of concentration polarization. The Van't Hoff equation (Equation 19) can be used to determine the osmotic pressure seawater with a certain salinity and temperature. Where M is the molarity of salt (mol L^{-1}), R the gas constant (0.0831 L bar mol^{-1} K^{-1}), and T the temperature (K). i is the Van't Hoff Factor, a measure of the number of ions a solute will form when dissolved in water, since NaCl in seawater is fully dissociated i is equal to 2 .

Equation 19

$$\pi = iMRT$$

In practice, Equation 19 was used to calculate the osmotic pressure of NaCl solutions, while water activity (Equation 18) was measured for seawater, as the salinity of the seawater used was unknown. The theoretical calculations discussed in the remainder of this section use Equation 19.

Figure 22 shows the osmotic pressure for seawater with increasing salinity for 4, 20, and 30°C. There is a linear increase in osmotic pressure with salinity, and increasing osmotic pressure with increasing temperature, however, the effect of temperature on osmotic pressure is low. Consequently, seasonal variations in temperature should not affect a full-scale plant operating using a seawater draw solution. In Denmark there are 27 WWTP within 1km of the coast, of these, 12 have a salinity of 10-19 PSU, 13 20-29 PSU, and two have access to 30+ PSU. As such, the majority of Danish WWTPs in the vicinity of the coast have access to seawater with salinity of 20+ PSU (13+ bar osmotic pressure).

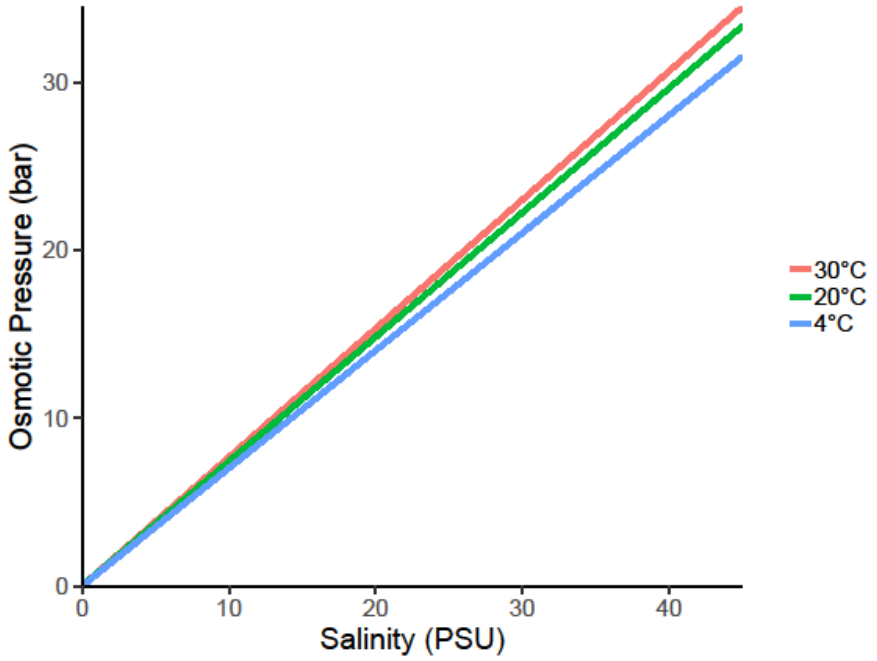

Figure 22 Calculated osmotic pressure for seawater

From the osmotic pressure, calculated in

Figure 22, the average flux can be estimated. This can be achieved using the water permeability of the membrane (in this instance 0.904 LMH bar^{-1} (from experiments carried out using TFC membrane) and Equation 3.

As seen in

Figure 23, this corresponds to an average water flux >2.8 LMH for WWTPs in Denmark.

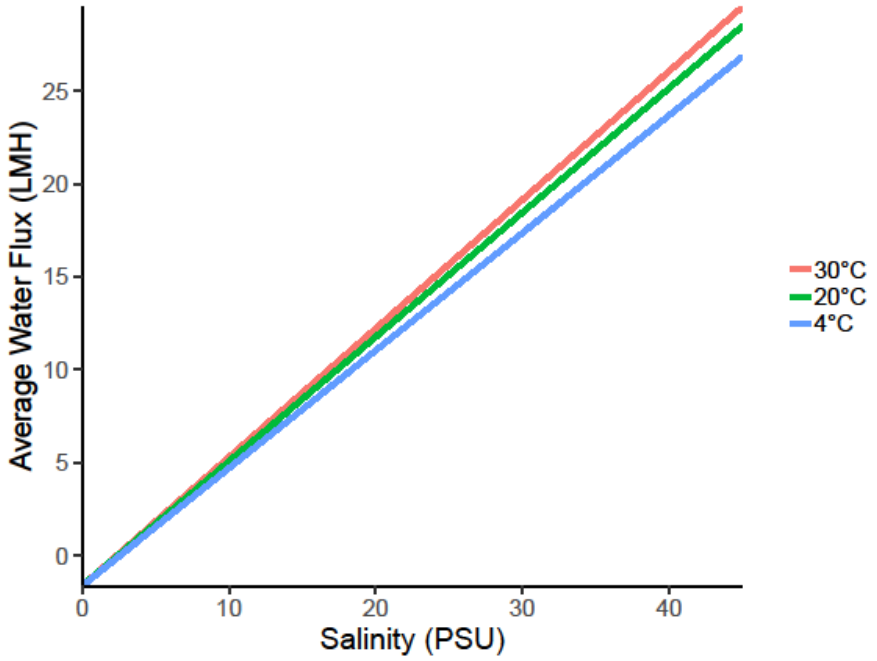

Figure 23 Calculated average water flux using seawater draw solution and digester centrate feed soluton

It is then possible to calculate the VCR to which the seawater draw solution is able to concentrate digester centrate. VCR can be calculated using Equation 20, which $V_{initial}$ and V_{final} are the initial and final feed solutions volumes.

Equation 20

$$VCR = \frac{V_{initial}}{V_{final}}$$

A WWTP with access to seawater with a salinity of greater than 20 PSU would be capable of achieving a VCR of 3 (as shown in Figure 24), thus attaining a decrease in P:Mg ratio from 1:1.3 to 1:1. Meaning that in Denmark alone, 15 WWTP are capable of utilizing this technology for phosphorus recovery based solely on draw solution availability.

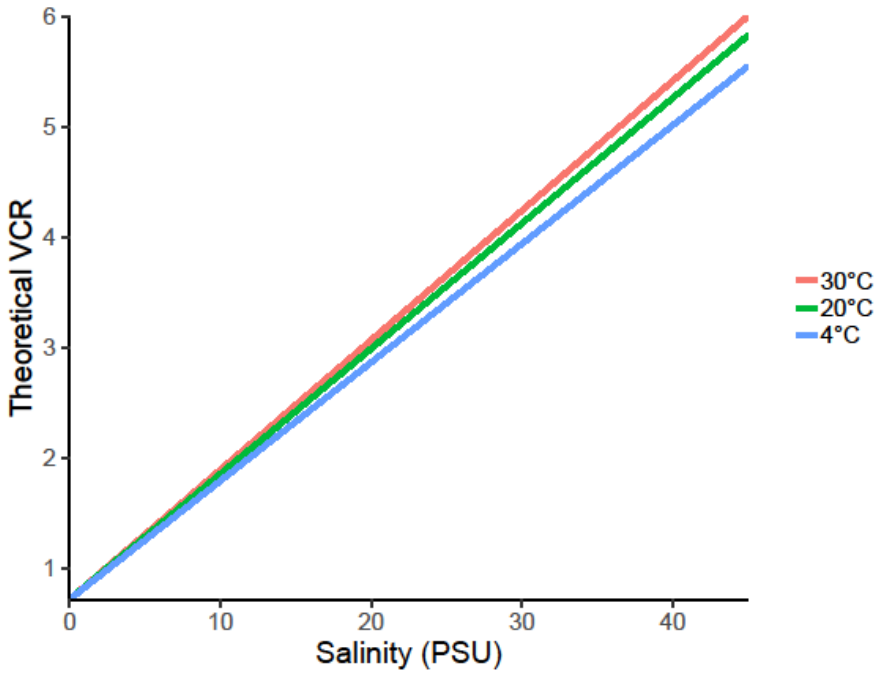

Figure 24 VCR seawater can be calculated using seawater draw solution to concentrate digester.

4.3. WATER FLUX & PERMEABILITY

Water flux and permeability were calculated for both biomimetic (Aquaporin A/S, Denmark) and TFC (Porifera, USA) membranes.

TFC membranes exhibited the higher water flux, achieving 49.7 LMH with deionized water feed solution and 54.5 bar osmotic pressure difference. For TFC membranes average water flux was 27.1 LMH and 5.2 LMH for deionized water and digester centrate feed solutions, respectively. When using deionized water feed solution biomimetic membranes achieved a water flux of 5.2 LMH, and 2.1 LMH for digester centrate feed solution. As shown in Figure 25.

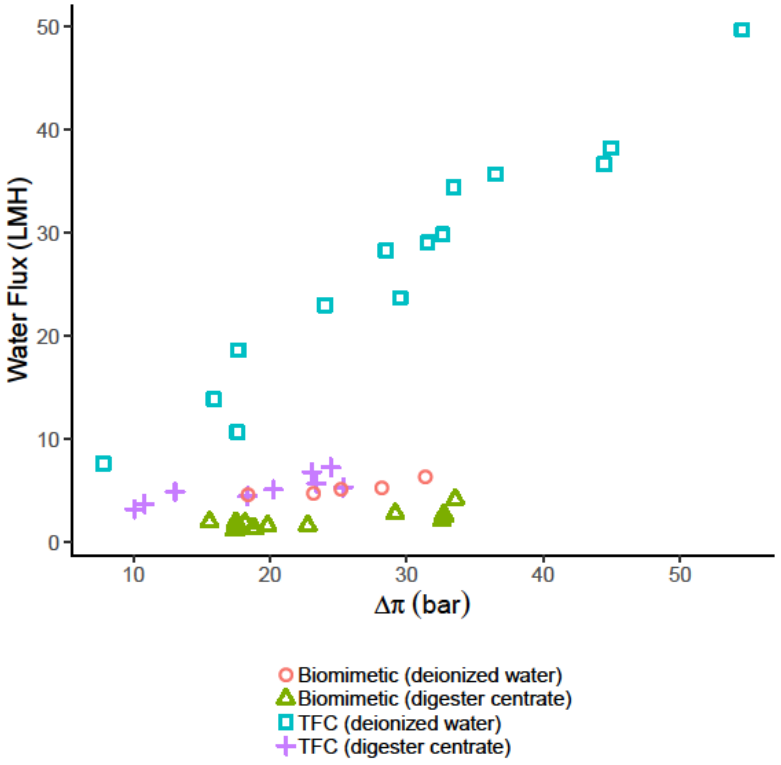

Figure 25 Water flux for both TFC and biomimetic membranes, using deionosed water and real digester centrate feed solutions.

Figure 26 shows water permeability (calculated using Equation 3). TFC membranes exhibited average water permeability of 1.1 and 0.3 LMH bar^{-1} for deionized water and digester centrate, respectively. Conversely, it was 0.21 and 0.09 LMH bar^{-1} for deionized water and digester centrate respectively when using biomimetic membrane. The difference between water permeability for deionized water and digester centrate feed solutions can be attributed to internal concentration polarization, as the support later is facing the feed (AL-DS) when using digester centrate and facing the draw (AL-FS) when using deionized water feed solution. With the support facing the feed when using deionized water the internal concentration polarization is reduced, giving a higher water flux. When this is no longer the case – as when using digester centrate- internal concentration polarization can occur in the membrane support layer. The gradient of water permeability against osmotic pressure difference for both TFC and biomimetic membranes is close to zero, showing external concentration polarization is not an issue.

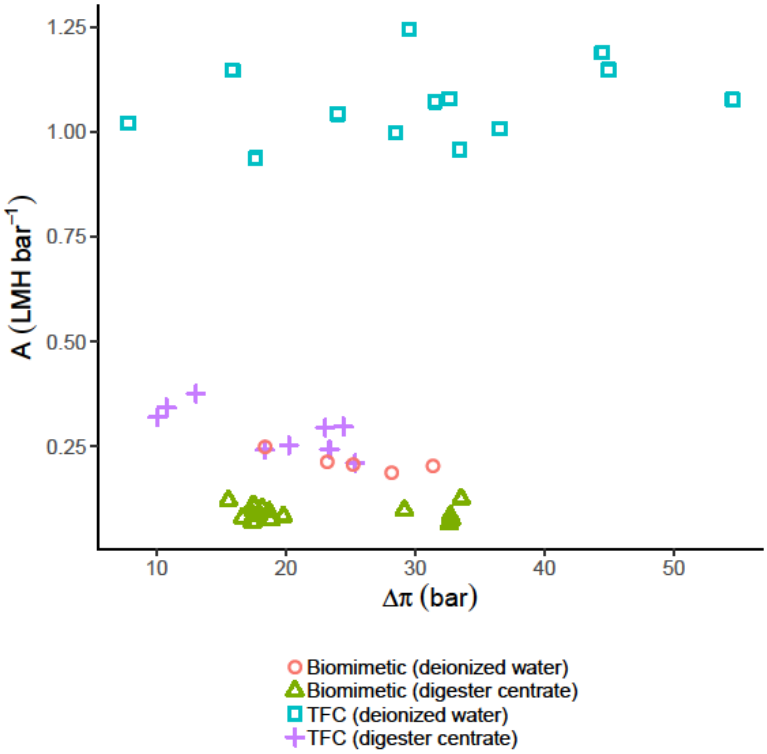

Figure 26 Water permeability (A) for both TFC and biomimetic membranes, using deionosed water and real digester centrate feed solutions.

In order to determine if long term operation could be successful the setup was run for three 22 hour periods, with a one hour cleaning cycle in between each 22 hour cycle. The 22 hour runs used seawater draw solution and digester centrate feed solution, while the cleaning cycle used deionized water feed solution and seawater draw solution. Water permeability (A) during the two cleaning cycles can be seen in Figure 27. Average water permeability was 0.23 and 0.21 for cleaning cycle 1 and 2 respectively. By the end of the cleaning cycle water permeability for both cleaning 1 and 2 were almost the same. It is therefore possible to conclude that membrane fouling is not an issue, as the water permeability is not affected over prolonged use.

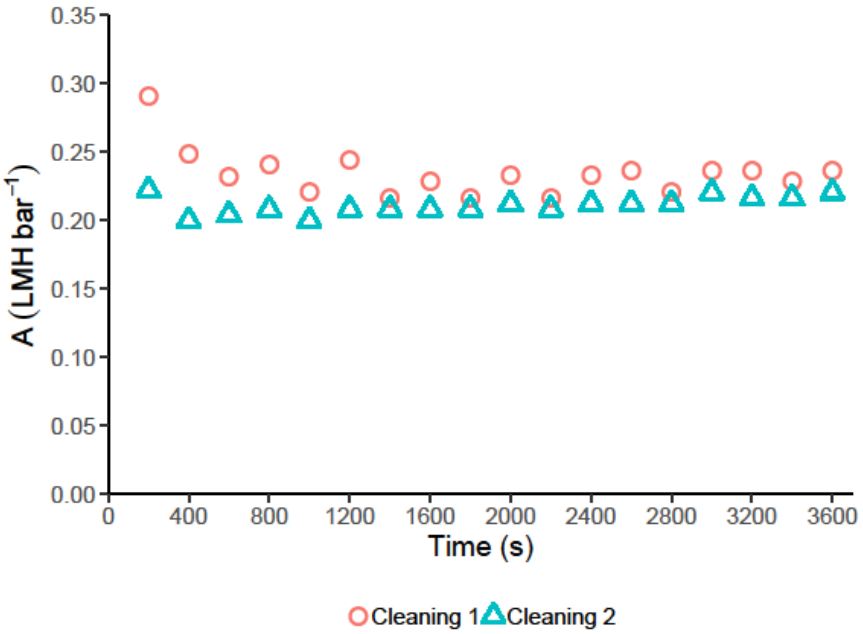

Figure 27 Water permeability during cleaning cycles, between 22 hour cycles using digester centrate feed solution and TFC membranes.

4.4. PHOSPHORUS

Rejection was calculated using Equation 11 [153]. As shown in Figure 28, average phosphorus rejection was 99.5% for TFC membrane. Similarly, previous studies reported phosphorus rejection >92% have been found for CTA membranes [149,152].

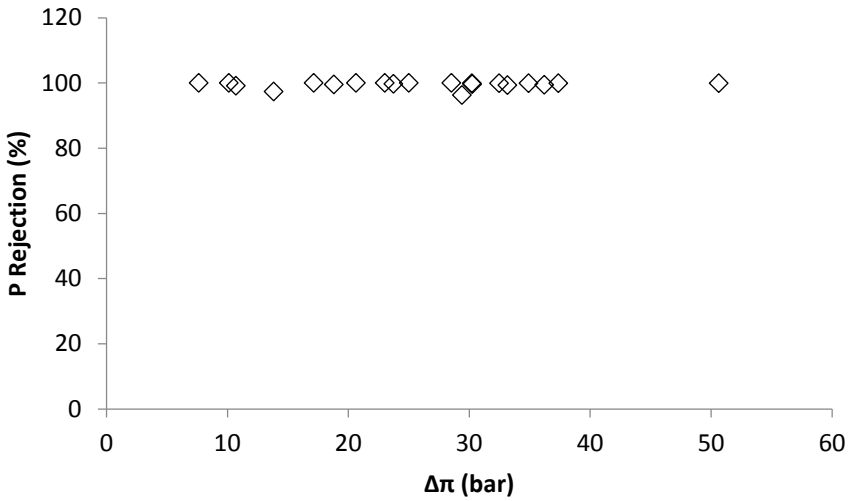

Figure 28 Phosphorus rejection for TFC membrane

In order to recover as much phosphorus as possible it is essential that the membrane have as high phosphorus rejection as possible. Figure 29 shows the percentage of phosphorus lost to the draw solution (from feed solution) at different pH using biomimetic membrane. Phosphate has increasing charge with increasing pH, corresponding to a decreasing percentage of phosphate lost to the draw solution, from 15.8% at pH 5 to 5.8% at pH 10. The biomimetic membrane relies on surface charge to repel ions; consequently, ions with greater charge are more easily rejected. Conversely, molecules will not be rejected and can diffuse through the membrane, as they have no charge.

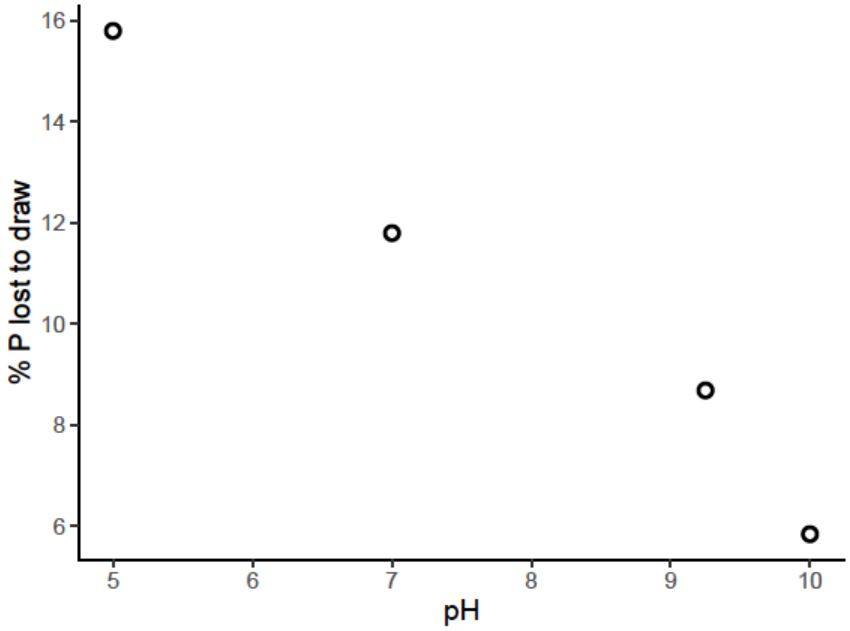

Figure 29 Phosphorus lost to draw solution using real digester centrate and biomimetic membrane.

4.5. AMMONIA

Figure 30 shows ammoniacal nitrogen diffusion for TFC and biomimetic membranes. TFC membrane exhibited a higher ammoniacal nitrogen flux than biomimetic membranes. For biomimetic membranes ammoniacal nitrogen diffusion stays steady up to pH 7, however, from pH 7 diffusion increases, corresponding to the increase in ammonia over ammonium. Uncharged ammonia can pass the membrane more easily than ammonium, which has a charge of +1, due to the membrane surface charge. As such, it would be necessary to keep pH low to reduce ammonical nitrogen diffusion across the membrane. Consequently, pH adjustment to aid struvite or calcium phosphate precipitation would need to take place after forward osmosis treatment, not before, as pH 9-10 is optimal for struvite precipitation.

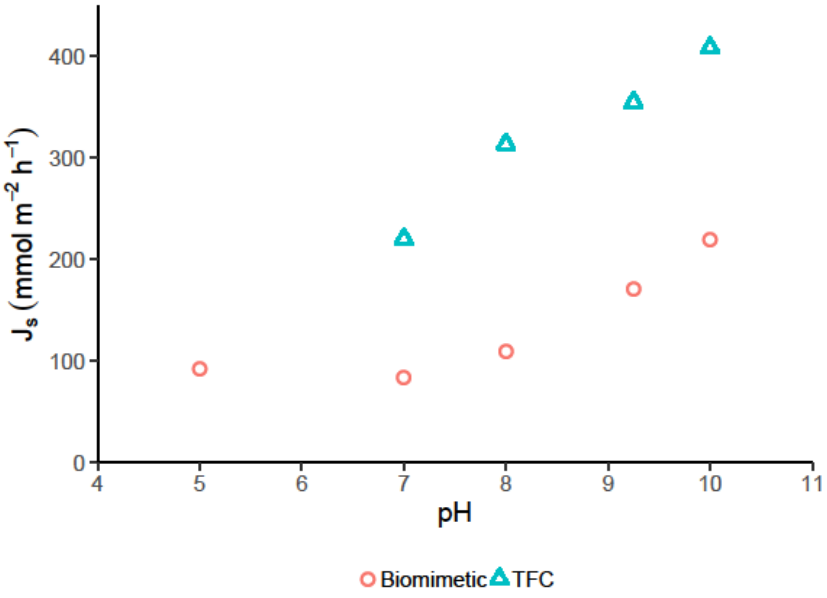

Figure 30 Diffusive TAN flux

Digester centrate from Aaby WWTP is pH = 8.7±0.2, therefore, ammonical nitrogen loss at pH 8 was calculated at increasing VCR using the average ammonical nitrogen flux at pH 8, as shown in

Figure 31. The percentage of ammonical nitrogen lost increases significantly between VCR 1 and 2 – with around 30% of the initial feed mass being lost to the draw. By VCR 10 this has increased to 50% and 56% for biomimetic and TFC membranes respectively. Consequently, seawater draw solution would require treatment prior to discharge or use as drinking water. Furthermore, if ammonia recovery is the main purpose alternative membranes or technology may be more suitable. However, phosphorus recovery through struvite would still be possible as the concentration of ammoniacal nitrogen is 10-20 times higher than that of phosphate. As such, a loss of 50% would not reduce the ammoniacal nitrogen concentration to below that of phosphate.

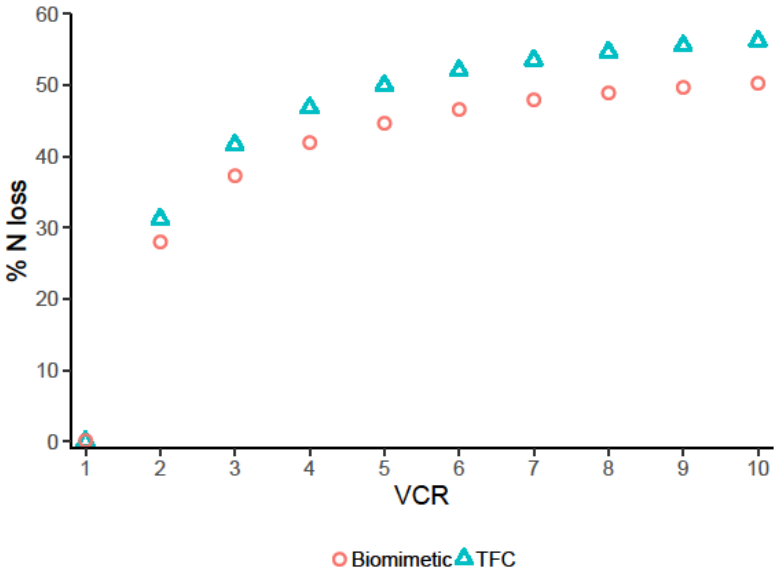

Figure 31 TAN loss, calculated using TAN flux at pH 8, it should be noted that this does not account for reductions in N loss due to struvite precipitation.

4.5.1. TRANSPORT MECHANISM THROUGH BIOMIMETIC MEMBRANE

Equation 21 can be used to calculate the flux of ammoniacal nitrogen. This can be used to determine the ratio of ammoniacal nitrogen flux to sodium ion reverse flux.

Equation 21

$$J_{NH_4^+} = k'(\text{pH}) + \lambda(-J_{Na^+})$$

Where λ is the fraction of the reverse sodium ion transport that is linked to the ammonium transport, and k' is the flux of ammonium with co-transport of an anion. The fraction of ammoniacal nitrogen present as ammonium ($\alpha_{NH_4^+}$) was calculated from Equation 22.

Equation 22

$$\alpha_{NH_4^+} = \frac{1}{1 + \frac{K_a}{[H^+]}}$$

Where $[H^+]$ is the concentration of hydrated protons and K_a is the dissociation constant which for ammoniacal nitrogen is $5.62 \cdot 10^{-10}$ M (calculated from pK_a = 9.25).

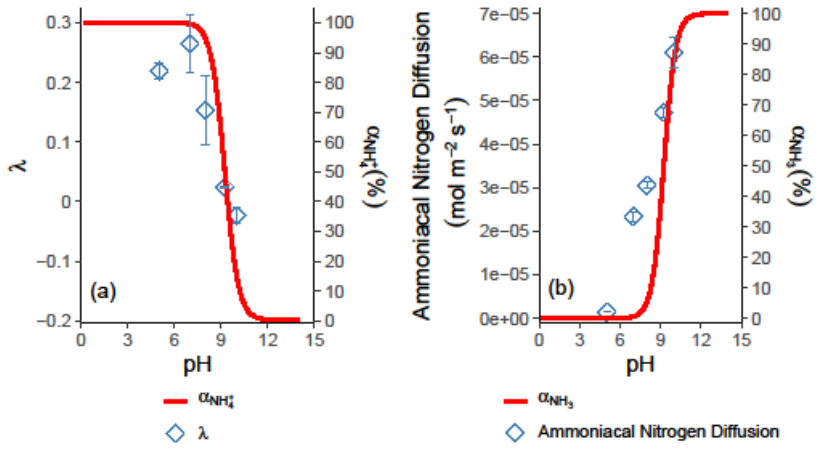

Figure 32 (a) Ratio of ammoniacal nitrogen to sodium flux (λ) (b) ammoniacal nitrogen diffusion as a function of pH (See Paper 2)

Ammoniacal nitrogen comes in two forms – ammonia (NH_3) and ammonium (NH_4^+). As mentioned previously, ammonia diffuses through the membrane with greater efficiency than ammonium since it is uncharged, and therefore not repelled by the charged surface of the membrane. Ammonium on the other hand is charged. As such, there are two ways by which it can pass the membrane;

1. When an ammonium ion moves from feed to draw a positive ion will move from draw to feed, i.e Na^+,
2. With a negative ion moving from feed to draw, i.e. Cl^-.

Figure 32 (a) shows the ratio of ammoniacal nitrogen flux to reverse Na^+ flux at increasing pH (λ). λ decreases with increasing pH, as seen from the red line, this corresponds with a decreasing concentration of ammonium (and increasing ammonia). However, Figure 32 (b) shows the diffusion of ammoniacal nitrogen increasing with increasing pH, corresponding to higher ammonia diffusion than ammonium transport at lower pH. Consequently, it would be necessary to either use an uncharged draw solution, or operate a low pH, where charged ammonium will be rejected more effectively by the membrane.

CHAPTER 5. SELECTRODIALYSIS

A four compartment selective electrodialysis setup (Figure 33) was used to recover phosphorus and ammonia in separate compartments. Phosphorus was concentrated in an anion concentrate stream, and ammonium was concentrated in a cation concentrate. Diluate was digester centrate, and electrode rinse solution was 20 gL^{-1} Na_2SO_4. In the anion compartment pH = 10 was maintained, in order to ensure a higher charge on the phosphate ions, thus preventing their passing the MVA membrane. In the cation compartment pH 4 and 8 were investigated to see the effect of increasing ammonia over ammonium. Results in this chapter are from Paper 3.

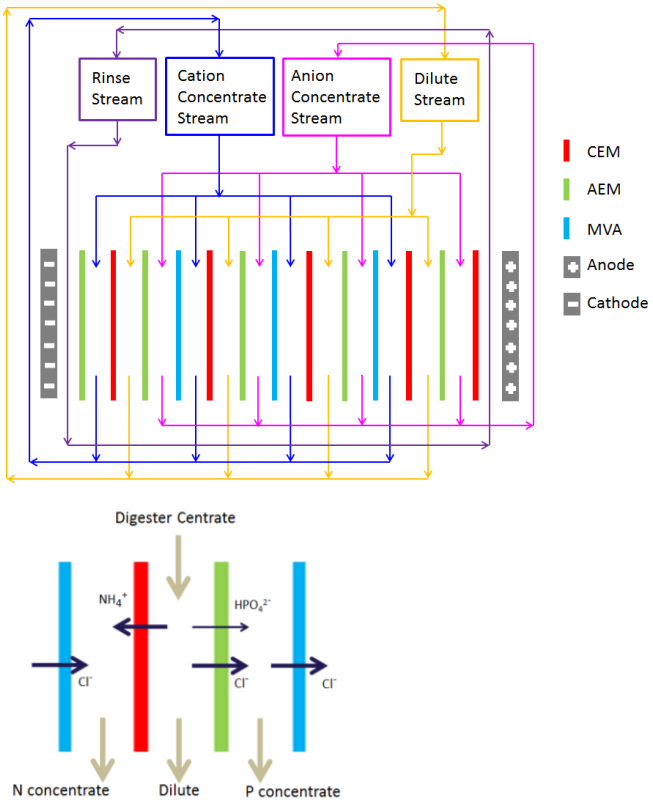

Figure 33 Selectrodialysis setup

5.1. ANION CONCENTRATE

Anions move from the diluate through the AEM membrane into the anion concentrate. Anions with a charge greater than one are then trapped in the anion concentrate, as they cannot pass the MVA membrane. In order for phosphate to move into the anion concentrate two single charge anions must pass the MVA membrane. In this case two chloride ions will move through the MVA membrane. Consequently it is necessary to have an abundant supply of chloride ions in the anion concentrate compartment, therefore 10 gL^{-1} NaCl was added to the concentrate streams.

Figure 34 shows the phosphate concentration decreasing in the diluate compartment and increasing in the anion concentrate compartment. Within four hours the diluate was depleted of phosphate and recovery >95% was recorded for both pH 4 and 8. The initial recovery rate for the first two hours of operation was 0.028 ± 0.006 mmol $m^{-2}s^{-1}$ (calculated using Equation 23).

Equation 23

$$J_i = \frac{\alpha}{A}$$

Where A is the membrane area (m^2) and α is $\Delta c/\Delta t$

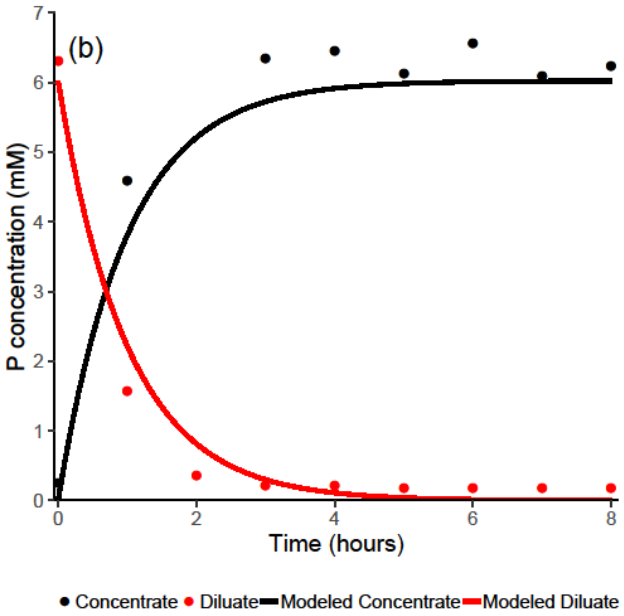

Figure 34 P concentration in diluate and concentrate for experiments with pH 4 (a) and 8(b) cation compartment.

Figure 35 shows the phosphate, chloride, and sulphate concentrations in the diluate and anion concentrate compartments. Phosphate concentration decrease in the diluate and increase in the anion concentrate, while chloride decreases in both diluate and anion concentrate compartments. Sulphate on the other hand, initially increases in the diluate, then decreases, and increases in the anion concentrate. The initial increase in diluate sulphate concentration is likely due to sulphate ions passing from the electrode rinse in to the diluate, these ions then pass through the AEM membrane into the anion concentrate. Sulphate causes an issue when entering the anion concentrate as it is unable to pass the MVA membrane, since it has a 2- charge. Since sulphate cannot leave the anion compartment it reduces the purity of any potential phosphorus product. In total 104.mM chloride leaves the anion compartment, while 6.7mM and 9.5mM of phosphate and sulphate respectively enter it. By charge, the phosphate and sulphate movement corresponds to 37.5% of chloride movement. This raises the issue of what other ions are moving into the anion concentrate, and whether these other ions have a single charge or remain in the concentrate. Nitrite was also measured, but was found to be below detectable limits. As seen in the figure, the chloride concentration is 17.6mM after 8 hours, in order to reduce costs in a full-scale system chloride concentration could be reduced.

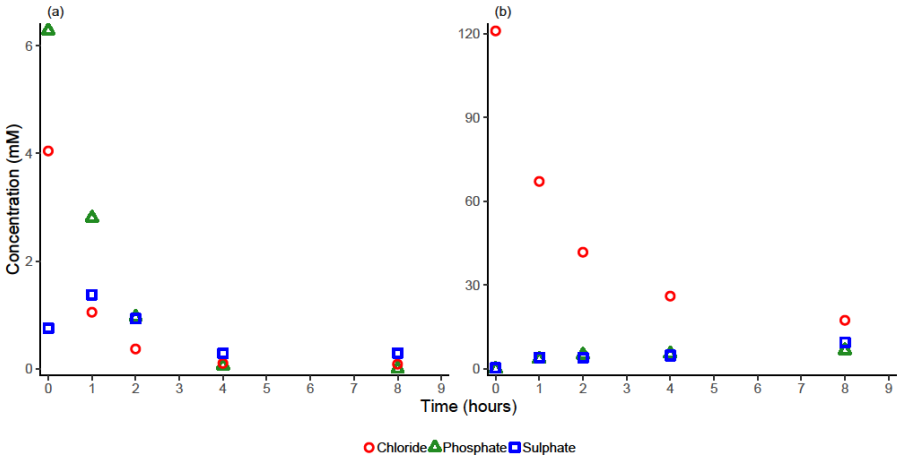

Figure 35 Chloride, sulphate and phosphate concentrations in diluate (a) and anion concentrate (b) compartments, when using pH = 4 cation concentrate.

5.2. CATION CONCENTRATE

Figure 36 shows the ammoniacal nitrogen concentration in the diluate and cation concentrate for pH 4 and 8 cation concentrate. Ammoniacal nitrogen concentration decreases from 84-125 mM to 3-6 mM during the 8 hour experiment. The initial recovery rate of ammonium was calculated to be 0.6 ± 0.3 mmol $m^{-2}s^{-1}$ for the first two hours (calculated using Equation 23). The average current efficiency was calculated to be 85 ± 15% for the first 4 hours of operation (calculated using Equation 12). Ammoniacal nitrogen recovery was calculated using Equation 16, and was found to be 71.3% and 71.9% for pH 4 and 8 respectively. Some ammoniacal nitrogen was found to be lost due to evaporation of ammonia, this corresponded to 7.8% and 11.4% of the initial diluate ammoniacal nitrogen concentration for pH 4 and 8 respectively.

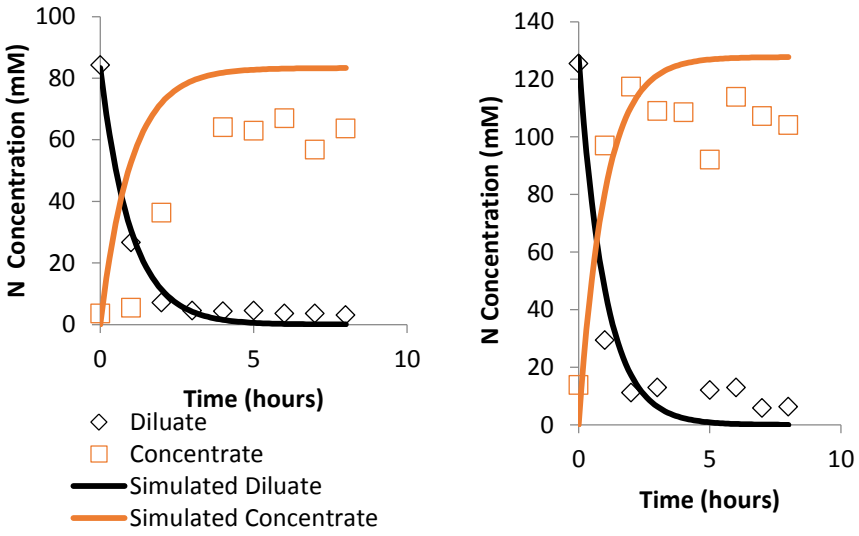

Figure 36 N concentration in diluate and concentrate for experiments with pH 4 (a) and 8(b) cation compartment.

5.3. SIMULATIONS

Phosphate and ammoniacal nitrogen concentrations can be simulated as an exponential decline in the dilute in order to model the membrane area and power required for increasing recovery. The rate constant (k) was used to estimate the membrane area required to treat digester centrate at Aaby WWTP. k was found to be 1 h for both phosphate and ammoniacal nitrogen.

Equation 24 was used to calculate the development in concentration in order to determine the required membrane area for a digester centrate stream of 10 m^3 h^{-1} with a phosphate concentration of 6 mM and an ammonium concentration of 105 mM. The phosphate concentration was calculated throughout an electrodialysis cell with dimensions l x h x w, where l is the length, h is the height (0.1 m) and w is the width (0.05 m). The single flow chamber was divided into a number of control volumes to solve the concentration as function of length and time in the cell. The area of the membrane was $A_{cell} = \Delta l$ x h, and the volume of each cell was $V_{cell} = \Delta l$ x h x w.

Equation 24

$$C_{C,t+\Delta t,l} = C_{C,t,l} + \left(\frac{QC_{C,t,l-\Delta l} - QC_{C,t,l} - JA_{cell}}{V_{cell}}\right)\Delta t$$

Equation 24 takes account of the convective transport in and out of each control volume, and the loss of phosphorus or ammonia through the membrane, with Δl = 0.4 m and Δt = 1 s. Concentrations of a given length and new time ($C_{C,t+\Delta t,l}$) were predicted from concentrations at current and previous length and at previous time ($C_{C,t,l}$ and $C_{C,t,l-\Delta l}$, respectively). This was done until a steady state was reached ($dC/dt = 0$). The boundary condition was that initial concentrations throughout the cell equalled the inlet concentrations of 6 mM phosphate and 105 mM ammonium, and the flow was 10 m^3h^{-1}. The required cell length was calculated as function of the degree of recovery. The energy consumption (W) can be calculated by using Equation 25.

Equation 25

$$E = iA\Delta V$$

where i is the current density and ΔV is the voltage drop for one stack. (From Paper 3)

Figure 37 shows the area of AEM membrane required in a stack to recover phosphate from Aaby WWTP, and the power needed to move phosphate across the membrane. As seen in the figure, the slope of the line increases after 70% recovery. Consequently, it is more cost efficient to only recover up to 70% P.

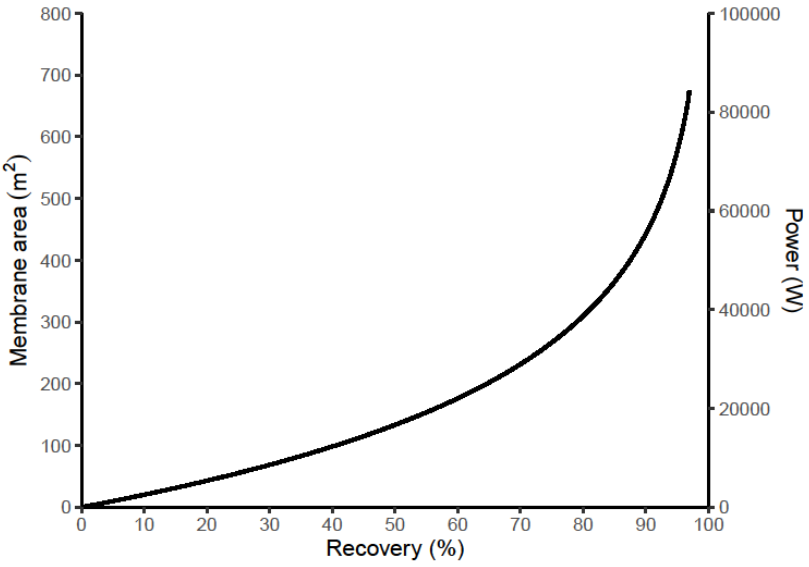

Figure 37 Membrane area and power required to recover P (Paper 3)

CHAPTER 6. ECONOMIC CASE STUDY – AABY WWTP

Aaby WWTP has a struvite recovery facility which treats $10m^3$ day^{-1} digester centrate, containing around 6 mM PO_4-P. The plant runs for 340 days a year. Costs have been calculated for both a forward osmosis and selectrodialysis system at Aaby WWTP. A number of assumptions have been made in order to simplify the costs involved in installing forward osmosis or selectiodialysis at Aaby WWTP, these are:

Forward osmosis:

- Membrane modules cost assumed to be €1320 ($1500), with each module being $27m^2$, price includes membrane housing (based on pricing by for Porifera Inc.) [187]

Selectrodialysis:

- Membrane cost based on those of 85% of those of lab-scale membranes purchased from PCCell GmbH (€347 per square meter for CEM and AEM membranes and €459 per square meter for MVA membranes (including 15% price reduction for bulk purchase)).
- Draw solution is seawater (pumping costs only) and WWTP is adjacent to coast (within 1km)
- Concentrate compartments are half the volume of diluate compartment.

General:

- Cost incurred by redundant (existing) equipment has been excluded.
- 5% loss of membrane area every 3 years [188].
- Maintenance costs calculated using 5% membrane area replacement plus 1 day (8 man hours for 2 men) of installation per 27 m^2 membrane module installed.
- General man-hour costs are estimated based on normal weekly checking of 1 hour per week.
- 1 man-hour is equal to €25
- 1 kWh costs €0.35.
- Bulk purchase of NaCl equates to cost of €133 ($150) per tonne [189].
- Cost of magnesium chloride €261 (1950 Danish Krone) per tonne (current price paid by Aaby WWTP).
- All P recovered is precipitated as struvite using a 1:1 Mg:P ratio.

- All costs converted to Euros (€) using x-rates.com and exchange rate at time of calculating (28.11.2018).

6.1. FORWARD OSMOSIS

6.1.1. MEMBRANE COSTS

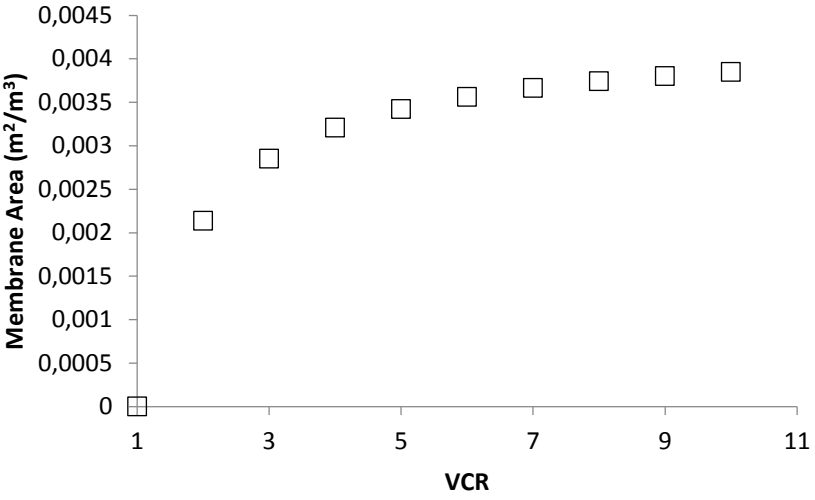

Figure 38 shows a cost estimate for TFC membrane. The membrane area required was based on the average water permeability, discussed in Chapter 4 (0.287 LMH bar^{-1} for TFC membranes). An osmotic pressure difference of 20 bar was assumed (seawater draw solution is capable of this osmotic pressure difference) and membrane area required was calculated using Equation 26. TFC membrane was only considered in this calculation because it had higher water permeability therefore requiring a smaller membrane area, resulting in a lower cost.

Equation 26

$$A_m = \frac{V_P}{J_W \, x \, t}$$

Where A_m is the membrane area (m^2), and V_P is the volume of permeate (L).

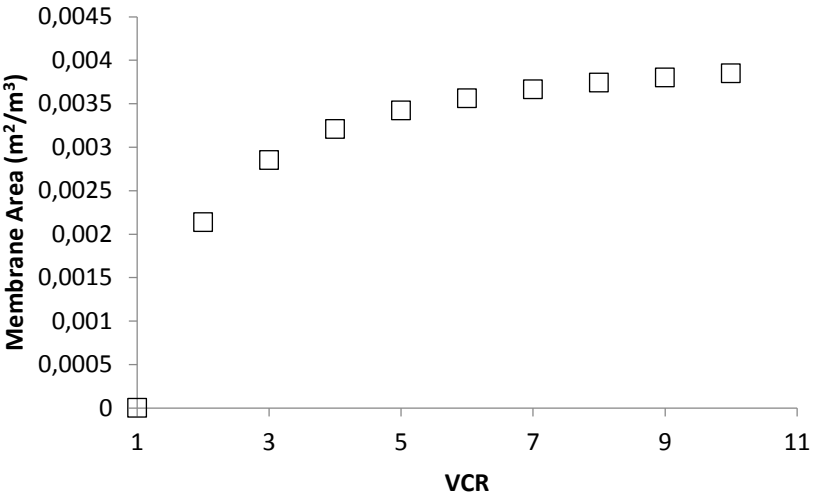

Figure 38 Membrane area per cubic meter digester centrate treated at Aaby WWTP using TFC membranes. Calculation based on a membrane flux of 5.7LMH.

In order to determine the membrane area required for forward osmosis, it is necessary to decide on an average flux the membrane is capable of achieving, and the VCR to which the draws solution will be concentrated.

Figure 39 shows the relationship between membrane costs per cubic meter of treated digester centrate by flux for various VCRs. From the figure it is possible to see the cost decreasing with increasing water flux. Since the average water flux when using TFC membranes was 5.2 LMH, a conservative water flux of 5 LMH was used for estimating the membrane area required. While a VCR of 7 was achieved using TFC membranes [124], theoretically a VCR of only 3 is required to reduce the P:Mg ratio from 1:1.3 to 1:1, therefore, in order to keep costs to a minimum a VCR of 4 is optimal as it ensures adequate concentration of phosphate, but does not require the time or energy demand of higher VCR.

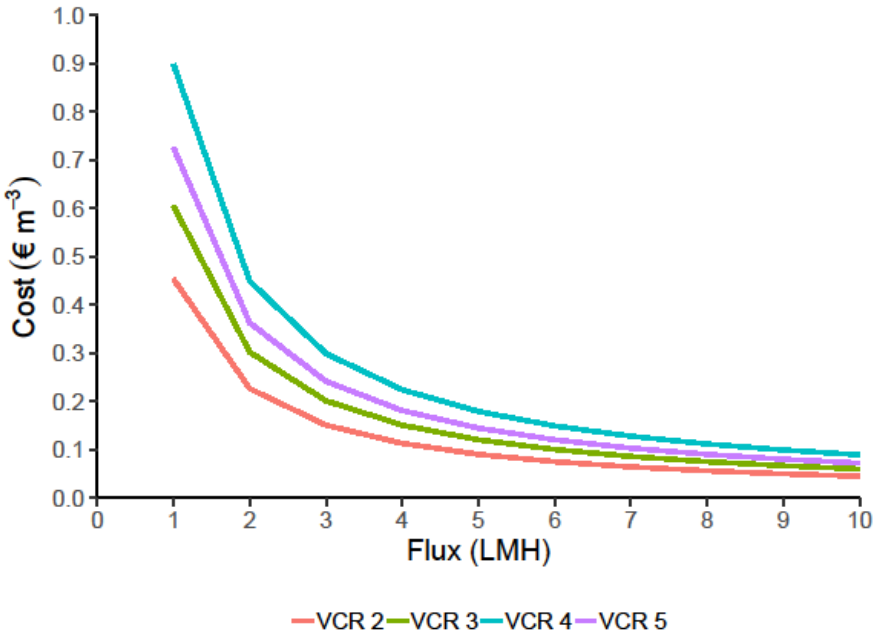

Figure 39 Membrane cost of treating digester centrate with as a function of flux for VCRs between 2 and 5

6.1.2. PUMPING COSTS

Pumping costs can be determined by calculating the energy required to move the feed or draw solution through a specific length of pipe, with a certain number of fittings or fixtures.

In order to determine the power required, the cross sectional area of the pipe must be calculated, using Equation 27. Where v is the free stream velocity (m s^{-1}), A is the cross sectional area of the pipe (m^2), and Q is the flow rate (m^3 s^{-1}). The pipe diameter can be calculated from A.

Equation 27

$$A = \frac{Q}{v}$$

After this the Reynolds number must be calculated to determine the flow type (laminar or turbulent). This was done using Equation 28:

Equation 28

$$Re = \frac{\rho v d}{\mu}$$

Where *Re* is the Reynolds number, ρ is the density (kg m^{-3}), d is the pipe diameter (m), and μ is the dynamic viscosity (Ns m^{-2}). For seawater draw solution the Reynolds number was calculated to be 4889.28, since it is >4000 the flow is considered turbulent, as such Moody's diagrams were consulted to determine the Darcy-Weisbach friction factor (λ) using relative pipe roughness (ε/d) of 0.04, giving a friction factor of 0.07. This was then used in Equation 29 to calculate the friction losses in the pipe. Where H_f is the loss of head due to friction (m), l is the pipe length (m), g is gravitational force (9.81 m s^{-2}).

Equation 29

$$H_f = \lambda \frac{l}{d} \frac{v^2}{2g}$$

This was calculated for up to 1000m of pipework. Next the fitting losses were calculated using Equation 30.

Equation 30

$$H = k_{fitting} \frac{v^2}{2g}$$

The fitting coefficient values ($k_{fitting}$) used are shown in Table 11.

Table 11 Fittings used to estimate head loss in pipe

Fitting	$k_{fitting}$	**Quantity**
Sharp edged entrance	0.5	1
Close radius 90 degree bend	0.75	2
Close radius 45 degree bend	0.3	2
Gate Valve (fully open)	0.12	1

Although through completing proper design work for the pipeline the number of fittings could change it has been assumed that the pipe would have an entrance, a number of bends and a gate valve to isolate the pump during maintenance.

H_f and H can then be combined with the static head loss (20m assumed in this case) to give the total head loss from which power (P) can be calculated using Equation 31.

Equation 31

$$P = \frac{Q\rho gH}{3.6 * 10^6}$$

From this the energy required can be determined, and then the cost.

Figure 40 shows the power and cost per cubic meter digester centrate treated for pumping seawater up to 1 km, assuming 20 m^3 day^{-1} is required. As seen, the cost is not significant compared to that of the membrane, as such, a pipeline of 1 km is feasible.

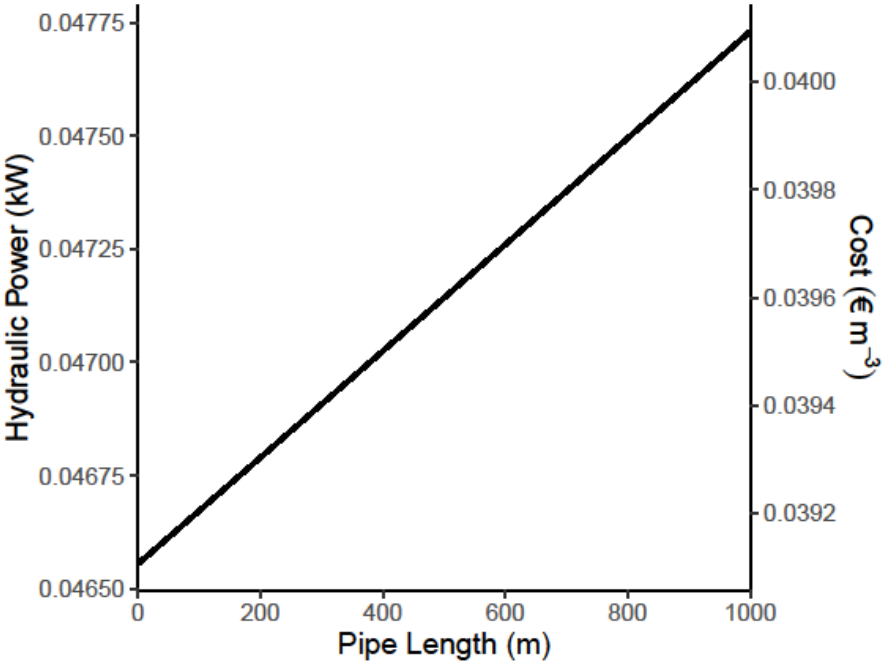

Figure 40 Cost and power demand of pumping seawater draw solution by distance

The pumping costs and power requirement were also calculated for digester centrate. However, Reynolds number was 3457.24, as such, the friction factor was calculated using the Swamee-Jain approximation. The simplified expression (Equation 32) was used as 5.74/Re0.9 << κ/3.7D (κ is the pipe roughness value (mm)) [190].

Equation 32

$$\lambda = \frac{0.25}{\left[\log\left(\frac{\kappa}{3.7\,d}\right)\right]^2}$$

As with draw solution, the power and cost for pumping digester centrate feed solution can be seen in

Figure 41. The cost is around half of that of seawater as $10m^3\ day^{-1}$ is being pumped rather than $20m^3\ day^{-1}$. It is unlikely that digester centrate will require pumping 1km, but it has been calculated to this distance for comparative purposes.

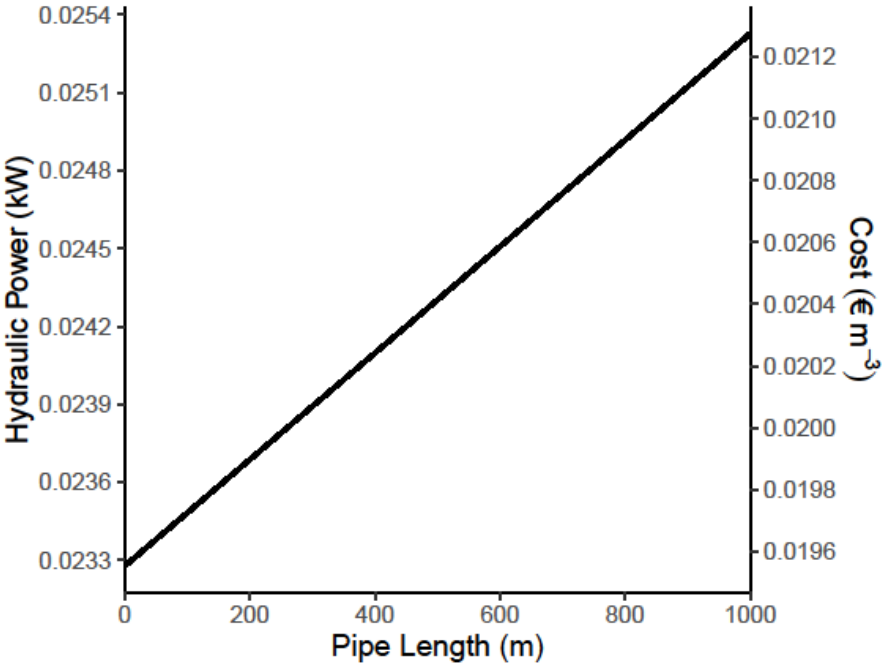

Figure 41 Cost and power demand of pumping digester centrate feed solution by distance

6.1.3. CAPITAL EXPENDITURE

The initial cost incurred a membrane plant, can be calculated using past projects. Capital expenditure (CAPEX) can be calculated without the initial cost of membranes using previous projects CAPEX excluding membranes (Equation 33) [191].

Equation 33

$$K_F = K_{FR}\left(\frac{A}{A_R}\right)^m$$

Where K_F is the plant costs for the new plant (€), K_{FR} is the plant cost for the existing plant (€), A is the membrane area for for the new plant (m^2), A_R is the membrane area for the existing plant (m^2), and m is the degrading exponent (0.8 for cross-flow plants). Data in Table 12 were used to calculate the plant costs at Aaby using Equation 33. The costs amounted to €52000.

Table 12 Data used to calculate plant costs for Aaby WWTP [187]

Element	Value
Equipment and materials (€)	17750000
Pumps (€)	5183000
Others (€)	32660000
Membrane Area (m^2)	416664

The final CAPEX cost is associated with construction. For previous forward osmosis plants construction costs have represented 48.1% of the CAPEX [187], as such ,it is possible to estimate them for Aaby WWTP using the membrane and plant costs. This gives a figure of €52000.

6.1.4. TOTAL COST

Table 13 shows the costs associated with implementing forward osmosis at Aaby WWTP for 20 years, one year, and the cost per cubic meter of treated digester centrate. The required membrane area was calculated using Equation 26. For a VCR of 4, and 10 m^3 day^{-1}, the permeate volume is equal to 7500 L in 24 hours. The membrane area calculated was 62.5 m^2, however, TFC membranes come in 27m^2 modules, as such, it would be necessary to base the cost on three of these modules (81 m^2), as two would not provide a large enough area. Similarly, when calculating membrane area loss, the module would not be able to be replaced until most of the area was lost, as such, it would only need to be replaced every 20 years.

Table 13 Costings associated with FO treatment at Aaby WWTP.

Cost (€)	20 years	1 year	Per cubic meter digester centrate treated
Plant	52000	2600	0.76
Construction	52000	2600	0.76
Power (seawater, 1km)	1300	65	0.02

Pumping (digester centrate, 50m)	2700	135	0.04
Initial membrane	4000	200	0.06
Membrane maintenance/ replacement	1300	65	0.02
Man-hours (maintenance)	400	20	0.01
Man-hours (general)	25000	1250	0.37
Magnesium Chloride (struvite precipitation)	10000	500	0.15
TOTAL	148700	7435	2.19

Figure 42 shows an estimate of cost for membranes, plant and construction for increasing membrane area. It assumes cost increases linearly with membrane area, i.e, it does not account for cost savings when bulk purchasing products/materials etc. Increasing costs suggest that forward osmosis may be suitable when dealing with small membrane area, but may not be cost effective for large membrane areas.

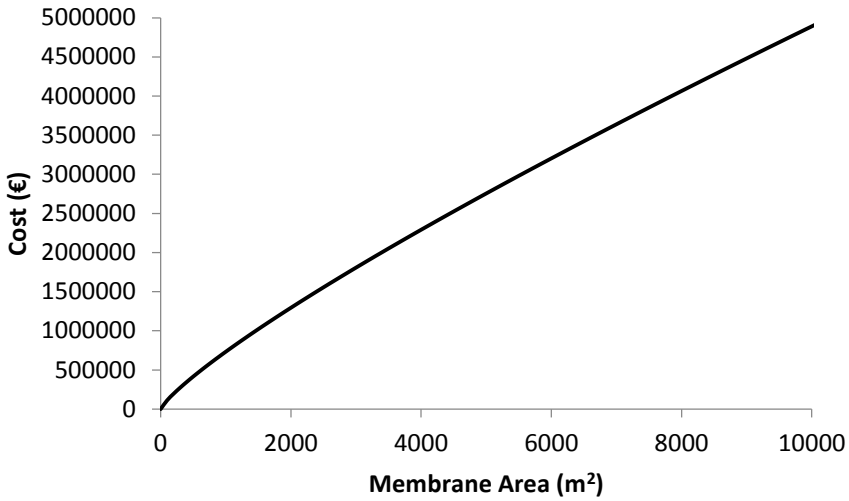

Figure 42 Membrane, plant and construction costs for increasing membrane area

6.2. SELECTRODIALYSIS

In order to cost for implementing selectrodialysis at Aaby WWTP it is necessary to determine the recovery in order to calculate membrane area and power needs.

Figure 43 shows the membrane and power costs for increasing recovery. As seen in the figure, the slope of both power and membrane costs increase after 70% recovery, therefore, increasing the cost of treatment. Consequently, it is practical to recover 70% phosphate and ammonium, but not higher (calculated using Equation 24).

In order to recover 70% a membrane area of 231.6m^2 is required for the AEM membrane. This has been calculated using the model discussed in Paper 3. Due to the membrane configuration used, each membrane will need to be 57.9 m^2 (the AEM membrane at the end of the stack does not count towards the 231.6 m^2 required as it is purely used to protect the electrode). A membrane stack containing 5no. AEM and CEM and 4no. MVA membranes were used, as per the setup used in Paper 3. Costings were calculated assuming this number of membranes was used, each with an area of 57.9m^2. The power consumption was calculated using Equation 25.

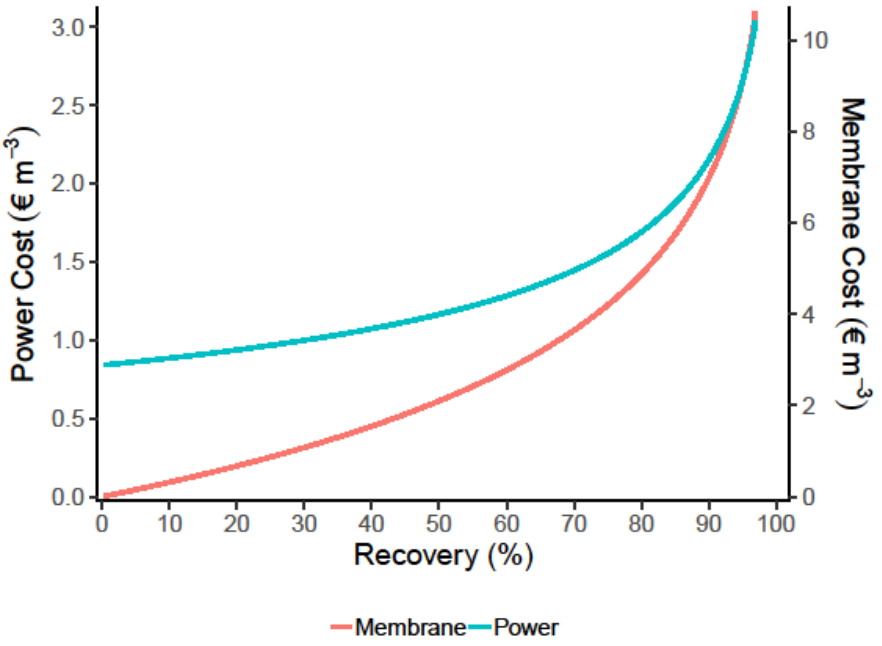

Figure 43 Membrane and power costs per m3 digester centrate treated using selectrodialysis

Costs associated with plant, construction, and pumping power were calculated in the same manner as forward osmosis, and are shown in Table 14.

Table 14 Costings associated with implementing selectrodialysis at Aaby WWTP.

Costs (€)	**20 years**	**1 year**	**Per cubic meter digester centrate treated**
Plant	140000	7000	2.06
Construction	130000.	6500	1.91
Power (pumping, diluate 50m)	1300	65	0.02
Power (pumping rinse, 50m	1300	65	0.02

Power (pumping anion concentrate 50m)	660	33	0.01
Power (pumping cation concentrate 50m)	660	33	0.01
Initial membrane	310000	15500	4.56
Power (across membrane stack)	100000	5000	1.47
Membrane maintenance	100000	5000	1.47
Man-hours (maintenance)	4000	200	0.06
Man-hours (general)	25000	1250	0.37
Magnesium chloride (struvite precipitation)	7000	350	0.10
Sodium chloride (concentrate streams)	90000	4500	1.32
TOTAL	909920	45496	13.38

Costs are generally higher for selectrodialyis, due to the need for multiple membranes (in the stack) and power needed to draw ions into the concentrate. The larger membrane area also increases the cost of plant and construction. However, the technology has a few benefits over forward osmosis. Selectrodialysis creates a 'pure' concentrate, as such there will be fewer issues with heavy metal contamination, or biological contamination in the product. Furthermore, as shown in Chapter 5, it is possible to concentrate ammonium and phosphate in separate concentrate streams, allowing a greater number of potential uses/customers.

6.3. OUTCOME

Aaby WWTP is capable of producing 300kg struvite per day, equal to 102 tonnes per year. Struvite has a potential sale value of €225 (£200) [83]. This equates to €67.50 per day, as such each cubic meter of digester centrate treated should cost less than €6.75 in order to secure a profit.

Therefore, from a purely cost-orientated view it would be beneficial to use forward osmosis at Aaby WWTP, however, in reality many other factors play a role in deciding which technology is suitable, such as;

- Available space.
- WWTP consents/restrictions (both volume and concentration).
- Available power supply.
- Training costs.
- Write-off cost of redundant equipment.
- Draw solution availability (i.e seawater).

Selectrodialysis, however, would not currently be a suitable option, as it is expensive (€13.38 per cubic meter digester centrate treated). However, as more selectrodialysis membranes enter the market costs are likely to decrease, which will make the technology more cost effective.

CHAPTER 7. CONCLUSION

Forward osmosis was capable of concentrating digester centrate for subsequent phosphorus recovery using TFC or biomimetic membrane. A VCR of 7 was achieved by concentrating digester centrate using seawater draw solution and TFC membrane. It was determined that theoretically a VCR of 3 is achievable using seawater with salinity >20PSU (corresponding to pressure of 15 atm). This would allow the reduction of added magnesium to a P:Mg ratio of 1:1 rather than 1:1.3 for un-concentrated digester centrate. The TFC membrane tested was found to have higher water permeability than biomimetic membranes, 0.092 and 0.29 LMH bar^{-1} for biomimetic and TFC membranes respectively when concentrating digester centrate. However, biomimetic membranes exhibited a smaller water permeability difference between deionized water and digester centrate feed solutions.

Membrane fouling was not observed during a 68 hour (3x 22 hour digester centrate concentrating plus 2x 1 hour cleaning cycles using deionized water) operating period when using TFC membranes. Water permeability remained steady during both cleaning cycles.

Ortho-P permeability was seen to decrease with increasing pH, corresponding to increasing charge on the phosphoric acid species. This is likely due to the membrane relying on charge rejection. TFC membranes had average P rejection of 99.5%.

Conversely, ammoniacal nitrogen flux increased with increasing pH, as ammonium becomes ammonia, which is uncharged and not as easily rejected by the membrane. Furthermore, ammonium flux is supported by reverse Na^+ flux and Cl^- flux. Ammoniacal nitrogen contamination of a seawater draw means it would need treatment prior to discharge, therefore using seawater as a method to make forward osmosis cost effective for phosphorus recovery is not viable with membranes currently on the market. Using Aaby WWTP as an example, this corresponds to 41% and 46% ammoniacal nitrogen lost using biomimetic and TFC membranes, respectively.

Selectrodialysis is an alternative method where phosphate and ammonia can be concentrated in a ‘pure’ concentrate compartment. This separates ammonia and phosphorus from bacteria and some heavy metals in digester centrate. The membrane configuration used allowed ammonia and phosphate to be concentrated in separate concentrate streams. Cross-contamination between the concentrate streams was not observed. Initial recovery rates were measured to be 0.072 mmol $m^{-2}s^{-1}$ and 1.31 mmol m^{-2} s^{-1} for phosphate and ammonium respectively. With an average recovery of 72±0.4% and 90±10% for ammonium and phosphate observed after 3 h of operation. Ammonium recovery rate was 18 times higher than that for phosphate,

however, the ammonium concentration was a similar magnitude higher than phosphate.

Through modelling, it was determined that an AEM membrane area of 231.6 m^2 is required for 70% recovery, corresponding to a power requirement of 289044 W to treat digester centrate from Aaby WWTP. In order to optimize phosphate recovery, pH in the diluate should be kept low in order to dissolve phosphorus products formed at high pH, thus allowing their recovery.

From cost calculations, it was estimated that forward osmosis using TFC membrane at Aaby will cost €2.19 per cubic meter digester centrate treated, while selectrodialysis costs €13.38. In order to be cost effective cost of treatment must be <€6.75, as such selectrodialysis would not currently be a cost effective solution. Decreasing membrane costs and area would make selectrodialysis more cost appropriate as this would decrease maintenance, man –hour, and build costs.

NOMENCLATURE

Symbol/Abbreviation	Definition	Unit
EBPR	Enhanced biological phosphorus removal	-
PE	Population equivalent	-
WWTP	Wastewater treatment plant	-
	Forward Osmosis	
a_w	Water activity	-
A	Water permeability	LMH bar^{-1}
A_m	Membrane area	m^2
B	Salt permeability coefficient	$m^2\ s^{-1}$
C_{Feed}	Feed concentration	M
$C_{s,F,initial}$	Initial feed concentration	M
$C_{s,F,final}$	Final feed concentration	M
d_h	Hydraulic diameter	m
D	Diameter	m
i	Dissociation factor	-
J_w	Water flux	L $m^{-2}\ h^{-1}$ (LMH)
J_i	Ion flux	mmol $m^{-2}\ h^{-1}$ or g $m^{-2}\ h^{-1}$ (gMH)
$-J_{Na^+}$	Reverse sodium flux	mmol $m^{-2}\ h^{-1}$ or g $m^{-2}\ h^{-1}$ (gMH)
$J_{NH_4^+}$	Ammonium flux	mmol $m^{-2}\ h^{-1}$ or g $m^{-2}\ h^{-1}$ (gMH)
J_s	Reverse salt flux	mmol $m^{-2}\ h^{-1}$ or g $m^{-2}\ h^{-1}$ (gMH)
k	Mass transfer coefficient	-
K_a	Dissociation constant	M
L	Length of pipe or channel	m
M	Molarity	M
R	Ideal gas constant	L bar $mol^{-1}\ K^{-1}$
Re	Reynolds number	-
$R\ (\%)$	Rejection	%
Sc	Schmidt number	-
Sh	Sherwood number	-
t	time	hours
t_m	Membrane thickness	m
T	Temperature	K

V_{final}	Final volume	L
$V_{initial}$	Initial volume	L
V_m	Partial molar volume of water	m^3
ε	Membrane porosity	-
$\alpha_{NH_4^+}$	Percentage of ammoniacal nitrogen as ammonium	%
λ	Ratio of ammonical nitrogen flux to sodium flux	-
$\pi_{D,b}$	Osmotic pressure of draw solution	Bar
$\pi_{F,b}$	Osmotic pressure of feed solution	Bar
τ	Tortuosity of support layer	-
AL-FS	Active layer facing feed solution	-
AL-DS	Active layer facing draw solution	-
CNT	Carbon nanotube	-
CTA	Cellulose triacetate	-
ECP	External concentration polarization	-
HTI	Hydration technology industries	-
ICP	Internal concentration polarization	-
PAO	Pressure assisted osmosis	-
PSU	Practical salinity unit	$g\ kg^{-1}$
S	Membrane structural parameter	-
TFC	Thin-film composite	-
VCR	Volume concentration ratio	-

Selectrodialysis

A_{cell}	Area of cell	m^2
C	Concentration	M
C_A	Concentration of ion A	M
C_B	Concentration of ion B	M
$C_{C,i}$	Initial concentration in concentrate compartment	M
$C_{C,t}$	Concentration in concentrate compartment at time t	M
$C_{D,i}$	Initial concentration in diluate compartment	M
CE	Current efficiency	%
D	Diffusion coefficient	-
E	Energy supplied	J
E_m	Potential difference across cell	V
F	Faradays constant	$A{\cdot}s{\cdot}mol^{-1}$
i	Current density	$V\ m^{-2}$

i_{lim}	Limiting current density	A m^{-2}
I	Applied current	A
J	Ion flux	g m^{-2} h^{-1} (gMH)
m_A	Total weight of transferred ion	g
M_A	Molar mass of ion	g
n	Number of cell trios	-
Q	Flow rate	m^3 s^{-1}
R	Ideal gas constant	L bar mol^{-1} K^{-1}
S_B^A	Separation efficiency	-
t	time	S
t_i'	Membrane transport number	-
t_m	Ion transport number in membrane	-
t_s	Ion transport number in solution	-
T	Temperature	K
V_{cell}	Cell volume	m^3
$V_{C,i}$	Initial volume in concentrate compartment	L
$V_{C,t}$	Volume in concentrate compartment at time t	L
V_D	Diluate volume	L
$V_{D,i}$	Initial volume in diluate compartment	L
z_A	Charge on ion	-
δ	Boundary layer thickness	m
ΔV	Voltage drop	V
AEM	Anion exchange membrane	-
CEM	Cation exchange membrane	-
MVA	Monovalent anion exchange membrane	-
MVC	Monovalent cation exchange membrane	-

Economic Case Study

A	Membrane area of new plant	m^2
A_m	Membrane area	m^2
A_R	Membrane area of existing plant	m^2
d	Pipe diameter	m
g	Gravitational constant	m s^{-2}
H	Headloss	m
H_f	Headloss due to friction	M
J_W	Water flux	L m^{-2} h^{-1} (LMH)

$k_{fitting}$	Fitting coefficient	-
K_F	Plant costs for new plant	€
K_{FR}	Plant costs for existing plant	€
l	Pipe length	m
m	Degrading exponent	-
P	Power	W
Q	Flow rate	$m^3\ s^{-1}$
Re	Reynolds number	-
t	Time	hours
v	Free stream velocity	$m\ s^{-1}$
V_P	Permeate volume	L
κ	Pipe roughness	mm
λ	Friction coefficient	-
μ	Dynamic viscosity	$Ns\ m^{-2}$
ρ	density	$Kg\ m^{-3}$
CAPEX	Capital expenditure	-

LITERATURE LIST

[1] J. Elser, E. Bennett, A broken biogeochemical cycle, Nature. 478 (2011) 29. https://doi.org/10.1038/478029a.

[2] D. Cordell, J.O. Drangert, S. White, The story of phosphorus: Global food security and food for thought, Glob. Environ. Chang. 19 (2009) 292–305. doi:10.1016/j.gloenvcha.2008.10.009.

[3] P. Dery, B. Anderson, Peak Phosphorus, Energy Bull. (2007). http://www.greb.ca/GREB/Publications_files/Peakphosphorus.pdf (accessed January 25, 2019).

[4] D. Cordell, S. White, D. Cordell, S. White, Peak Phosphorus: Clarifying the Key Issues of a Vigorous Debate about Long-Term Phosphorus Security, Sustainability. 3 (2011) 2027–2049. doi:10.3390/su3102027.

[5] S. Van Kauwenbergh, World Phosphate reserves and Resources, (2010).

[6] D.E.C. Corbridge, Phosphorus: Chemistry, Biochemistry and Technology, Sixth Edit, CRC Press, 2013.

[7] C. Lu, H. Tian, Global nitrogen and phosphorus fertilizer use for agriculture production in the past half century: shifted hot spots and nutrient imbalance, Earth Ststem Sci. Data. 9 (2017) 181–192.

[8] Mosaic, Crop Nutrition, (2018). https://www.cropnutrition.com/efu-phosphorus (accessed December 13, 2018).

[9] J.A. Foley, R. DeFries, G.P. Asner, C. Barford, G. Bonan, S.R. Carpenter, F.S. Chapin, M.T. Coe, G.C. Daily, H.K. Gibbs, J.H. Helkowski, T. Holloway, E.A. Howard, C.J. Kucharik, C. Monfreda, J.A. Patz, I.C. Prentice, N. Ramankutty, P.K. Snyder, Global Consequences of Land Use, Science (80-.). 309 (2005) 570 LP-574. doi:10.1126/science.1111772.

[10] D. Teegarden, R.M. Lyle, G.P. McCabe, L.D. McCabe, W.R. Proulx, K. Michon, A.P. Knight, C.C. Johnston, C.M. Weaver, Dietary calcium, protein, and phosphorus are related to bone mineral density and content in young women, Am. J. Clin. Nutr. 68 (1998) 749–754. http://dx.doi.org/10.1093/ajcn/68.3.749.

[11] J.. Schröder, D. Cordell, A.. Smit, A. Rosemarin, Sustainable Use of Phosphorus, Wageningen, 2009. http://ec.europa.eu/environment/natres/pdf/phosphorus/sustainable_use_pho

sphorus.pdf.

[12] OECD, Material Resources, Productivity and the Environment, Paris, 2015.

[13] H. Depoorter, J. Nys, A. Van Dormael, New classes of phosphorus-containing dyes, Tetrahedron Lett. 2 (1961) 199–205. doi:10.1016/S0040-4039(01)99231-7.

[14] M.R. Reidmeyer, M. Rajaram, D.E. Day, Preparation of phosphorus oxynitride glasses, J. Non. Cryst. Solids. 85 (1986) 186–203. doi:10.1016/0022-3093(86)90090-6.

[15] G. Lusvardi, G. Malavasi, F. Tarsitano, L. Menabue, M.C. Menziani, A. Pedone, Quantitative Structure−Property Relationships of Potentially Bioactive Fluoro Phospho-silicate Glasses, J. Phys. Chem. B. 113 (2009) 10331–10338. doi:10.1021/jp809805z.

[16] D.C.G. Muir, Phosphate Esters. In: Anthropogenic Compounds, in: PThe Handb. Environ. Chem. Vol 3 / 3C, Springer, Berlin, Heidelberg, 1984. doi:https://doi.org/10.1007/978-3-540-38819-7_2.

[17] A.M. Cook, C.G. Daughton, M. Alexander, Phosphorus-containing pesticide breakdown products: quantitative utilization as phosphorus sources by bacteria, Appl. Environ. Microbiol. 36 (1978) 668–672. https://www.ncbi.nlm.nih.gov/pubmed/727784.

[18] P.M. Smith, Review of Chemistry of Pyrotechnics: Basic Principles and Theory, J. Chem. Educ. 89 (2012) 698. doi:10.1021/ed3001864.

[19] Ș.-B. Ivan, I. Popescu, I. Fechete, F. Garin, V.I. Pârvulescu, I.-C. Marcu, The effect of phosphorus on the catalytic performance of nickel oxide in ethane oxidative dehydrogenation, Catal. Sci. Technol. 6 (2016) 6953–6964. doi:10.1039/C6CY00946H.

[20] R.W. Keyes, The Electrical Properties of Black Phosphorus, Phys. Rev. 92 (1953) 580–584. doi:10.1103/PhysRev.92.580.

[21] H.Z. Toama, World Phosphate Industry, Iraqi Bull. Geol. Min. Special Is (2017) 5–23.

[22] P. Logue, Industrial uses of phosphates., J. Chem. Educ. 23 (1946) 529. doi:10.1021/ed023p529.

[23] Y. Jaffer, T.. Clark, P. Pearce, S.. Parsons, Potential phosphorus recovery by

struvite formation, Water Res. 36 (2002) 1834–1842. doi:10.1016/S0043-1354(01)00391-8.

[24] L. Egle, H. Rechberger, J. Krampe, M. Zessner, Phosphorus recovery from municipal wastewater: An integrated comparative technological, environmental and economic assessment of P recovery technologies, Sci. Total Environ. 571 (2016) 522–542. doi:10.1016/J.SCITOTENV.2016.07.019.

[25] R. Cho, Phosphorus: Essential to Life—Are We Running Out?, State Planet, Earth Institute, Columbia Univ. (2013). https://blogs.ei.columbia.edu/2013/04/01/phosphorus-essential-to-life-are-we-running-out/ (accessed January 21, 2019).

[26] G. Reta, X. Dong, Z. Li, B. Su, X. Hu, H. Bo, D. Yu, H. Wan, J. Liu, Y. Li, G. Xu, K. Wang, S. Xu, Environmental impact of phosphate mining and benefication: review, Int. J. Hydrol. 2 (2018) 424–431.

[27] T. Hvitved-Jacobsen, N.B. Johansen, Y.A. Yousef, Treatment systems for urban and highway run-off in Denmark, Sci. Total Environ. 146–147 (1994) 499–506. doi:10.1016/0048-9697(94)90275-5.

[28] E. White, A.R. Gibson, Phosphorus and nitrate run-off in hill pasture and forest catchments, Taita, New Zealand AU - McColl, R. H. S., New Zeal. J. Mar. Freshw. Res. 11 (1977) 729–744. doi:10.1080/00288330.1977.9515709.

[29] K.A. Smith, D.R. Jackson, P.J.A. Withers, Nutrient losses by surface run-off following the application of organic manures to arable land. 2. Phosphorus, Environ. Pollut. 112 (2001) 53–60. doi:10.1016/S0269-7491(00)00098-1.

[30] G.M. Barnett, Phosphorus forms in animal manure, Bioresour. Technol. 49 (1994) 139–147. doi:10.1016/0960-8524(94)90077-9.

[31] N.R. Gollehon, M. Caswell, M. Ribaudo, R.L. Kellogg, C. Lander, D. Letson, Confined Animal Production and Manure Nutrients, Agric. Inf. Bull. 33763 United States Dep. Agric. Econ. Res. Serv. (2001).

[32] S.M. Heilmann, J.S. Molde, J.G. Timler, B.M. Wood, A.L. Mikula, G. V Vozhdayev, E.C. Colosky, K.A. Spokas, K.J. Valentas, Phosphorus Reclamation through Hydrothermal Carbonization of Animal Manures, Environ. Sci. Technol. 48 (2014) 10323–10329. doi:10.1021/es501872k.

[33] E. Desmidt, K. Ghyselbrecht, Y. Zhang, L. Pinoy, B. Van der Bruggen, W.

Verstraete, K. Rabaey, B. Meesschaert, Global Phosphorus Scarcity and Full-Scale P-Recovery Techniques: A Review, Crit. Rev. Environ. Sci. Technol. 45 (2015) 336–384. doi:10.1080/10643389.2013.866531.

[34] P.M.J. Janssen, K. Meinema, H.F. van der Roest, Biological Phosphorus Removal: Manual for design and operation, First, IWA Publishing, London, 2002.

[35] L. Ju, H. Shah, J. Porteous, Phosphorus release in aerobic sludge digestion., Water Env. Res. 77 (2005) 553–9.

[36] I. Metcalf & Eddy, Wastewater engineering : treatment and reuse, Fourth edition / revised by George Tchobanoglous, Franklin L. Burton, H. David Stensel. Boston : McGraw-Hill, [2003] ©2003, n.d. https://search.library.wisc.edu/catalog/999935704402121.

[37] G. Thelin, eco:P, eco:N, eco:S Resource recovery from organic waste products, (2018).

[38] P. Balslev, Phosphogreen technology, (2018).

[39] C. Meyer, V. Preyl, H. Steinmetz, R. Maier, W., Mohn, H. Schönberger, The Stuttgart Process (Germany), in: Phosphorus Recover. Recycl., Springer, Singapore, 2018. doi:https://doi.org/10.1007/978-981-10-8031-9_19.

[40] A. Amann, O. Zoboli, J. Krampe, H. Rechberger, M. Zessner, L. Egle, Environmental impacts of phosphorus recovery from municipal wastewater, Resour. Conserv. Recycl. 130 (2018) 127–139. doi:10.1016/J.RESCONREC.2017.11.002.

[41] K. Stendahl, S. Jäfverström, Recycling of sludge with the Aqua Reci process, Water Sci. Technol. 49 (2004) 233–240. doi:10.2166/wst.2004.0652.

[42] A. Campos, J. Judex, P-recovery potential from thermal gasified sludge, Phosphorus Recover. from Wastewater, with Focus Potential Thermochem. Sludge Treat. Work. (2018).

[43] E. Sellering, P-recovery with Pyreg, (2018).

[44] L. Rossi, Phosphorus recovery in Finland, (2018).

[45] T. Schaaf, A. Orth, Outotec AshDec Process, (2018).

[46] Y. Cohen, Ash2Phos Clean commercial phosphorus products from sewage sludge ash, (2018).

[47] S. Donatello, C.R. Cheeseman, Recycling and recovery routes for incinerated sewage sludge ash (ISSA): A review, Waste Manag. 33 (2013) 2328–2340. doi:10.1016/J.WASMAN.2013.05.024.

[48] J. Arundel, Sewage and industrial effluent treatment: a practical guide., Oxford, 1995.

[49] M. Cyr, M. Coutand, P. Clastres, Technological and environmental behavior of sewage sludge ash (SSA) in cement-based materials, Cem. Concr. Res. 37 (2007) 1278–1289. doi:10.1016/J.CEMCONRES.2007.04.003.

[50] A. Amann, O. Zoboli, J. Krampe, H. Rechberger, M. Zessner, L. Egle, Environmental impacts of phosphorus recovery from municipal wastewater, Resour. Conserv. Recycl. 130 (2018) 127–139. doi:10.1016/J.RESCONREC.2017.11.002.

[51] P.M. Melia, A.B. Cundy, S.P. Sohi, P.S. Hooda, R. Busquets, Trends in the recovery of phosphorus in bioavailable forms from wastewater, Chemosphere. 186 (2017) 381–395. doi:10.1016/J.CHEMOSPHERE.2017.07.089.

[52] H. Herzel, O. Krüger, L. Hermann, C. Adam, Sewage sludge ash — A promising secondary phosphorus source for fertilizer production, Sci. Total Environ. 542 (2016) 1136–1143. doi:10.1016/J.SCITOTENV.2015.08.059.

[53] P.S. Kidd, M.J. Domínguez-Rodríguez, J. Díez, C. Monterroso, Bioavailability and plant accumulation of heavy metals and phosphorus in agricultural soils amended by long-term application of sewage sludge, Chemosphere. 66 (2007) 1458–1467. doi:10.1016/J.CHEMOSPHERE.2006.09.007.

[54] L. Tuhy, M. Samoraj, K. Chojnacka, Evaluation of nutrients bioavailability from fertilizers in in vivo tests, Interdiscip. J. Eng. Sci. 1 (2013) 10–13.

[55] P. Guedes, N. Couto, L.M. Ottosen, A.B. Ribeiro, Phosphorus recovery from sewage sludge ash through an electrodialytic process, Waste Manag. 34 (2014) 886–892. doi:10.1016/J.WASMAN.2014.02.021.

[56] B. Ebbers, L.M. Ottosen, P.E. Jensen, Comparison of two different electrodialytic cells for separation of phosphorus and heavy metals from sewage sludge ash, Chemosphere. 125 (2015) 122–129.

doi:10.1016/J.CHEMOSPHERE.2014.12.013.

[57] M. Takahashi, S. Kato, H. Shima, E. Sarai, T. Ichioka, S. Hatyakawa, H. Miyajiri, Technology for recovering phosphorus from incinerated wastewater treatment sludge, Chemosphere. 44 (2001) 23–29. doi:10.1016/S0045-6535(00)00380-5.

[58] W. Xue, T. Tobino, F. Nakajima, K. Yamamoto, Seawater-driven forward osmosis for enriching nitrogen and phosphorous in treated municipal wastewater: effect of membrane properties and feed solution chemistry., Water Res. 69 (2015) 120–30. doi:10.1016/j.watres.2014.11.007.

[59] G.. Morse, S.. Brett, J.. Guy, J.. Lester, Review: Phosphorus removal and recovery technologies, Sci. Total Environ. 212 (1998) 69–81. doi:10.1016/S0048-9697(97)00332-X.

[60] S. Donatello, D. Tong, C.R. Cheeseman, Production of technical grade phosphoric acid from incinerator sewage sludge ash (ISSA), Waste Manag. 30 (2010) 1634–1642. doi:https://doi.org/10.1016/j.wasman.2010.04.009.

[61] T. Schütte, C. Niewersch, T. Wintgens, S. Yüce, Phosphorus recovery from sewage sludge by nanofiltration in diafiltration mode, J. Memb. Sci. 480 (2015) 74–82. doi:10.1016/J.MEMSCI.2015.01.013.

[62] S. Petzet, B. Peplinski, P. Cornel, On wet chemical phosphorus recovery from sewage sludge ash by acidic or alkaline leaching and an optimized combination of both, Water Res. 46 (2012) 3769–3780. doi:10.1016/J.WATRES.2012.03.068.

[63] A.M. Rawn, Multiple-Stage Sewage Sludge Digestion, Proc. Am. Soc. Civ. Eng. 63 (1937) 1673–1700.

[64] J.D. Doyle, S.A. Parsons, Struvite formation, control and recovery, Water Res. 36 (2002) 3925–3940. doi:10.1016/S0043-1354(02)00126-4.

[65] W.G. Breck, Water chemistry (Snoeyink, V. L.; Jenkins, D.), J. Chem. Educ. 58 (1981) A382. doi:10.1021/ed058pA382.2.

[66] C. V. Booram, R. J. Smith, T. E. Hazen, Crystalline Phosphate Precipitation from Anaerobic Animal Waste Treatment Lagoon Liquors, Trans. ASAE. 18 (1975) 340–343. doi:https://doi.org/10.13031/2013.36584.

[67] N.A. Booker, A.J. Priestley, I.H. Fraser, Struvite Formation in Wastewater Treatment Plants: Opportunities for Nutrient Recovery, Environ. Technol.

20 (1999) 777–782. doi:10.1080/09593332008616874.

[68] J. R. Buchanan, C. R. Mote, R. B. Robinson, Struvite Control by Chemical Treatment, Trans. ASAE. 37 (1994) 1301–1308. doi:https://doi.org/10.13031/2013.28211.

[69] J. R. Buchanan, C. R. Mote, R. B. Robinson, Thermodynamics of Struvite Formation, Trans. ASAE. 37 (1994) 617–621. doi:https://doi.org/10.13031/2013.28121.

[70] K.N. Ohlinger, T.M. Young, E.D. Schroeder, Predicting struvite formation in digestion, Water Res. 32 (1998) 3607–3614. doi:10.1016/S0043-1354(98)00123-7.

[71] A.C. Quist-Jensen, M. Koustrup Jørgensen, L.M. Christensen, Treated Seawater as a Magnesium Source for Phosphorous Recovery from Wastewater—A Feasibility and Cost Analysis, Membr. . 6 (2016). doi:10.3390/membranes6040054.

[72] P. Battistoni, P. Pavan, M. Prisciandaro, F. Cecchi, Struvite crystallization: a feasible and reliable way to fix phosphorus in anaerobic supernatants, Water Res. 34 (2000) 3033–3041. doi:10.1016/S0043-1354(00)00045-2.

[73] I. Stratful, S. Brett, M.B. Scrimshaw, J.N. Lester, Biological Phosphorus Removal, Its Role in Phosphorus Recycling, Environ. Technol. 20 (1999) 681–695. doi:10.1080/09593332008616863.

[74] J.L. Pérez Rodriguez, C. Maqueda, J. Lebrato, M.I. Carretero, Influence of clay minerals, used as supports in anaerobic digesters, in the precipitation of struvite, Water Res. 26 (1992) 497–506. doi:10.1016/0043-1354(92)90051-5.

[75] K. Suzuki, Y. Tanaka, K. Kuroda, D. Hanajima, Y. Fukumoto, Recovery of phosphorous from swine wastewater through crystallization, Bioresour. Technol. 96 (2005) 1544–1550. doi:10.1016/J.BIORTECH.2004.12.017.

[76] O.K. N., Y.T. M., S.E. D., Postdigestion Struvite Precipitation Using a Fluidized Bed Reactor, J. Environ. Eng. 126 (2000) 361–368. doi:10.1061/(ASCE)0733-9372(2000)126:4(361).

[77] Y.-H. Song, G.-L. Qiu, P. Yuan, X.-Y. Cui, J.-F. Peng, P. Zeng, L. Duan, L.-C. Xiang, F. Qian, Nutrients removal and recovery from anaerobically digested swine wastewater by struvite crystallization without chemical additions, J. Hazard. Mater. 190 (2011) 140–149.

doi:10.1016/J.JHAZMAT.2011.03.015.

[78] P. Battistoni, C. Morini, P. Pavan, F. Latini, The Retrofitting of an Extended Aeration Process to Optimise Biological Nitrogen Removal in Liquid Industrial Wastes, Environ. Technol. 20 (1999) 563–573. doi:10.1080/09593332008616851.

[79] B.J.C. Bergmans, A.M. Veltman, M.C.M. van Loosdrecht, J.B. van Lier, L.C. Rietveld, Struvite formation for enhanced dewaterability of digested wastewater sludge, Environ. Technol. 35 (2014) 549–555. doi:10.1080/09593330.2013.837081.

[80] E. V Münch, K. Barr, Controlled struvite crystallisation for removing phosphorus from anaerobic digester sidestreams, Water Res. 35 (2001) 151–159. doi:10.1016/S0043-1354(00)00236-0.

[81] X. Liu, Z. Hu, J. Mu, H. Zang, L. Liu, Phosphorus recovery from urine with different magnesium resources in an air-agitated reactor, Environ. Technol. 35 (2014) 2781–2787. doi:10.1080/09593330.2014.921732.

[82] Y. Matsumiya, T. Yamasita, Y. Nawamura, Phosphorus Removal from Sidestreams by Crystallisation of Magnesium-Ammonium-Phosphate Using Seawater, Water Environ. J. 14 (2000) 291–296. doi:10.1111/j.1747-6593.2000.tb00263.x.

[83] Y. Jaffer, T.. Clark, P. Pearce, S.. Parsons, Potential phosphorus recovery by struvite formation, Water Res. 36 (2002) 1834–1842. doi:10.1016/S0043-1354(01)00391-8.

[84] A. Guadie, S. Xia, W. Jiang, L. Zhou, Z. Zhang, S.W. Hermanowicz, X. Xu, S. Shen, Enhanced struvite recovery from wastewater using a novel cone-inserted fluidized bed reactor, J. Environ. Sci. 26 (2014) 765–774. doi:10.1016/S1001-0742(13)60469-6.

[85] B. Li, I. Boiarkina, B. Young, W. Yu, Substance Flow Analysis of Phosphorus in China, Int. J. Environ. Sci. Dev. 6 (2015) 9–13.

[86] Y. Wang, S.-J. Zheng, L.-Y. Pei, L. Ke, D. Peng, S.-Q. Xia, Nutrient release, recovery and removal from waste sludge of a biological nutrient removal system, Environ. Technol. 35 (2014) 2734–2742. doi:10.1080/09593330.2014.920048.

[87] X. Li, J. Li, Dead-End Filtration BT - Encyclopedia of Membranes, in: E. Drioli, L. Giorno (Eds.), Springer Berlin Heidelberg, Berlin, Heidelberg,

2015: pp. 1–3. doi:10.1007/978-3-642-40872-4_2196-1.

[88] GE, Cross Flow Filtration Method Handbook, n.d. https://cdn.gelifesciences.com/dmm3bwsv3/AssetStream.aspx?mediaformatid=10061&destinationid=10016&assetid=17054.

[89] K. Lutchmiah, A.R.D. Verliefde, K. Roest, L.C. Rietveld, E.R. Cornelissen, Forward osmosis for application in wastewater treatment: a review., Water Res. 58 (2014) 179–97. doi:10.1016/j.watres.2014.03.045.

[90] T.-S. Chung, S. Zhang, K.Y. Wang, J. Su, M.M. Ling, Forward osmosis processes: Yesterday, today and tomorrow, Desalination. 287 (2012) 78–81. doi:10.1016/J.DESAL.2010.12.019.

[91] Forward osmosis: Principles, applications, and recent developments, J. Memb. Sci. 281 (2006) 70–87. doi:10.1016/J.MEMSCI.2006.05.048.

[92] J.R. McCutcheon, M. Elimelech, Influence of concentrative and dilutive internal concentration polarization on flux behavior in forward osmosis, J. Memb. Sci. 284 (2006) 237–247. doi:10.1016/j.memsci.2006.07.049.

[93] G.T. Gray, J.R. McCutcheon, M. Elimelech, Internal concentration polarization in forward osmosis: role of membrane orientation, Desalination. 197 (2006) 1–8. doi:10.1016/J.DESAL.2006.02.003.

[94] M. Mulder, Basic Principles of Membrane Technology, Springer Netherlands, Enschede, 1991. doi:10.1007/978-94-017-0835-7.

[95] C.Y. Tang, Q. She, W.C.L. Lay, R. Wang, A.G. Fane, Coupled effects of internal concentration polarization and fouling on flux behavior of forward osmosis membranes during humic acid filtration, J. Memb. Sci. 354 (2010) 123–133. doi:10.1016/J.MEMSCI.2010.02.059.

[96] E. Cornelissen, D. Harmsen, K. Dekorte, C. Ruiken, J. Qin, H. Oo, L. Wessels, Membrane fouling and process performance of forward osmosis membranes on activated sludge, J. Memb. Sci. 319 (2008) 158–168. doi:10.1016/j.memsci.2008.03.048.

[97] J.T. Arena, S.S. Manickam, K.K. Reimund, B.D. Freeman, J.R. McCutcheon, Solute and water transport in forward osmosis using polydopamine modified thin film composite membranes, Desalination. 343 (2014) 8–16. doi:10.1016/J.DESAL.2014.01.009.

[98] J. Heikkinen, H. Kyllönen, E. Järvelä, A. Grönroos, C.Y. Tang, Ultrasound-

assisted forward osmosis for mitigating internal concentration polarization, J. Memb. Sci. 528 (2017) 147–154. doi:10.1016/j.memsci.2017.01.035.

[99] J.C. Ortega-Bravo, G. Ruiz-Filippi, A. Donoso-Bravo, I.E. Reyes-Caniupán, D. Jeison, Forward osmosis: Evaluation thin-film-composite membrane for municipal sewage concentration, Chem. Eng. J. 306 (2016) 531–537. doi:10.1016/j.cej.2016.07.085.

[100] W. Xue, K. Yamamoto, T. Tobino, Membrane Fouling and Long-Term Performance of Seawater-Driven Forward Osmosis for Enrichment of Nutrients in Treated Municipal Wastewater, J. Memb. Sci. (2015). doi:10.1016/j.memsci.2015.11.009.

[101] S.E. Kwan, E. Bar-Zeev, M. Elimelech, Biofouling in forward osmosis and reverse osmosis: Measurements and mechanisms, J. Memb. Sci. 493 (2015) 703–708. doi:10.1016/J.MEMSCI.2015.07.027.

[102] C. Boo, M. Elimelech, S. Hong, Fouling control in a forward osmosis process integrating seawater desalination and wastewater reclamation, J. Memb. Sci. 444 (2013) 148–156. doi:10.1016/J.MEMSCI.2013.05.004.

[103] B. Mi, M. Elimelech, Organic fouling of forward osmosis membranes: Fouling reversibility and cleaning without chemical reagents, J. Memb. Sci. 348 (2010) 337–345. doi:10.1016/j.memsci.2009.11.021.

[104] S. Lee, C. Boo, M. Elimelech, S. Hong, Comparison of fouling behavior in forward osmosis (FO) and reverse osmosis (RO), J. Memb. Sci. 365 (2010) 34–39. doi:10.1016/j.memsci.2010.08.036.

[105] T.Y. Cath, N.T. Hancock, C.D. Lundin, C. Hoppe-Jones, J.E. Drewes, A multi-barrier osmotic dilution process for simultaneous desalination and purification of impaired water, J. Memb. Sci. 362 (2010) 417–426. doi:10.1016/j.memsci.2010.06.056.

[106] N.T. Hancock, P. Xu, M.J. Roby, J.D. Gomez, T.Y. Cath, Towards direct potable reuse with forward osmosis: Technical assessment of long-term process performance at the pilot scale, J. Memb. Sci. 445 (2013) 34–46. doi:10.1016/J.MEMSCI.2013.04.056.

[107] K.L. Hickenbottom, N.T. Hancock, N.R. Hutchings, E.W. Appleton, E.G. Beaudry, P. Xu, T.Y. Cath, Forward osmosis treatment of drilling mud and fracturing wastewater from oil and gas operations, Desalination. 312 (2013) 60–66. doi:10.1016/J.DESAL.2012.05.037.

[108] Y. Gao, Z. Fang, P. Liang, X. Huang, Direct concentration of municipal sewage by forward osmosis and membrane fouling behavior, Bioresour. Technol. 247 (2018) 730–735. doi:10.1016/J.BIORTECH.2017.09.145.

[109] C. Boo, S. Lee, M. Elimelech, Z. Meng, S. Hong, Colloidal fouling in forward osmosis: Role of reverse salt diffusion, J. Memb. Sci. 390–391 (2012) 277–284. doi:10.1016/J.MEMSCI.2011.12.001.

[110] L.F. Greenlee, D.F. Lawler, B.D. Freeman, B. Marrot, P. Moulin, Reverse osmosis desalination: Water sources, technology, and today's challenges, Water Res. 43 (2009) 2317–2348. doi:10.1016/J.WATRES.2009.03.010.

[111] D. Hasson, A. Drak, R. Semiat, Inception of CaSO4 scaling on RO membranes at various water recovery levels, Desalination. 139 (2001) 73–81. doi:10.1016/S0011-9164(01)00296-X.

[112] A. Rahardianto, J. Gao, C.J. Gabelich, M.D. Williams, Y. Cohen, High recovery membrane desalting of low-salinity brackish water: Integration of accelerated precipitation softening with membrane RO, J. Memb. Sci. 289 (2007) 123–137. doi:10.1016/J.MEMSCI.2006.11.043.

[113] J.R. McCutcheon, R.L. McGinnis, M. Elimelech, Desalination by ammonia–carbon dioxide forward osmosis: Influence of draw and feed solution concentrations on process performance, J. Memb. Sci. 278 (2006) 114–123. doi:10.1016/j.memsci.2005.10.048.

[114] S. Phuntsho, H.K. Shon, S. Hong, S. Lee, S. Vigneswaran, A novel low energy fertilizer driven forward osmosis desalination for direct fertigation: Evaluating the performance of fertilizer draw solutions, J. Memb. Sci. 375 (2011) 172–181. doi:10.1016/J.MEMSCI.2011.03.038.

[115] S. Phuntsho, H.K. Shon, T. Majeed, I. El Saliby, S. Vigneswaran, J. Kandasamy, S. Hong, S. Lee, Blended Fertilizers as Draw Solutions for Fertilizer-Drawn Forward Osmosis Desalination, Environ. Sci. Technol. 46 (2012) 4567–4575. doi:10.1021/es300002w.

[116] S. Sahebi, S. Phuntsho, J. Eun Kim, S. Hong, H. Kyong Shon, Pressure assisted fertiliser drawn osmosis process to enhance final dilution of the fertiliser draw solution beyond osmotic equilibrium, J. Memb. Sci. 481 (2015) 63–72. doi:10.1016/j.memsci.2015.01.055.

[117] A. Razmjou, G.P. Simon, H. Wang, Effect of particle size on the performance of forward osmosis desalination by stimuli-responsive polymer hydrogels as a draw agent, Chem. Eng. J. 215–216 (2013) 913–920.

doi:10.1016/J.CEJ.2012.11.088.

[118] D. Li, X. Zhang, J. Yao, G.P. Simon, H. Wang, Stimuli-responsive polymer hydrogels as a new class of draw agent for forward osmosis desalination, Chem. Commun. 47 (2011) 1710–1712. doi:10.1039/C0CC04701E.

[119] D. Li, X. Zhang, G.P. Simon, H. Wang, Forward osmosis desalination using polymer hydrogels as a draw agent: Influence of draw agent, feed solution and membrane on process performance, Water Res. 47 (2013) 209–215. doi:10.1016/J.WATRES.2012.09.049.

[120] D. Li, X. Zhang, J. Yao, Y. Zeng, G.P. Simon, H. Wang, Composite polymer hydrogels as draw agents in forward osmosis and solar dewatering, Soft Matter. 7 (2011) 10048–10056. doi:10.1039/C1SM06043K.

[121] A. Achilli, T.Y. Cath, A.E. Childress, Selection of inorganic-based draw solutions for forward osmosis applications, J. Memb. Sci. 364 (2010) 233–241. doi:10.1016/J.MEMSCI.2010.08.010.

[122] H.T. Nguyen, N.C. Nguyen, S.-S. Chen, H.H. Ngo, W. Guo, C.-W. Li, A new class of draw solutions for minimizing reverse salt flux to improve forward osmosis desalination, Sci. Total Environ. 538 (2015) 129–136. doi:10.1016/J.SCITOTENV.2015.07.156.

[123] B. Corzo, T. de la Torre, C. Sans, E. Ferrero, J.J. Malfeito, Evaluation of draw solutions and commercially available forward osmosis membrane modules for wastewater reclamation at pilot scale, Chem. Eng. J. 326 (2017) 1–8. doi:10.1016/j.cej.2017.05.108.

[124] K.C. Kedwell, C.A. Quist-Jensen, G. Giannakakis, M.L. Christensen, Forward osmosis with high-performing TFC membranes for concentration of digester centrate prior to phosphorus recovery, Sep. Purif. Technol. 197 (2018) 449–456. doi:10.1016/j.seppur.2018.01.034.

[125] Y. Zhao, C. Qiu, X. Li, A. Vararattanavech, W. Shen, J. Torres, C. Hélix-Nielsen, R. Wang, X. Hu, A.G. Fane, C.Y. Tang, Synthesis of robust and high-performance aquaporin-based biomimetic membranes by interfacial polymerization-membrane preparation and RO performance characterization, J. Memb. Sci. 423–424 (2012) 422–428. doi:10.1016/J.MEMSCI.2012.08.039.

[126] N.T. Hancock, T.Y. Cath, Solute Coupled Diffusion in Osmotically Driven Membrane Processes, Environ. Sci. Technol. 43 (2009) 6769–6775. doi:10.1021/es901132x.

[127] L. Chen, Y. Gu, C. Cao, J. Zhang, J.-W. Ng, C. Tang, Performance of a submerged anaerobic membrane bioreactor with forward osmosis membrane for low-strength wastewater treatment, Water Res. 50 (2014) 114–123. doi:10.1016/J.WATRES.2013.12.009.

[128] K.S. Bowden, A. Achilli, A.E. Childress, Organic ionic salt draw solutions for osmotic membrane bioreactors, Bioresour. Technol. 122 (2012) 207–216. doi:10.1016/J.BIORTECH.2012.06.026.

[129] N.T. Hau, S.S. Chen, N.C. Nguyen, K.Z. Huang, H.H. Ngo, W. Guo, Exploration of EDTA sodium salt as novel draw solution in forward osmosis process for dewatering of high nutrient sludge, J. Memb. Sci. 455 (2014) 305–311. doi:10.1016/j.memsci.2013.12.068.

[130] J.T. Arena, S.S. Manickam, K.K. Reimund, B.D. Freeman, J.R. McCutcheon, Solute and water transport in forward osmosis using polydopamine modified thin film composite membranes, Desalination. 343 (2014) 8–16. doi:10.1016/J.DESAL.2014.01.009.

[131] S. Sahebi, S. Phuntsho, J. Eun Kim, S. Hong, H. Kyong Shon, Pressure assisted fertiliser drawn osmosis process to enhance final dilution of the fertiliser draw solution beyond osmotic equilibrium, J. Memb. Sci. 481 (2015) 63–72. doi:10.1016/J.MEMSCI.2015.01.055.

[132] L. Chekli, S. Phuntsho, J.E. Kim, J. Kim, J.Y. Choi, J.-S. Choi, S. Kim, J.H. Kim, S. Hong, J. Sohn, H.K. Shon, A comprehensive review of hybrid forward osmosis systems: Performance, applications and future prospects, J. Memb. Sci. 497 (2016) 430–449. doi:10.1016/J.MEMSCI.2015.09.041.

[133] S. Jamil, S. Jeong, S. Vigneswaran, Application of pressure assisted forward osmosis for water purification and reuse of reverse osmosis concentrate from a water reclamation plant, Sep. Purif. Technol. 171 (2016) 182–190. doi:10.1016/J.SEPPUR.2016.07.036.

[134] V. Yangali-Quintanilla, Z. Li, R. Valladares, Q. Li, G. Amy, Indirect desalination of Red Sea water with forward osmosis and low pressure reverse osmosis for water reuse, Desalination. 280 (2011) 160–166. doi:10.1016/J.DESAL.2011.06.066.

[135] C.H. Tan, H.Y. Ng, A novel hybrid forward osmosis - nanofiltration (FO-NF) process for seawater desalination: Draw solution selection and system configuration, Desalin. Water Treat. 13 (2010) 356–361. doi:10.5004/dwt.2010.1733.

[136] S. Zhao, L. Zou, D. Mulcahy, Brackish water desalination by a hybrid forward osmosis–nanofiltration system using divalent draw solute, Desalination. 284 (2012) 175–181. doi:10.1016/J.DESAL.2011.08.053.

[137] M.M. Ling, T.-S. Chung, Desalination process using super hydrophilic nanoparticles via forward osmosis integrated with ultrafiltration regeneration, Desalination. 278 (2011) 194–202. doi:10.1016/J.DESAL.2011.05.019.

[138] S.K. Yen, F. Mehnas Haja N., M. Su, K.Y. Wang, T.-S. Chung, Study of draw solutes using 2-methylimidazole-based compounds in forward osmosis, J. Memb. Sci. 364 (2010) 242–252. doi:10.1016/J.MEMSCI.2010.08.021.

[139] J.R. McCutcheon, R.L. McGinnis, M. Elimelech, A novel ammonia—carbon dioxide forward (direct) osmosis desalination process, Desalination. 174 (2005) 1–11. doi:10.1016/J.DESAL.2004.11.002.

[140] Q. Ge, M. Ling, T.-S. Chung, Draw solutions for forward osmosis processes: Developments, challenges, and prospects for the future, J. Memb. Sci. 442 (2013) 225–237. doi:10.1016/J.MEMSCI.2013.03.046.

[141] K.Y. Wang, M.M. Teoh, A. Nugroho, T.-S. Chung, Integrated forward osmosis–membrane distillation (FO–MD) hybrid system for the concentration of protein solutions, Chem. Eng. Sci. 66 (2011) 2421–2430. doi:10.1016/J.CES.2011.03.001.

[142] M. Ghanbari, D. Emadzadeh, W.J. Lau, H. Riazi, D. Almasi, A.F. Ismail, Minimizing structural parameter of thin film composite forward osmosis membranes using polysulfone/halloysite nanotubes as membrane substrates, Desalination. 377 (2016) 152–162. doi:10.1016/J.DESAL.2015.09.019.

[143] D.L. Shaffer, J.R. Werber, H. Jaramillo, S. Lin, M. Elimelech, Forward osmosis: Where are we now?, Desalination. 356 (2015) 271–284. doi:10.1016/J.DESAL.2014.10.031.

[144] R.C. Ong, T.-S. Chung, J.S. de Wit, B.J. Helmer, Novel cellulose ester substrates for high performance flat-sheet thin-film composite (TFC) forward osmosis (FO) membranes, J. Memb. Sci. 473 (2015) 63–71. doi:10.1016/J.MEMSCI.2014.08.046.

[145] L.A. Hoover, J.D. Schiffman, M. Elimelech, Nanofibers in thin-film composite membrane support layers: Enabling expanded application of forward and pressure retarded osmosis, Desalination. 308 (2013) 73–81.

doi:10.1016/j.desal.2012.07.019.

[146] K. Goh, L. Setiawan, L. Wei, W. Jiang, R. Wang, Y. Chen, Fabrication of novel functionalized multi-walled carbon nanotube immobilized hollow fiber membranes for enhanced performance in forward osmosis process, J. Memb. Sci. 446 (2013) 244–254. doi:10.1016/j.memsci.2013.06.022.

[147] K.Y. Wang, T.-S. Chung, G. Amy, Developing thin-film-composite forward osmosis membranes on the PES/SPSf substrate through interfacial polymerization, AIChE J. 58 (2011) 770–781. doi:10.1002/aic.12635.

[148] N.Y. Yip, A. Tiraferri, W.A. Phillip, J.D. Schiffman, M. Elimelech, High Performance Thin-Film Composite Forward Osmosis Membrane, Environ. Sci. Technol. 44 (2010) 3812–3818. doi:10.1021/es1002555.

[149] N.C. Nguyen, S.S. Chen, H.Y. Yang, N.T. Hau, Application of forward osmosis on dewatering of high nutrient sludge, Bioresour. Technol. 132 (2013) 224–229. doi:10.1016/j.biortech.2013.01.028.

[150] H.T. Madsen, N. Bajraktari, C. Hélix-Nielsen, B. Van der Bruggen, E.G. Søgaard, Use of biomimetic forward osmosis membrane for trace organics removal, J. Memb. Sci. 476 (2015) 469–474. doi:10.1016/j.memsci.2014.11.055.

[151] X. Song, L. Wang, C.Y. Tang, Z. Wang, C. Gao, Fabrication of carbon nanotubes incorporated double-skinned thin film nanocomposite membranes for enhanced separation performance and antifouling capability in forward osmosis process, Desalination. 369 (2015) 1–9. doi:10.1016/j.desal.2015.04.020.

[152] A.J. Ansari, F.I. Hai, W.E. Price, L.D. Nghiem, Phosphorus recovery from digested sludge centrate using seawater-driven forward osmosis, Sep. Purif. Technol. 163 (2016) 1–7. doi:10.1016/j.seppur.2016.02.031.

[153] R.W. Holloway, A.E. Childress, K.E. Dennett, T.Y. Cath, Forward osmosis for concentration of anaerobic digester centrate, Water Res. 41 (2007) 4005–4014. doi:10.1016/J.WATRES.2007.05.054.

[154] A.J. Ansari, F.I. Hai, W.E. Price, J.E. Drewes, L.D. Nghiem, Forward osmosis as a platform for resource recovery from municipal wastewater - A critical assessment of the literature, J. Memb. Sci. 529 (2017) 195–206. doi:10.1016/j.memsci.2017.01.054.

[155] R.W. Holloway, A.E. Childress, K.E. Dennett, T.Y. Cath, Forward osmosis

for concentration of anaerobic digester centrate, Water Res. 41 (2007) 4005–4014. doi:10.1016/j.watres.2007.05.054.

[156] D.J. Conley, H.W. Paerl, R.W. Howarth, D.F. Boesch, S.P. Seitzinger, K.E. Havens, C. Lancelot, G.E. Likens, Controlling Eutrophication: Nitrogen and Phosphorus, Sci. Mag. (2009) 1014–1015.

[157] W. Kühn, Oxidation Techniques in Drinking Water Treatment: Papers Presented at the Conference Held in Karlsruhe, Federal Republic of Germany, September 11-13, 1978, 1979.

[158] A.J. Ansari, F.I. Hai, W.E. Price, J.E. Drewes, L.D. Nghiem, Forward osmosis as a platform for resource recovery from municipal wastewater - A critical assessment of the literature, J. Memb. Sci. (2017). doi:10.1016/j.memsci.2017.01.054.

[159] J.C. Ortega-Bravo, G. Ruiz-Filippi, A. Donoso-Bravo, I.E. Reyes-Caniupán, D. Jeison, Forward osmosis: Evaluation thin-film-composite membrane for municipal sewage concentration, Chem. Eng. J. 306 (2016) 531–537. doi:10.1016/J.CEJ.2016.07.085.

[160] C.R. Company., CRC handbook of chemistry and physics., CRC Press, Boca Raton, 1993.

[161] C. Schneider, R.S. Rajmohan, A. Zarebska, P. Tsapekos, C. Hélix-Nielsen, Treating anaerobic effluents using forward osmosis for combined water purification and biogas production, Sci. Total Environ. 647 (2019) 1021–1030. doi:10.1016/J.SCITOTENV.2018.08.036.

[162] M. Xie, H.K. Shon, S.R. Gray, M. Elimelech, Membrane-based processes for wastewater nutrient recovery: Technology, challenges, and future direction, Water Res. 89 (2016) 210–221. doi:https://doi.org/10.1016/j.watres.2015.11.045.

[163] I.M. Khan, R. Luque, S. Akhtar, A. Shaheen, A. Mehmood, S. Idress, A.S. Buzdar, A. Ur Rehman, Design of Anion Exchange Membranes and Electrodialysis Studies for Water Desalination, Mater. . 9 (2016). doi:10.3390/ma9050365.

[164] A.T.K. Tran, Y. Zhang, N. Jullok, B. Meesschaert, L. Pinoy, B. Van der Bruggen, RO concentrate treatment by a hybrid system consisting of a pellet reactor and electrodialysis, Chem. Eng. Sci. 79 (2012) 228–238. doi:10.1016/J.CES.2012.06.001.

[165] F. Valero, Electrodialysis Technology - Theory and Applications, in: A. Barceló (Ed.), IntechOpen, Rijeka, 2011: p. Ch. 1. doi:10.5772/14297.

[166] T. Xu, Ion exchange membranes: State of their development and perspective, J. Memb. Sci. 263 (2005) 1–29. doi:10.1016/J.MEMSCI.2005.05.002.

[167] S. Mulyati, R. Takagi, A. Fujii, Y. Ohmukai, H. Matsuyama, Simultaneous improvement of the monovalent anion selectivity and antifouling properties of an anion exchange membrane in an electrodialysis process, using polyelectrolyte multilayer deposition, J. Memb. Sci. 431 (2013) 113–120. doi:10.1016/J.MEMSCI.2012.12.022.

[168] X. Wang, X. Zhang, Y. Wang, Y. Du, H. Feng, T. Xu, Simultaneous recovery of ammonium and phosphorus via the integration of electrodialysis with struvite reactor, J. Memb. Sci. 490 (2015) 65–71. doi:10.1016/j.memsci.2015.04.034.

[169] R. Liu, Y. Wang, G. Wu, J. Luo, S. Wang, Development of a selective electrodialysis for nutrient recovery and desalination during secondary effluent treatment, Chem. Eng. J. 322 (2017) 224–233. doi:10.1016/j.cej.2017.03.149.

[170] Y. Zhang, E. Desmidt, A. Van Looveren, L. Pinoy, B. Meesschaert, B. Van der Bruggen, Phosphate Separation and Recovery from Wastewater by Novel Electrodialysis, Environ. Sci. Technol. 47 (2013) 5888–5895. doi:10.1021/es4004476.

[171] Y. Zhang, B. Van der Bruggen, L. Pinoy, B. Meesschaert, Separation of nutrient ions and organic compounds from salts in RO concentrates by standard and monovalent selective ion-exchange membranes used in electrodialysis, J. Memb. Sci. 332 (2009) 104–112. doi:10.1016/J.MEMSCI.2009.01.030.

[172] A.T.K. Tran, Y. Zhang, D. De Corte, J.-B. Hannes, W. Ye, P. Mondal, N. Jullok, B. Meesschaert, L. Pinoy, B. Van der Bruggen, P-recovery as calcium phosphate from wastewater using an integrated selectrodialysis/crystallization process, J. Clean. Prod. 77 (2014) 140–151. doi:10.1016/J.JCLEPRO.2014.01.069.

[173] A.T.K. Tran, Y. Zhang, J. Lin, P. Mondal, W. Ye, B. Meesschaert, L. Pinoy, B. Van der Bruggen, Phosphate pre-concentration from municipal wastewater by selectrodialysis: Effect of competing components, Sep. Purif. Technol. 141 (2015) 38–47. doi:10.1016/J.SEPPUR.2014.11.017.

[174] E. James Watkins, P.H. Pfromm, Capacitance spectroscopy to characterize organic fouling of electrodialysis membranes, J. Memb. Sci. 162 (1999) 213–218. doi:10.1016/S0376-7388(99)00144-1.

[175] V. Lindstrand, G. Sundström, A.-S. Jönsson, Fouling of electrodialysis membranes by organic substances, Desalination. 128 (2000) 91–102. doi:10.1016/S0011-9164(00)00026-6.

[176] H.-J. Lee, M.-K. Hong, S.-D. Han, S.-H. Cho, S.-H. Moon, Fouling of an anion exchange membrane in the electrodialysis desalination process in the presence of organic foulants, Desalination. 238 (2009) 60–69. doi:10.1016/J.DESAL.2008.01.036.

[177] L. Bazinet, M. Araya-Farias, Effect of calcium and carbonate concentrations on cationic membrane fouling during electrodialysis, J. Colloid Interface Sci. 281 (2005) 188–196. doi:10.1016/J.JCIS.2004.08.040.

[178] E. Ayala-Bribiesca, M. Araya-Farias, G. Pourcelly, L. Bazinet, Effect of concentrate solution pH and mineral composition of a whey protein diluate solution on membrane fouling formation during conventional electrodialysis, J. Memb. Sci. 280 (2006) 790–801. doi:10.1016/J.MEMSCI.2006.02.036.

[179] K.C. Kedwell, M.L. Christensen, C.A. Quist-Jensen, M.K. Jørgensen, Effect of reverse sodium flux and pH on ammoniacal nitrogen transport through biomimetic membranes, Sep. Purif. Technol. 217 (2019) 40–47. doi:https://doi.org/10.1016/j.seppur.2019.02.001.

[180] R. Elmgren, U. Larsson, Nitrogen and the Baltic Sea: Managing Nitrogen in Relation to Phosphorus, ScientificWorldJournal. 1 (2001) 371–377.

[181] S.A.G. Leroy, F. Marret, E. Gibert, F. Chalié, J.-L. Reyss, K. Arpe, River inflow and salinity changes in the Caspian Sea during the last 5500 years, Quat. Sci. Rev. 26 (2007) 3359–3383. doi:10.1016/J.QUASCIREV.2007.09.012.

[182] P.P. Povinec, H.D. Livingston, S. Shima, M. Aoyama, J. Gastaud, I. Goroncy, K. Hirose, L. Huynh-Ngoc, Y. Ikeuchi, T. Ito, J. La Rosa, L. Liong Wee Kwong, S.-H. Lee, H. Moriya, S. Mulsow, B. Oregioni, H. Pettersson, O. Togawa, IAEA'97 expedition to the NW Pacific Ocean—results of oceanographic and radionuclide investigations of the water column, Deep Sea Res. Part II Top. Stud. Oceanogr. 50 (2003) 2607–2637. doi:10.1016/S0967-0645(03)00138-3.

[183] M. Thiel, I.A. Hinojosa, T. Joschko, L. Gutow, Spatio-temporal distribution of floating objects in the German Bight (North Sea), J. Sea Res. 65 (2011) 368–379. doi:10.1016/J.SEARES.2011.03.002.

[184] J.D. Reimer, M. Herrera, R. Gatins, M.B. Roberts, J.E. Parkinson, M.L. Berumen, Latitudinal variation in the symbiotic dinoflagellate Symbiodinium of the common reef zoantharian Palythoa tuberculosa on the Saudi Arabian coast of the Red Sea, J. Biogeogr. 44 (2017) 661–673. doi:10.1111/jbi.12795.

[185] B.C. Cho, Heterotrophic Flagellates in Hypersaline Waters BT - Adaptation to Life at High Salt Concentrations in Archaea, Bacteria, and Eukarya, in: N. Gunde-Cimerman, A. Oren, A. Plemenitaš (Eds.), Springer Netherlands, Dordrecht, 2005: pp. 541–549.

[186] J.L. Reid, On the temperature, salinity, and density differences between the Atlantic and Pacific oceans in the upper kilometre, Deep Sea Res. 7 (1961) 265–275. doi:10.1016/0146-6313(61)90044-2.

[187] R. Valladares Linares, Z. Li, V. Yangali-Quintanilla, N. Ghaffour, G. Amy, T. Leiknes, J.S. Vrouwenvelder, Life cycle cost of a hybrid forward osmosis – low pressure reverse osmosis system for seawater desalination and wastewater recovery, Water Res. 88 (2016) 225–234. doi:10.1016/J.WATRES.2015.10.017.

[188] M.J. Pryor, E.P. Jacobs, J.P. Botes, V.L. Pillay, A low pressure ultrafiltration membrane system for potable water supply to developing communities in South Africa, Desalination. 119 (1998) 103–111. doi:10.1016/S0011-9164(98)00126-X.

[189] Salt Sellers, Econ. (2010). https://www.economist.com/finance-and-economics/2010/01/14/salt-sellers.

[190] S. Judd, Watermaths, Second, Judd and Judd Ltd, 2013.

[191] S. Ripperger, Cross-flow micro- and ultra-filtration, in: Short Course - World Filtr. Congr. 2008, Leipzig, 2008.

.

ISSN (online): 2446-1636
ISBN (online): 978-87-7210-412-6

AALBORG UNIVERSITY PRESS